



Comprehensive Model for Epidermal Growth Factor Receptor Ligand Binding Involving Conformational States of the Extracellular and the Kinase Domains

Tímea Hajdu^{1,2}, Tímea Váradi¹, István Rebenku¹, Tamás Kovács¹, János Szöllösi^{1,3} and Peter Nagy^{1}*

OPEN ACCESS

Edited by:

Venkaiah Betapudi,
Chemical and Biological Defense
Division (DHS), United States

Reviewed by:

Sarvenaz Sarabipour,
Johns Hopkins University,
United States
Paul Van Bergen En Henegouwen,
Utrecht University, Netherlands

*Correspondence:

Peter Nagy
nagy.p@med.unideb.hu;
peter.v.nagy@gmail.com

Specialty section:

This article was submitted to
Cellular Biochemistry,
a section of the journal
*Frontiers in Cell and Developmental
Biology*

Received: 17 April 2020

Accepted: 23 July 2020

Published: 11 August 2020

Citation:

Hajdu T, Váradi T, Rebenku I,
Kovács T, Szöllösi J and Nagy P
(2020) Comprehensive Model
for Epidermal Growth Factor Receptor
Ligand Binding Involving
Conformational States of the
Extracellular and the Kinase Domains.
Front. Cell Dev. Biol. 8:776.
doi: 10.3389/fcell.2020.00776

¹ Department of Biophysics and Cell Biology, Faculty of Medicine, University of Debrecen, Debrecen, Hungary, ² Doctoral School of Molecular Medicine, Faculty of Medicine, University of Debrecen, Debrecen, Hungary, ³ MTA-DE Cell Biology and Signaling Research Group, Faculty of Medicine, University of Debrecen, Debrecen, Hungary

The epidermal growth factor (EGF) receptor (EGFR) undergoes ligand-dependent dimerization to initiate transmembrane signaling. Although crystallographic structures of the extracellular and kinase domains are available, ligand binding has not been quantitatively analyzed taking the influence of both domains into account. Here, we developed a model explicitly accounting for conformational changes of the kinase and extracellular domains, their dimerizations and ligand binding to monomeric and dimeric receptor species. The model was fitted to ligand binding data of suspended cells expressing receptors with active or inactive kinase conformations. Receptor dimers with inactive, symmetric configuration of the kinase domains exhibit positive cooperativity and very weak binding affinity for the first ligand, whereas dimers with active, asymmetric kinase dimers are characterized by negative cooperativity and subnanomolar binding affinity for the first ligand. The homodimerization propensity of EGFR monomers with active kinase domains is ~100-times higher than that of dimers with inactive kinase domains. Despite this fact, constitutive, ligand-independent dimers are mainly generated from monomers with inactive kinase domains due to the excess of such monomers in the membrane. The experimental finding of increased positive cooperativity at high expression levels of EGFR was recapitulated by the model. Quantitative prediction of ligand binding to different receptor species revealed that EGF binds to receptor monomers and dimers in an expression-level dependent manner without significant recruitment of monomers to dimers upon EGF stimulation below the phase transition temperature of the membrane. Results of the fitting offer unique insight into the workings of the EGFR.

Keywords: EGF receptor, ligand binding, cooperativity, dimerization, kinase domain

INTRODUCTION

The ErbB/HER family of receptor tyrosine kinases (RTKs) comprises four transmembrane receptors activated by a large number and variety of peptide growth factors (Yarden and Sliwkowski, 2001). ErbB1, also known as the epidermal growth factor (EGF) receptor (EGFR), is activated by ligand binding followed by tyrosine phosphorylation of its C-terminal domain and recruitment of SH2 and PTB domain-containing proteins (Wagner et al., 2013). While EGFR is one of the most studied transmembrane receptors, perplexing questions remain about the fine details of its activation (Jovin, 2014). Although larger clusters of EGFR has also been described (Szabó et al., 2008; Needham et al., 2016), dimerization is believed to be the key in regulating receptor activation, a notion strongly supported by crystallographic structures of the extracellular and kinase domains of the receptor (Ogiso et al., 2002; Zhang et al., 2006). The tethered or closed structure of the extracellular domain (ECD) undergoes a rearrangement to an extended conformation forming back-to-back, ligand-bound dimers stabilized by the exposed dimerization arm (Lemmon, 2009; Ziomkiewicz et al., 2013). Besides this dimeric species, ligand-bound head-to-head dimers (Garrett et al., 2002) and ligand-free dimeric species, including side-to-side dimers have also been reported (Moriki et al., 2001; Zanetti-Domingues et al., 2018). Dimerization is not only mediated by the ECD, but also by the transmembrane (TMD) and intracellular domains under the influence of the lipid environment of the plasma membrane (Kovacs et al., 2015; Kovács et al., 2016; Zákány et al., 2020). The TMD of EGFR contains two dimerization motifs, with the N- and C-terminal ones suggested to stabilize active and inactive dimers, respectively (Fleishman et al., 2002). The kinase domain (KD) is also capable of forming at least two different dimeric species. The kinase is activated in an asymmetric dimer by a mechanism recapitulating how cyclins activate cyclin-dependent kinases, while the symmetric dimer, although harboring KDs in their active conformation, is unlikely to be capable of signal transduction (Landau et al., 2004; Zhang et al., 2006; Jura et al., 2009; Kovacs et al., 2015). Most tyrosine kinase inhibitors bind to the ATP-binding pocket of the kinase. Type I inhibitors, including erlotinib, stabilize the active conformation of the kinase, while type II inhibitors, e.g., lapatinib, stabilize its inactive structure (Stamos et al., 2002; Wood et al., 2004; Zhang et al., 2009). Interactions of the juxtamembrane segment with negatively charged lipids in the inner leaflet of the plasma membrane prevent formation of active kinase dimers, while the juxtamembrane segment also forms activating interactions with the KD (Jura et al., 2009). Although the large variety of dimeric structures is complicated, a scheme seems to emerge in which the asymmetric, active kinase dimer, the TMD dimer stabilized by its N-terminal dimerization motif and the liganded, back-to-back ECD dimer mutually favor each other, since this conformation of the ECD holds the C-terminal dimerization motifs of the TMD apart and the asymmetric KD dimer pulls the N-terminal dimerization motifs of the TMD together (Diwanji et al., 2019). The finding of coupling between the KD activated by the L858R mutation and the unliganded, dimerization competent

ECD also supports the previous model (Valley et al., 2015). Interactions between different parts of inactive receptors is more controversial. While coupling of the symmetric kinase dimer to the TMD dimer stabilized by its C-terminal dimerization motif is widely accepted, conformational coupling of this symmetric kinase dimer and the transmembrane domains to the ECD is debated. While some evidence suggests that the liganded ECD can couple to both the symmetric and asymmetric kinase dimers (Mi et al., 2011), a strict linkage between symmetric kinase dimers and the closed conformation of the ECD has also been put forward (Bessman et al., 2014; Macdonald-Obermann and Pike, 2018). In addition, the ECD of inactive receptors has been suggested to form alternative structures as well, like side-to-side dimers (Moriki et al., 2001) or head-to-head oligomers (Zanetti-Domingues et al., 2018).

Although significant progress has been made in revealing conformational transitions of isolated receptor parts upon activation, correlations between these receptor states in the full-length protein have not been described due to the flexibility of the juxtamembrane domains and the difficulty of studying structurally homogenous EGFR populations (Mi et al., 2011; Diwanji et al., 2019). These correlations implicitly determine the concentration dependence of ligand binding. Oligomerization linkage takes place when a liganded monomer undergoes dimerization differently than its unliganded counterpart revealing ligand-induced conformational transitions. Throughout the paper this phenomenon will be briefly referred to as linkage. When ligands bind cooperatively to a dimer, the dissociation constants for consecutive ligand bindings are not identical implying conformational changes taking place in the dimer. Although this phenomenon has been named homotropic ligand linkage, the term cooperativity has been so widely accepted that it will be used for referring to this phenomenon (Wyman and Gill, 1990; Pike, 2012). Analysis of equilibrium ligand binding is often carried out by fitting the Hill equation to data providing the Hill cooperativity coefficient. Although a Hill coefficient different from one is interpreted as a sign of cooperativity, we are going to refer to this phenomenon as apparent or phenomenological cooperativity since linkage and molecular cooperativity collectively determine the Hill coefficient.

Quantitative EGF binding assays may produce concave-up Scatchard plots, which were attributed to two independent binding sites for decades (Defize et al., 1988; Bellot et al., 1990; Özcan et al., 2006). However, negative cooperativity has been invoked to account for the apparent heterogeneity of EGF binding sites (Macdonald and Pike, 2008). This phenomenon requires that binding of the first ligand to an EGFR dimer decreases the ligand binding affinity of the other subunit by inducing an asymmetric ECD dimer with a constrained ligand binding site on the unoccupied receptor. While the drosophila EGFR, whose isolated ECD retains negative cooperativity, has indeed been reported to form such asymmetric dimers (Alvarado et al., 2010), its human counterpart only exhibits negative cooperativity when ligands bind to full-length receptors in cells. Although low affinity ligands bound to human EGFR stabilize an asymmetric ECD dimer (Freed et al., 2017), such an asymmetry

has not been observed when high affinity ligands, like EGF, are complexed with the receptor (Martin-Fernandez, 2012). These facts suggest that other receptor regions, conformations and/or unknown cellular components must be involved in the regulation of ligand affinity of EGFR in the cellular environment. Although negative cooperativity became the dogma in EGF binding studies, several investigators reported positive cooperative ligand binding to EGFR (Sherrill and Kyte, 1996; Lemmon et al., 1997; Teramura et al., 2006; Chung et al., 2010) with a recent report linking positive cooperativity to receptor dimers with symmetric kinase dimers, but without quantitative analysis based on molecular structures (Macdonald-Obermann and Pike, 2018). The present study was undertaken to generate a structure-based model of EGF binding involving conformational transitions of the extracellular and intracellular domains. The obtained equations not only fit the experimental data well, but are in accordance with most published structural results and can resolve the aforementioned contradictions regarding cooperativity of ligand binding.

MATERIALS AND METHODS

Cells

The CHO-K1 cell line (ATCC CCL-61) was obtained from the American Type Culture Collection (Manassas, VA, United States). Its subline, F1-4, stably expresses EGFR-GFP (Brock et al., 1999). F1-4 cells were maintained at 37°C and 5% CO₂ in Dulbecco's Modified Eagle's medium (DMEM) supplemented with 10% fetal calf serum and 50 µg/ml gentamicin. The number of passages of cells used for the experiments never exceeded 15. The expression level of EGFR was determined by flow cytometry using Qifikit (Agilent Technologies, Santa Clara, CA, United States). For stimulation of EGFR, cells were cultured in DMEM containing 0.1% fetal calf serum and 50 µg/ml gentamicin for 12 h followed by incubation with 130 nM EGF (R&D Systems, Minneapolis, MN, United States) in Hank's balanced salt solution at 37°C or 4°C for 15 min or 1 h.

Reagents

For microscopic experiments cells were cultured on µ-slide 8-well chambered coverglass (Ibidi, Martinsried, Germany). For flow cytometry cells were harvested by trypsinization. Human EGF (cat. no: 236-EG) was purchased from R&D Systems (Minneapolis, MN, United States). Tetramethylrhodamine-labeled EGF (cat. no: E3481) was purchased from Thermo Fisher Scientific (Waltham, MA, United States). EGF-stimulated tyrosine phosphorylation was visualized by labeling with an antibody against phosphotyrosine (PY99, cat. no: sc-7020; Santa Cruz, Dallas, TX, United States) followed by secondary staining with AlexaFluor647-conjugated goat-anti-mouse IgG (cat. no: A-21235; Thermo Fisher Scientific). Tunicamycin (cat. no: T7765), latrunculin-B (cat. no: L5288) and jasplakinolide (Cat. no: J4580) were purchased from Sigma-Aldrich (St. Louis, MO, United States). Tetramethylrhodamine B isothiocyanate-labeled phalloidin (TRITC-phalloidin, cat. no: P1951) and 4',6-diamidino-2'-phenylindole (DAPI, cat. no: D9542) were obtained

from Sigma Aldrich. Lapatinib (cat. no: S2111) and erlotinib (cat. no: S7786) were purchased from Selleckchem (Houston, TX, United States).

Labeling of Cells With Fluorescent EGF

Tetramethylrhodamine-conjugated EGF (TAMRA-EGF) was reconstituted at a concentration of 10 µM. A two-fold dilution series of TAMRA-EGF was prepared with each vial containing 500 µl TAMRA-EGF dissolved in phosphate-buffered saline supplemented with 1% (w/v) BSA. The solutions were kept on ice before adding 20 µl of a cold cell suspension containing 100,000 cells. Cells were incubated in the presence of TAMRA-EGF for 1 h on ice with shaking. The fluorescence intensity of the samples was measured on a FACS Aria III flow cytometer (BD Biosciences, San Jose, CA, United States) without washing to prevent the dissociation of fluorescent EGF. TAMRA was excited at 561 nm, and its emission was detected through a 595 nm band-pass filter. Analysis of flow cytometric data was carried out with FCS Express (Denovo Software, Thornhill, ON, Canada). Mean fluorescence intensities were background-corrected followed by fitting the Hill equation to the binding curves:

$$I = I_{\min} + \frac{I_{\max} - I_{\min}}{1 + 10^{n(\log K_d - \log c)}} \quad (1)$$

where I is the intensity of the sample labeled with concentration c of fluorescent EGF, I_{\min} and I_{\max} are the minimal and maximal intensities, respectively. K_d and n are the dissociation constant and the Hill coefficient, respectively. The same datasets were also used for fitting of the model described in the present manuscript.

Treatment of Cells With Kinase Inhibitors

In order to measure the effect of kinase inhibitors on EGF-induced phosphorylation cells were grown on µ-slide 8-well chambered coverglass and were serum-starved for 12 h. Then, they were exposed to erlotinib or lapatinib at a concentration of 5 µM at 37°C for 1 h followed by stimulation with EGF at a concentration of 130 nM for 15 min at 37°C. Cells were fixed in 3.7% (v/v) formaldehyde, permeabilized with a solution of 0.1% (v/v) Triton-X100 containing 1% (w/v) BSA in PBS followed by secondary staining with a pan-phosphotyrosine antibody (PY99) and AlexaFluor647 goat anti-mouse IgG. Samples were observed using a Zeiss LSM880 confocal microscope with a C-Apochromat 40 × (N.A. = 1.2) water immersion objective. GFP and AlexaFluor647 were excited at 488 and 633 nm, respectively. Emissions of GFP and AlexaFluor647 were measured in the wavelength range of 490–570 nm and 635–755 nm, respectively. In order to measure the effect of kinase inhibitors on EGF binding trypsinized cells were treated with erlotinib or lapatinib at a concentration of 5 µM at 37°C for 1 h followed by labeling with TAMRA-EGF as described previously.

Inhibition of Glycosylation of EGFR

F1-4 cells were treated with tunicamycin at a concentration of 1 µg/ml for 24 h followed by trypsinization and labeling with TAMRA-EGF as described above. In order to show the effect of deglycosylation on the molecular weight of EGFR control

and tunicamycin-treated cells were lysed and scraped followed by running the lysate in a 7% SDS-PAGE gel. Proteins were transferred to PVDF membranes, and the blots were incubated with an antibody against EGFR (anti-EGFR, clone F4, Thermo Fisher Scientific; Cat. no: MA1-24226) at 4°C overnight followed by labeling with anti-mouse IgG-peroxidase (Sigma-Aldrich; cat no: AP124P) for detection with a chemiluminescence kit (Thermo Fisher Scientific; cat no: 34577, 34095).

Inhibition or Promotion of Actin Polymerization

Cells were treated with latrunculin-B at a concentration of 2 μ M at 37°C for 10 min or by 1 μ M jasplakinolide at 37°C for 30 min followed by labeling with a concentration series of TAMRA-EGF as described above. In order to visualize the effect of latrunculin-B or jasplakinolide on microfilaments, control and treated cells were permeabilized with acetone followed by staining with 4 μ g/ml TRITC-phalloidin and 10 μ g/ml DAPI. Samples were observed with a Zeiss LSM880 confocal microscope using a C-Apochromat 40 \times (N.A. = 1.2) water immersion objective. DAPI and TRITC were excited at 405 nm and 543 nm, respectively. The emissions of DAPI and TRITC were detected in the wavelength range of 410–482 nm and 557–655 nm, respectively.

Homo-FRET Measurements

F1-4 cells were seeded at a density of 5×10^4 cells/well on μ -slide 8-well chambered coverglass, and serum-starved overnight. After washing with Hank's balanced salt solution, cells were treated with erlotinib or lapatinib at a concentration of 5 μ M at 37°C for 1 h followed by stimulation with EGF at a concentration of 130 nM for 15 min at 37°C or 4°C. Imaging was carried out with a Zeiss LSM880 confocal microscope without washing or diluting the samples. Samples were examined with a C-Apochromat 40 \times (N.A. = 1.2) water immersion objective. Stepwise bleaching of GFP was accomplished by a 405-nm laser line till the GFP signal completely faded. Fluorescence was observed in two tracks detecting the fluorescence emission polarized parallel (I_{\parallel}) and perpendicular (I_{\perp}) to the excitation beam by a Quasar detector in the L-format arrangement. Intensities were summed in membrane pixels, identified by manually seeded watershed segmentation, after subtracting background fluorescence determined in a cell-free area of the image. Intensities were corrected for high numerical aperture detection followed by calculating anisotropy (r) as follows (Jovin, 1979):

$$r = \frac{I_{\parallel} - G I_{\perp}}{I_{\parallel} + 2 G I_{\perp}} \quad (2)$$

The G factor, characterizing the sensitivity of the detection system to the parallel and perpendicular intensity components, was determined by imaging a GFP solution using microscope settings identical to the ones used for the cells.

Homo-FRET implemented in microscopy or flow cytometry has been used previously to analyze receptor clustering (Lidke et al., 2003; Yeow and Clayton, 2007; Szabó et al., 2008; Hofman et al., 2010). In order to estimate homoclustering of EGFR, the

anisotropy, calculated from membrane pixels, of each image in the bleaching sequence was plotted against the residual fractional intensity of GFP, and an equation describing the anisotropy of a mixture of monomers and homoclustered receptors was fitted to the measured data points. We assumed that a fraction of proteins (mon) is unclustered, whereas the rest of them form clusters consisting of N fluorophores. The equation describing the anisotropy of such a population of fluorophores ($r_{s,N}$) was fitted to the measured data (Szabó et al., 2008):

$$r_{s,N} = \frac{(1 - mon)}{Ns} \sum_{k=0}^N \left[\left(\frac{N}{k} \right) s^k (1-s)^{N-k} k \left(r_1 \frac{1+d^6}{1+kd^6} + r_{FRET} \frac{(k-1)d^6}{1+kd^6} \right) \right] + mon \cdot r_1 \quad (3)$$

where s is the fraction of unbleached fluorophores, r_1 and r_{FRET} are the anisotropies of an isolated fluorophore and a fluorophore excited by homo-FRET, respectively, and d is the reciprocal of the distance between the fluorophores in the clusters normalized to R_0 . r_1 was assumed to be 0.34 (Volkmer et al., 2000), while the anisotropy of fluorophores excited by homo-FRET (r_{FRET}) was assumed to be zero (Runnels and Scarlata, 1995). The distance between two fluorophores in a cluster was assumed to be equal to the Förster distance for a GFP-GFP homo-FRET pair (4.8 nm), which is in the same order of magnitude as the size of a GFP barrel (Yang et al., 1996; Kremers and Goedhart, 2009). Fitting provided the number of proteins in a homocluster (N , cluster size) and the fraction of monomeric receptors (mon). The reliability of the estimation at the given biological variability and measurement error was determined by Monte Carlo simulation. Five hundred anisotropy vs. fractional residual intensity curves were generated using the mean and the standard deviation of the anisotropies. All curves were fitted generating 500 estimations for the cluster size and monomeric fraction. The histograms of these values and their 95% confidence intervals provided an estimation for the reliability of the fitting (Szabó et al., 2008).

RESULTS

Equilibrium Binding of EGF to Cells With or Without Kinase Inhibitor Treatment

Coupling between the conformations of the intra- and extracellular parts of EGFR are expected to affect the apparent cooperativity and affinity of EGF binding, which can be estimated by analyzing the dependence of these parameters on the expression level of the receptor. In order to look at cell populations having different EGFR expression levels without disturbing the homeostasis of cells significantly, we used F1-4 cells, a CHO subline stably transfected with EGFR-GFP. Flow cytometric gating on the GFP fluorescence makes selection of subpopulations with different expression levels of EGFR possible (Supplementary Figure 1). Although quantitative imaging of fluorescent EGF bound to attached cells is possible (Teramura et al., 2006; Chung et al., 2010), the statistical reliability of such measurements, especially when restricted to a subpopulation

with a certain receptor expression level, is poor due to the low number of analyzed cells. We expected that such noisy data would have prevented successful fitting of a complex model. In order for our flow cytometric approach to be relevant for the physiological state of EGFR, we showed that trypsinization, used for detaching cells from culture flasks, had negligible effect on the expression level and molecular weight of EGFR on the cell surface (**Supplementary Figure 2**). In spite of these findings, it must be pointed out that all binding measurements were carried out with suspended cells. We also established that the EGF binding characteristics of the EGFR-GFP fusion construct are identical to those of native EGFR (**Supplementary Figure 3**). Fitting of the Hill equation to the equilibrium EGF binding data in F1-4 cells revealed nanomolar apparent K_d and positive apparent cooperativity, which increased as a function of receptor expression (**Figure 1** and **Table 1**). Throughout the analyses presented in the manuscript ligand depletion was assumed to be negligible. The validity of this assumption is shown in the **Supplementary Information**. In order to test explicitly the influence of different states of the KD on EGF binding, inhibitors stabilizing the kinase in the active and inactive conformations were used. Their effect on EGF-induced tyrosine phosphorylation is shown in **Supplementary Figure 4**. Erlotinib, binding and stabilizing the active conformation of the kinase, increased the affinity of the receptor for EGF and reduced the Hill coefficient to a range characteristic of negative apparent cooperativity in all cell populations except for those exhibiting the highest expression. Cells treated with lapatinib, an inhibitor stabilizing the inactive conformation of the KD, were characterized by positive cooperative EGF binding with reduced apparent affinity (**Figure 1** and **Table 1**). The results revealed that EGFR exhibits an expression level-dependent tendency for positive apparent cooperativity in ligand binding, which is also influenced by the conformation of the KD.

Development of a Model Involving Conformational States of the Ligand-Binding and Kinase Domains

Given the results obtained with cells treated with the two kinase inhibitors, establishing that the KD exerts significant effects on the characteristics of EGF binding, and structural evidence pointing at dimerization of the KD, we developed a molecular model of EGF binding based on the following assumptions. 1. The closed conformation of the ECD is in equilibrium with its extended structure (Klein et al., 2004). Although the ligandless ECD has been found to be dynamic, assuming other conformations as well (Kaplan et al., 2016), they were not included in the model in order to limit the number of free parameters. 2. Receptor dimerization only takes place with receptors whose ECD is in the extended conformation (Garrett et al., 2002; Ogiso et al., 2002). 3. The KD is assumed to adopt either an inactive or active conformation in receptor monomers. Although other conformations of the KD have also been reported (Shan et al., 2012), the number of molecular species had to be minimized so that the model remains tractable. Therefore, these intermediate conformations were excluded from the model.

4. The conformations of the intra- and extracellular domains are uncoupled from each other in monomeric receptors. 5. The extended conformation of the ECD dimers can couple with both symmetric and asymmetric KD dimers, in accordance with high resolution electron microscopic evidence (Mi et al., 2011). While assignment of symmetric and asymmetric configurations to the two different kinds of kinase dimers in the model is not based on firm structural evidence, the assumption of two different receptor dimerization pathways beginning from receptors harboring inactive and active KDs was absolutely required for successful fitting of the data. With this limitation in mind, we still refer to these kinase dimers as symmetric and asymmetric. The structure of kinase domain dimers assigned to these two different dimerization pathways will be further addressed in the Discussion. 6. Dimers with symmetric and asymmetric KD dimers are characterized by different affinities for EGF. Incorporation of this assumption was required so that the model could reproduce the significant dependence of apparent cooperativity on expression levels and on the presence of the two kinase inhibitors. A possible explanation for the validity of this assumption is provided in the Discussion. 7. Ligand binds only to the extended conformation of the ECD. Models describing EGF binding including or neglecting ligand binding to the closed conformation of the ECD have both been published (Klein et al., 2004; Macdonald and Pike, 2008). Since the affinity of a dimer harboring symmetric kinase dimers for binding of the first ligand turned out to be low, incorporation of another low affinity binding site, the closed ECD, would have made the model less reliable. Besides this model, several alternative ones have been tested. Receptor dimerization beginning from a monomer with extended ECD and an asymmetric kinase dimer was included in all of them. Without inclusion of another dimerization pathway the result of the fitting was poor. If the second dimerization pathway began from either of the monomers with closed ECD ("CA" or "CI"), fittings were also of poor quality. The approach taken to construct the model is a compromise between an even more detailed, but mathematically intractable model taking every possible state and transition into consideration and a biologically unrealistic, simplistic model, which is easy to handle. Such a golden mean has been suggested to result in realistic and experimentally verifiable models (Yates et al., 2001).

The model, presented in **Figure 2**, involves twelve molecular species, whose equilibrium state is described by eleven equations and nine constants. The following equations characterize the conformational transitions and ligand binding of monomeric species:

$$[CI] = K_1 [CA] \quad (4)$$

$$[CI] = K_2 [EI] \quad (5)$$

$$[EI] = K_1 [EA] \quad (6)$$

$$[EI] [EGF] = K_3 [EIL] \quad (7)$$

TABLE 1 | EGF binding fitted according to the Hill equation.

	Low expresser	Medium expresser	High expresser	All cells
Untreated	$n = 1.14 \pm 0.004$ $K_d = 4.4 \pm 0.005$ nM $N = 390,000$	$n = 1.33 \pm 0.008$ $K_d = 3.8 \pm 0.01$ nM $N = 630,000$	$n = 1.41 \pm 0.01$ $K_d = 3.8 \pm 0.01$ nM $N = 1,070,000$	$n = 1.26 \pm 0.006$ $K_d = 3.9 \pm 0.007$ nM $N = 560,000$
Erlotinib	$n = 0.92 \pm 0.02$ $K_d = 2 \pm 0.02$ nM $N = 390,000$	$n = 0.99 \pm 0.01$ $K_d = 1.8 \pm 0.01$ nM $N = 630,000$	$n = 1.03 \pm 0.01$ $K_d = 1.7 \pm 0.02$ nM $N = 1,000,000$	$n = 0.95 \pm 0.01$ $K_d = 1.9 \pm 0.01$ nM $N = 500,000$
Lapatinib	$n = 1.04 \pm 0.01$ $K_d = 6.3 \pm 0.01$ nM $N = 390,000$	$n = 1.21 \pm 0.01$ $K_d = 5.1 \pm 0.01$ nM $N = 630,000$	$n = 1.36 \pm 0.01$ $K_d = 4.9 \pm 0.02$ nM $N = 1,010,000$	$n = 1.2 \pm 0.01$ $K_d = 4.9 \pm 0.02$ nM $N = 520,000$

Equilibrium EGF binding data was fitted with the Hill equation. The apparent dissociation constant (K_d) and the Hill coefficient (n , \pm their standard deviations) are displayed for the control sample and cells treated with the kinase inhibitors. The standard deviations were estimated by multiplying the inverse of the Hessian with the standard deviation of the fitting error. The expression level of EGFR of the whole cell population was measured by flow cytometric calibration. EGFR expressions of the low, medium and high expresser subpopulations were determined by assuming that the maximum intensity of EGF fluorescence, determined from the Hill fits, is proportional to the receptor expression level. The number of receptors/cell, designated by N , is shown at the bottom of each cell. The experimental data and the fits are shown in **Figure 1**.

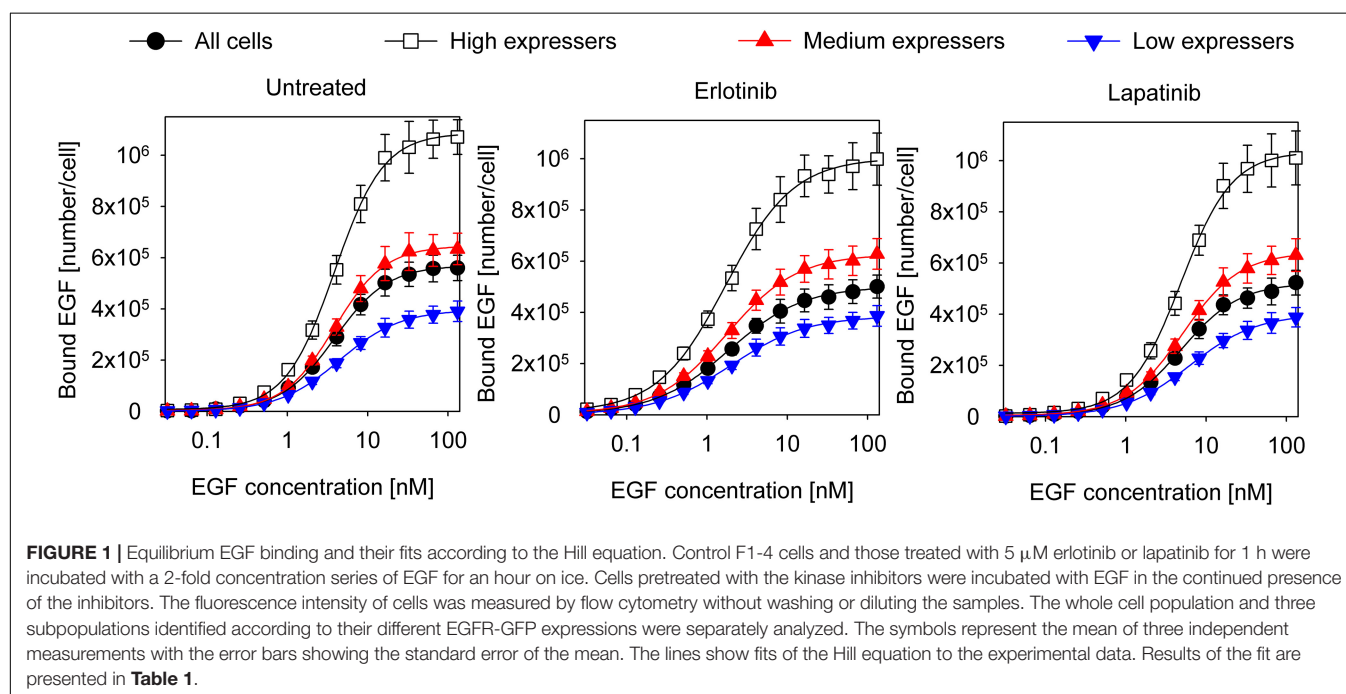


FIGURE 1 | Equilibrium EGF binding and their fits according to the Hill equation. Control F1-4 cells and those treated with 5 μ M erlotinib or lapatinib for 1 h were incubated with a 2-fold concentration series of EGF for an hour on ice. Cells pretreated with the kinase inhibitors were incubated with EGF in the continued presence of the inhibitors. The fluorescence intensity of cells was measured by flow cytometry without washing or diluting the samples. The whole cell population and three subpopulations identified according to their different EGFR-GFP expressions were separately analyzed. The symbols represent the mean of three independent measurements with the error bars showing the standard error of the mean. The lines show fits of the Hill equation to the experimental data. Results of the fit are presented in **Table 1**.

$$[EA][EGF] = K_3[EAL] \quad (8)$$

where K_1 and K_2 are the equilibrium constants for the conformational transitions of the KD and the ECD, respectively, and K_3 is the dissociation constant of EGF binding to a monomeric receptor having an extended ECD. The abbreviations of molecular species are defined in the legend to **Figure 2**. The following equations describe the dimerization of monomers leading to the formation of dimers with symmetric kinase dimers:

$$[EI][EI] = K_4[DES] \quad (9)$$

$$[DES][EGF] = K_5[DESL] \quad (10)$$

$$[DESL][EGF] = K_6[DES2L] \quad (11)$$

where K_4 is the dissociation constant of an unliganded dimer harboring extended ECD and symmetric KD dimer,

and the dissociation constants of the first and second EGF binding to this dimer are denoted by K_5 and K_6 , respectively. The dimerization and ligand binding pathway of species with asymmetric KD dimers are described by the equations below:

$$[EA][EA] = K_7[DEA] \quad (12)$$

$$[DEA][EGF] = K_8[DEAL] \quad (13)$$

$$[DEAL][EGF] = K_9[DEA2L] \quad (14)$$

where K_7 is the dissociation constant of an unliganded dimer with extended ECD and asymmetric KD dimer, while K_8 and K_9 denote the dissociation constants of the first and second EGF binding to this dimer, respectively. The relationships describing the quantity of cell-bound EGF and the conservation

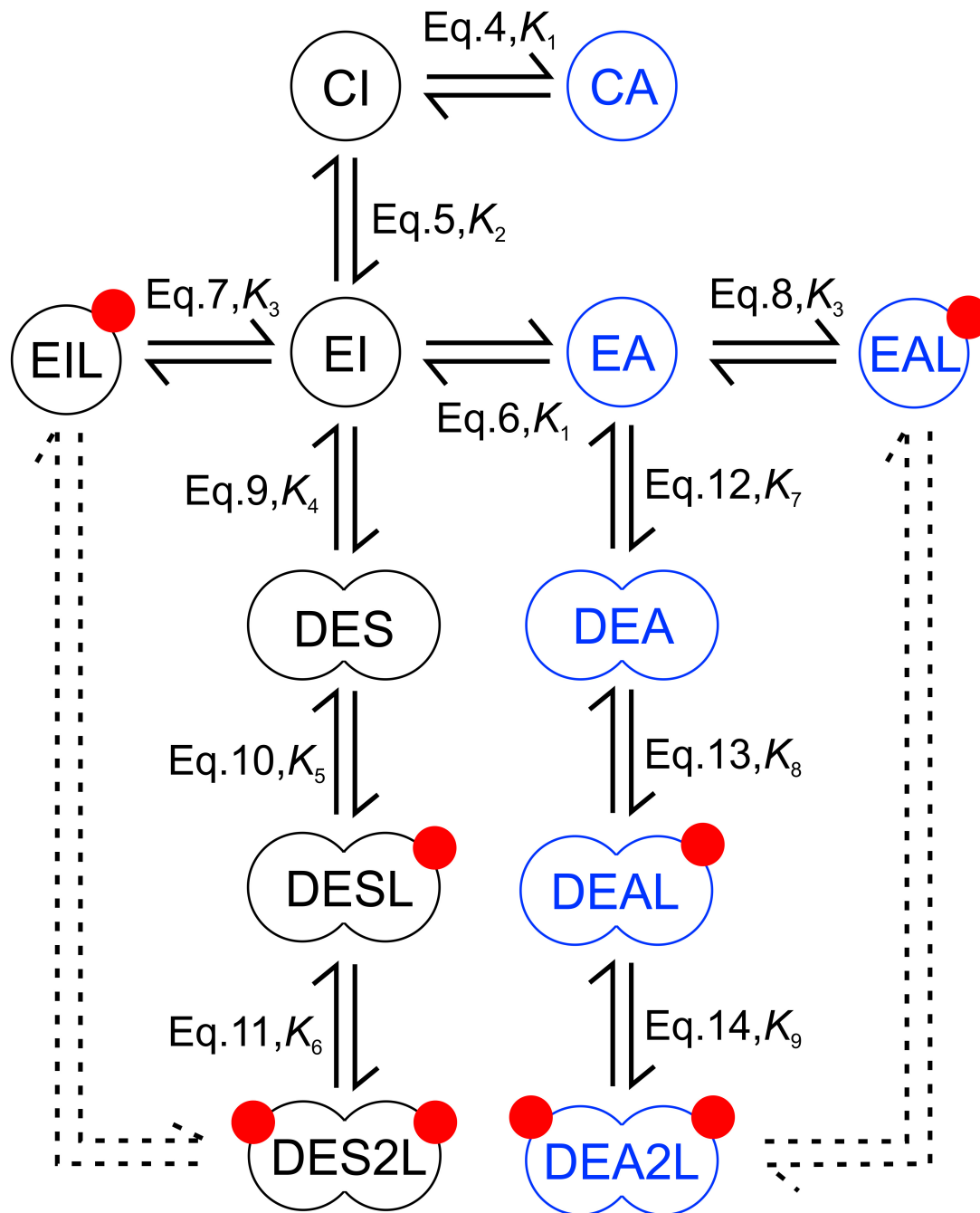


FIGURE 2 | Model for EGF binding involving conformations of the ligand binding and kinase domains. The extracellular part of the receptor is present in either a closed (C) or extended (E) conformation with both of these states coupled to either an active (A) or inactive (I) kinase domain generating four possible monomers (CI, CA – closed extracellular domain with inactive and active kinase domain, respectively; EI, EA – extended extracellular domain with inactive and active kinase domain, respectively). Receptors whose extracellular domain is in the extended conformation can bind EGF (red circles). Liganded species are designated by an ‘L’ at the end of their names. Receptors with extended extracellular domains can form dimers designated by a ‘D’ at the beginning of their names. Monomeric and dimeric species, whose kinase domain is in an active or inactive conformation, are shown in blue and black, respectively. Three different kinds of dimers with inactive, symmetric kinase dimers are present according to their ligand binding state (DES, DESL, DES2L – dimers with inactive, symmetric kinase dimers with 0, 1 and 2 bound EGF, respectively). The same designation principle applies to dimeric species with active, asymmetric kinase dimers (DEA, DEAL, DEA2L). The double arrows (continuous lines) show those transitions, which are explicitly included in describing the equilibrium. The descriptions beside the arrows show the equation and constant describing the equilibrium corresponding to the arrow. The equilibrium of all other conformational changes, ligand binding and dimerization events not explicitly shown in the figure are fully described by the equation set discussed in the main text since the equilibrium constants determine the standard Gibbs energy change of a reaction and consequently the ratio of the equilibrium concentrations of any pairwise selection of species. Although the dashed double arrow labeling the dimerization of liganded monomers is not explicitly included in the model, it is required for determining linkage in the system.

of receptor number constitute the final two equations of the system:

$$[EGF_{bound}] = [EIL] + [EAL] + [DESL] + [DEAL] + 2([DES2L] + [DEA2L]) \quad (15)$$

$$[R_{tot}] = [CI] + [CA] + [EI] + [EA] + [EIL] + [EAL] + 2([DES] + [DESL] + [DES2L] + [DEA] + [DEAL] + [DEA2L]) \quad (16)$$

where R_{tot} is the number of receptors/cell. The unit of ligand dissociation constants in the model is nM, whereas the unit of receptor dissociation constants is number of receptors/cell. Equations (4)–(16), constituting a quadratic equation set containing 13 unknowns (the concentration of the 12 molecular species and $[EGF_{bound}]$), were solved with Mathematica (Wolfram Research, Champaign, IL). The set of roots in which all 13 concentrations were positive was selected as the meaningful solution, which is presented as a Matlab (Mathworks, Natick, MA) file in the **Supplementary Information**.

Control cells and the samples treated with erlotinib or lapatinib were divided into three subpopulations corresponding to low, medium and high expressors of EGFR. In this way there were four cell populations for each experimental condition (the three gated subpopulations and the whole cell population), altogether constituting 12 experimental conditions. The sum of squared deviations between the fitted equations and the experimental data was minimized by an algorithm, which was global in two respects: (1) All 12 data sets were fitted simultaneously with parameters K_2 – K_9 shared between all of them, while K_1 characterizing the conformational equilibrium between the active and inactive KDs was allowed to have three different values for the control, erlotinib- and lapatinib-treated samples. In this way, the 11 free parameters in the model were globally fitted to 156 data points from the 12 data sets. (2) The Global Search algorithm of Matlab was used for finding the global minimum of the norm. In order to define the confidence interval of the fitted parameters the optimization procedure was repeated 100-times.

Fitting of the Model to Equilibrium EGF Binding Data

The data set analyzed previously with the Hill equation was fitted with the model described in the previous section (**Figure 3, Table 2**). The confidence intervals of the fitted parameters are shown in **Supplementary Figure 5**. The model reveals that the inactive conformation of the KD is favored under all experimental conditions in the absence of EGF, with the kinase inhibitors shifting this equilibrium in accordance with their presumed tendency to stabilize one of the kinase structures. In the absence of ligand, the ECD is preferentially in the closed conformation. Monomers with an inactive KD dimerize much less efficiently than monomers harboring an active KD. While the ligand binding affinity of EGFR monomers is in the nanomolar range, the KD exerts significant effects on the affinity and cooperativity of dimers. Dimeric structures with asymmetric kinase dimers exhibit subnanomolar affinity

for the first ligand, but the second EGF binds with a ~ 30 -times lower affinity due to significant negative cooperativity. Dimers with symmetric kinase dimers have an extremely low affinity for the first ligand, but a subnanomolar binding constant is found for the second EGF. The model parameters revealed that the KD is strongly coupled to ligand binding suggesting that its involvement cannot be neglected in analyzing EGF binding data.

Predictions of the Model for Different Molecular Species

The fitted model parameters not only describe the amount of cell-bound EGF, but they also predict the dependence of different receptor species on ligand concentration and receptor expression level. Calculation of the concentration of liganded receptor species revealed that a substantial fraction of EGF binds to monomeric EGFR with inactive KD, while monomers with active KDs do not contribute to ligand binding (**Supplementary Figure 6**). The fraction of EGF bound to monomer receptors decreases with increased EGFR expression, a feature, which could account for increased apparent positive cooperativity at high receptor expression levels. Dimers with both symmetric and asymmetric kinase dimers participate in ligand binding with the relative contribution of the latter increasing as a function of EGFR expression. Due to favoring the active conformation of the KD, erlotinib eliminates the binding of EGF to dimers with symmetric kinase dimers almost completely and significantly decreases the fraction of EGF binding to monomeric receptors. As a result, EGF binds almost exclusively to dimers harboring asymmetric kinase dimers in the presence of erlotinib. The model predicts that monomeric receptors with inactive KDs become the dominant EGF binding species in the presence of lapatinib at all receptor expression levels tested. In accordance with its ability to stabilize the inactive conformation of the kinase, lapatinib significantly decreases the percentage of liganded receptor dimers with active KDs.

Apparent cooperativity of ligand binding, captured by the Hill coefficient, is not only determined by the affinity of receptor dimers for the first and second EGF, but also by linkage. Linkage was determined by considering the equivalence of two pathways leading to the formation of doubly liganded receptor dimers: (i) dimerization of liganded receptor monomers, and (ii) dimerization of unliganded receptor monomers followed by successive binding of two EGFs (**Figure 2**). The dissociation constant for dimerization of a ligand-bound EGFR with inactive KD was found to be $K_4 K_5 K_6 / K_3^2 = 9.3 \cdot 10^5$, which implies negative linkage and decreased homodimerization tendency compared to unliganded monomers with inactive KDs. In contrast, the dissociation constant for homodimerization of liganded receptor monomers with active KD, described by the term $K_7 K_8 K_9 / K_3^2 = 84$, is significantly smaller than the same constant for unliganded monomers with active KD implying positive linkage. Due to the very strong dimerization tendency of unliganded and liganded EGFR with active KDs, EGF-bound receptor monomers with active KDs are predicted not to exist since they immediately dimerize upon their formation.

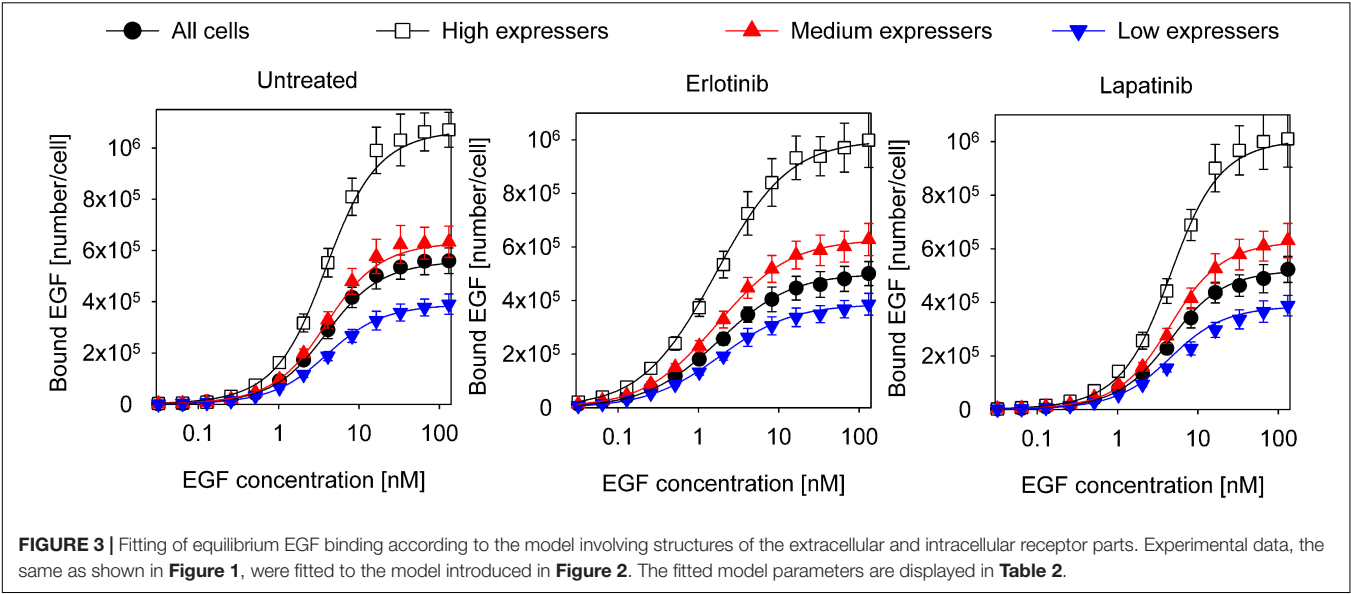


FIGURE 3 | Fitting of equilibrium EGF binding according to the model involving structures of the extracellular and intracellular receptor parts. Experimental data, the same as shown in **Figure 1**, were fitted to the model introduced in **Figure 2**. The fitted model parameters are displayed in **Table 2**.

TABLE 2 | Fitting of the proposed model to the equilibrium binding of EGF.

Parameter	Description	Scope of parameter	Value (95% CI)
K_1	equilibrium constant for inactive and active KD (>1 favors the inactive conformation)	untreated	104 (67–155)
		erlotinib (active KD)	25 (17–38)
		lapatinib (inactive KD)	162 (101–243)
K_2	equilibrium constant for the closed and extended conformations of the ECD (>1 favors the closed conformation)	global	2.9 (1.6–4.4)
K_3	K_d of EGF binding to a monomer with extended ECD	global	1.3 nM (0.8–1.8 nM)
K_4	dimerization of monomers with inactive KD	global	36,900 (15,600–68,700)
K_5	K_d of binding of the first EGF to a dimer with inactive, symmetric kinase dimer	global	95 nM (69–99 nM)
K_6	K_d of binding of the second EGF to a dimer with inactive, symmetric kinase dimer	global	0.45 nM (0.34–0.53 nM)
K_7	dimerization of monomers with active KD	global	480 (86–2,400)
K_8	K_d of binding of the first EGF to a dimer with active, asymmetric kinase dimer	global	0.1 nM (0.02–0.16 nM)
K_9	K_d of binding of the second EGF to a dimer with active, asymmetric kinase dimer	global	2.96 nM (2.93–2.97 nM)

The model involving conformational transitions of the kinase domain (KD) and extracellular domains (ECD) was fitted to equilibrium EGF binding. The measured data points and the fitted lines are shown in **Figure 3**. All twelve curves were fitted globally with the same value of parameters K_2 – K_9 , while three different values of K_1 were used for the three experimental conditions (untreated/erlotinib/lapatinib). The confidence interval was estimated by repeating the fitting 100-times. Constants describing conformational equilibria (K_1 , K_2) express concentration ratios according to equations (4) and (5), therefore they do not have a unit. The unit of equilibrium constants describing dimerizations (K_4 , K_7) is number of receptors/cell.

According to the model calculations only four molecular species bind EGF significantly under any of the experimental conditions: monomeric EGFR with inactive KD, singly liganded receptor dimer with asymmetric KD dimer and both kinds of doubly liganded receptor dimers (with symmetric and asymmetric KD dimers). The singly liganded dimer with asymmetric KD dimer exhibits the highest, subnanomolar affinity for EGF, while binding to the other three molecular species is saturated above 10 nM EGF (**Supplementary Figure 7**). Although there are six different, EGF-binding receptor species (two kinds of monomers with active and inactive KDs, singly and doubly liganded dimers of both kinds), only four of them bind EGF to a significant extent. The EGF-binding affinities of these binding sites is characterized by the dissociation constants in **Table 2** (K_3 , K_5 , K_6 , K_8 , K_9). It is worth pointing out that the ECD is assumed to adopt an extended conformation in all

of these EGF-binding receptor species in the model. Therefore, subtle alterations in the conformations and in the stability of the conformations may account for the different ligand-binding affinities. Along this line, the extended ECD of a receptor monomer exhibits nanomolar EGF affinity (**Table 2**), but this conformation of the ECD in a dimer with asymmetric KD dimers is characterized by subnanomolar EGF affinity, most likely because the dimeric structure stabilizes the extended conformation. The issue of different cooperativities of the two different receptor dimers with asymmetric and symmetric KD dimers will be further considered in the Discussion. Two of the six EGF binding receptor species do not reach significant concentration for the following reason: (i) the liganded receptor monomer with active KD immediately dimerizes; (ii) the singly liganded receptor dimer with symmetric KD dimer immediately binds the second ligand due to the strong positive cooperativity.

Besides confirming the previous conclusions, calculation of the amount of all kinds of receptor species for all experimental conditions also predicts that a substantial fraction of ligand-independent preformed dimers exist (**Supplementary Figure 8**). These constitutive dimers harbor kinase domains in a symmetric configuration. A peculiar prediction of these calculations is the lack of dependence of the total amount of receptor dimers on EGF concentration in the control and lapatinib-treated samples. In contrast, EGF induces a slight increase in the fraction of receptor dimers in erlotinib-treated cells.

EGF-Induced Changes in EGFR Clustering Revealed by Homo-FRET Experiments Are in Agreement With the Model

Although the lack of EGF-dependent recruitment of EGFRs to dimers may sound unexpected, one must bear in mind that the experiments were performed at 4°C, below the phase transition temperature of the plasma membrane, to prevent internalization. In order to confirm the predictions of the model, homo-FRET experiments were performed. Since the donor and the acceptor are spectroscopically identical in homo-FRET, energy migrates in a cluster of such fluorophores (Lidke et al., 2003). Therefore, homo-FRET has already been used extensively for characterizing homoclustering of receptors (Lidke et al., 2003; Yeow and Clayton, 2007; Szabó et al., 2008; Hofman et al., 2010). The extent of energy migration is inversely related to fluorescence anisotropy, the only read-out parameter influenced by homo-FRET. Since anisotropy is not only influenced by homo-FRET, the dependence of anisotropy on the density of fluorophores was utilized to determine the cluster size (the number of fluorophores in a cluster) and the fraction of monomeric, unclustered fluorophores according to a method developed previously (Szabó et al., 2008). Different fluorophore densities were generated by gradual photobleaching of EGFR-GFP.

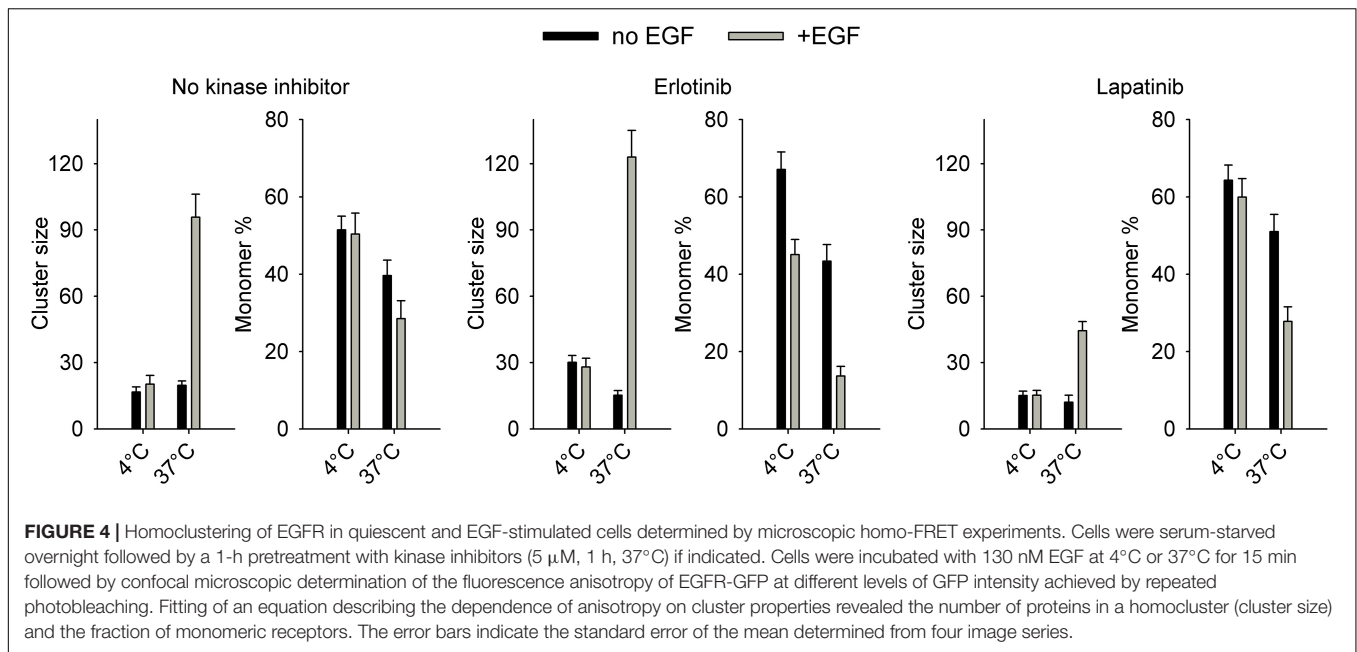
In control cells without pretreatment with kinase inhibitors, EGF did not induce any change in EGFR homoclustering at 4°C (**Figure 4**, **Supplementary Figure 9**). We have shown that 15-min and 60-min incubations were equally ineffective in bringing about changes in EGFR clustering at 4°C (**Supplementary Figure 10**). These results are in accordance with previous reports revealing that tyrosine phosphorylation of EGFR takes place and reaches saturation in ~5 min at 4°C, while effects requiring significant lateral diffusion (e.g., internalization) are blocked below the phase transition temperature of the membrane (Campos-Gonzalez and Glenney, 1991; Moehren et al., 2002). Therefore, all homo-FRET experiments were carried out with cells stimulated with EGF for 15 min. As opposed to no effect at 4°C, EGF induced a substantial increase in the cluster size and in the fraction of clustered receptors at 37°C (**Figure 4**, **Supplementary Figure 9**). The confidence intervals of the estimations are shown in **Supplementary Figure 11**, and representative anisotropy images are displayed in **Supplementary Figure 12**. Erlotinib-pretreated cells responded to EGF with a slight increase in the fraction of clustered receptors at 4°C corroborating this prediction of the model as

well. The EGF-induced increase in EGFR clustering at 37°C was augmented by erlotinib pretreatment in agreement with previous results (Coban et al., 2015). While lapatinib did not alter the lack of EGF-induced clustering at 4°C, it slightly decreased the EGF-elicited clustering of EGFR as evidenced by the smaller cluster size.

While the model describing EGF binding only differentiates between monomers and dimers, homo-FRET detects larger clusters as well (Szabó et al., 2008). Therefore, the fraction of dimeric EGFRs and the fraction of clustered receptors in the homo-FRET experiments are not directly comparable. However, changes in dimerization and large-scale clustering are correlated. EGF-induced changes in large-scale clustering only took place at 4°C in our experiments, similar to the requirement for EGF stimulation to be carried out at room temperature or at 37°C so that the growth factor induces dimerization (Gadella and Jovin, 1995). The remarkable correspondence between the homo-FRET experiments and the EGF-dependent changes in EGFR dimerization, shown in **Supplementary Figure 8**, lends significant support to the model describing ligand binding.

Experimental Conditions Eliminating Positive Apparent Cooperativity of EGF Binding

Since cytoskeletal anchoring has repeatedly been observed to affect ligand binding and activation of EGFR (Wiegant et al., 1986; Lidke et al., 2005; Low-Nam et al., 2011), we tested whether disassembling actin fibers exerts any effect on EGF binding. Latrunculin B treatment disrupted actin fibers and led to a decreased affinity and apparent cooperativity of EGF binding (control cells: $K_d = 4$ nM (3.9–4.1), $n = 1.24$ (1.21–1.26); latrunculin B-treated cells: $K_d = 8.2$ nM (7.9–8.5), $n = 1.03$ (1–1.05); the 95% confidence interval is displayed in the parentheses; **Figure 5A**, **Supplementary Figure 13**). We also tested if induction of nucleation of actin polymerization by jasplakinolide affects EGF binding. The affinity and apparent cooperativity of EGF binding were not altered by the treatment (**Supplementary Figure 14**), most likely as a result of jasplakinolide exerting minimal effects on the overall organization of actin filaments and on the subcortical actin meshwork (**Supplementary Figure 13**). Glycosylation of the ECD has been shown to alter the structure of EGFR significantly (Kaszuba et al., 2015). Tunicamycin treatment successfully deglycosylated EGFR, as evidenced by the decreased molecular weight of the protein (**Supplementary Figure 15**), and led to an even more pronounced reduction in EGF binding affinity and apparent cooperativity than disrupting actin fibers ($K_d = 15$ nM (14.6–15.4), $n = 0.77$ (0.75–0.78); **Figure 5A**). Although the model presented in **Figure 2** was fitted to the EGF binding data of tunicamycin- and latrunculin B-treated cells, the results of the fitting were unreproducible and unreliable. We attribute the failure to two circumstances: (i) Since both conditions compromised cell viability, we could not combine these treatments with kinase inhibitors leading to a low number of data points to be fitted. (ii) The low affinity of EGF binding, especially in the tunicamycin-treated cells, resulted in the lack of saturation. Although fitting the Hill equation to the data



points does not reveal the molecular background of the observed changes, the results still show that both glycosylation and an intact cytoskeleton are required for positive cooperative EGF binding and for maintaining the affinity of the binding site.

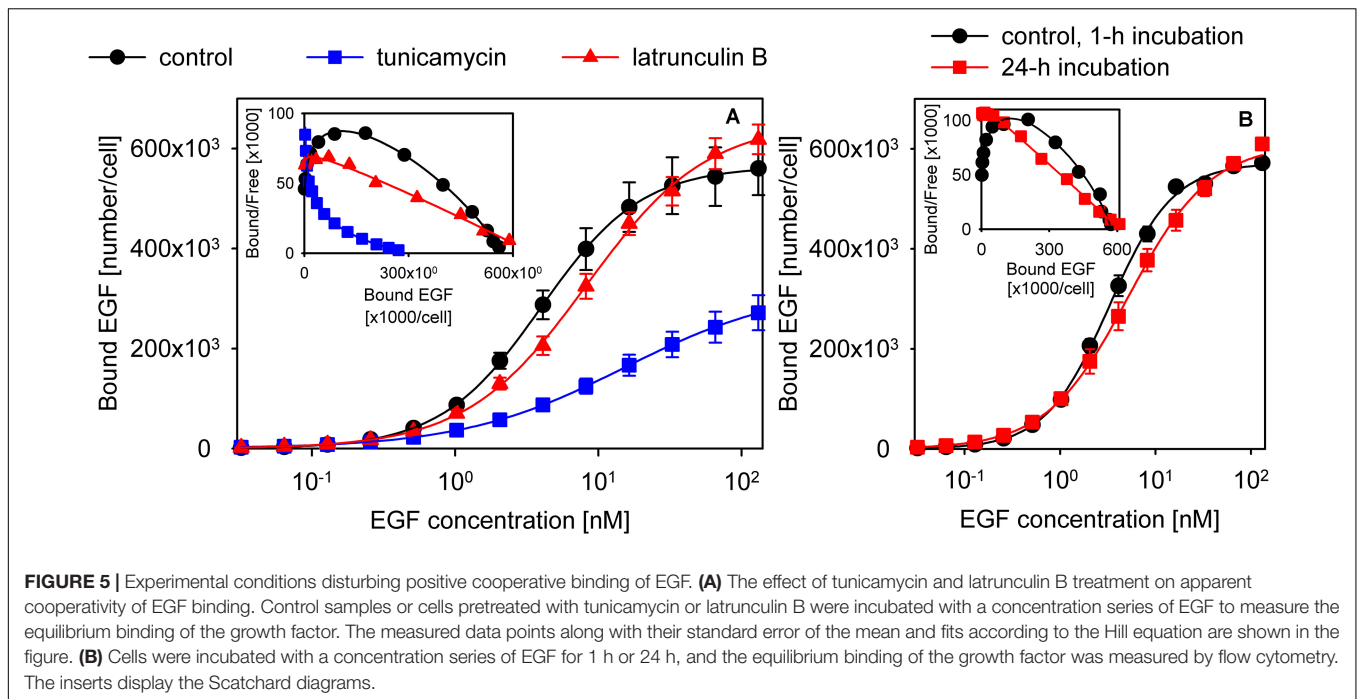
In all of the binding assays reported in the manuscript cells were incubated with EGF on ice for 1 h. The low temperature incubation “freezes” the membrane inhibiting internalization, which would completely invalidate the assumption of equilibrium. However, the low temperature also slows down the rate with which equilibrium binding at the plasma membrane is reached prompting some authors to increase the incubation time to 12–24 h (Macdonald and Pike, 2008; Macdonald-Obermann and Pike, 2018). In order to analyze the effect of a long incubation time EGF binding data obtained with a 1-h and a 24-h incubation with the growth factor were fitted by the Hill equation. The comparison revealed that the long incubation time substantially decreased the apparent cooperativity of EGF binding (1-h incubation: $K_d = 3.4$ nM (3.3–3.6); $n = 1.26$ (1.23–1.29); 24-h incubation: $K_d = 5.2$ nM (5–5.5); $n = 1.02$ (0.99–1.05); **Figure 5B**). Next, we recorded microscopic images of cells incubated with EGF for 1 h or 24 h, and compared the relative amount of fluorescence of TAMRA-EGF from within the intracellular space. Although both incubations were performed on ice, the 24-h incubation led to a significant increase in the intracellular concentration of EGF (**Supplementary Figure 16**). We concluded that long incubation times allow EGF to be internalized even at low temperatures questioning the assumption that equilibrium binding of EGF to membrane receptors is measured under such experimental conditions.

Since measuring the cell-bound fraction of EGF before reaching equilibrium can increase the apparent cooperativity of ligand binding (see **Supplementary Information** for a detailed derivation), it was essential to show that the 1-h incubation time

used in the experiments is sufficient for EGF binding to reach equilibrium. Time-correlated analysis of flow cytometric data enabled us to conclude that EGF binding is saturated in less than 1 h (**Supplementary Figure 17**).

DISCUSSION

In this manuscript we developed and tested a structure-based model for the ligand binding and dimerization of EGFR, whose defining feature is the different dimerization and ligand binding propensity of receptors harboring a kinase in its active or inactive conformation. In order to keep the number of model parameters as low as possible, several kinds of molecular species and processes were neglected, e.g., conformations of the ECD other than the extended and the closed ones, dimerization of monomers with an ECD conformation other than the extended structure, dimers formed only by interactions between the kinase domains, conformational states of the juxta- and transmembrane domains, interactions of the juxtamembrane domain with the membrane and local heterogeneity of receptor concentrations. Oligomerization is not explicitly involved in the model either, although interpretation of the different ligand binding affinities of EGFR dimers harboring active and inactive KDs involves higher-order receptor complexes, a feature of the model to be explained later. Therefore, although the absolute values of the fitted parameters may be inaccurate, the general tendencies and properties have reliably been identified, a conclusion supported by the fact that our experimental data were successfully fitted and that the predictions of the model are in accordance with most published data. Analysis of the fitted model allowed us to reach the following major conclusions: (i) dimers harboring asymmetric and symmetric KD dimers exhibit negative and positive cooperative ligand binding, respectively;



(ii) the homodimerization tendency of erlotinib-stabilized active KDs is higher than that of lapatinib-bound, inactive KDs; (iii) the dimerization tendency of liganded EGFR with active KD is stronger than that of unliganded monomers (positive linkage), while the opposite tendency applies to the inactive KD; (iv) both receptor monomers and dimers contribute to EGF binding with the importance of dimers increasing at high receptor expression levels; (v) A significant amount of preformed, ligand-independent dimers harboring inactive, symmetric KD dimers are present, and the fraction of receptor dimers does not change significantly upon ligand binding. While this latter conclusion may seem to be at odds with common sense, the gel-like state of the plasma membrane at the temperature of the experiments (4°C) most likely prevents diffusion-driven alterations of the monomer-dimer equilibrium in the plasma membrane. This prediction is also in accordance with our homo-FRET experiments and with previous results showing that EGF bound to cells on ice only induces receptor dimerization upon elevation of the temperature to 20°C or 37°C (Gadella and Jovin, 1995). The quantitative model proposed by Macdonald and Pike, neglecting structural transitions of the ECD and different conformations of the KD, predicts that EGF binding leads to a decreased fraction of receptor dimers (see recalculation of the model in the **Supplementary Material**). This feature is the consequence of the lower dimerization propensity of liganded monomers compared to their unliganded counterparts. We believe that predictions of our model are in better agreement with experimental findings than those of the previous model. The fact that our homo-FRET experimental results are in agreement also with the prediction of increased dimerization of EGFRs, whose KD is locked in the active conformation, confirms the major properties of the proposed model. This erlotinib-induced

increase in EGFR dimerization has also been reported by Coban et al. (2015).

According to our model, dimerization of EGFR monomers with active and inactive KDs leads to the formation of dimers harboring asymmetric and symmetric KD dimers, respectively. While the formation of asymmetric KD dimers from the active conformation of the kinase is in accordance with the proposed resemblance of EGFR activation to cyclin-induced activation of cyclin-dependent kinases (Zhang et al., 2006; Kovacs et al., 2015), the structural identity of the other KD dimer is dubious. The assumption of two different KD dimers was required for fitting the measurement data successfully. The hypothesis that the KD dimer other than the asymmetric dimer is identical to symmetric KD dimers is somewhat arbitrary. While symmetric KD dimers have been suggested to contain the kinase in the active conformation (Stamos et al., 2002; Landau et al., 2004), our observation that this dimeric species increased in abundance in the presence of lapatinib (**Supplementary Figure 8**) argues that they contain the kinase in its inactive conformation. While assignment of a specific structure to this KD dimer is arguable based on our experiments, the fact that a KD dimer different from the asymmetric dimer must exist and that this KD dimer is coupled to an ECD whose ligand binding properties are markedly different from the negatively cooperative, high affinity binding site seems certain. We also tested a model in which formation of this dimeric species containing a symmetric kinase dimer began from the “CI” monomer (containing inhibited kinase and closed ECD), but fitting of this model to the experimental data was not successful (data not shown).

Other aspects of the predictions of the proposed model are also in agreement with previous literature data. The fact that a significant fraction of EGF binds to monomeric

receptor species may be the consequence of hindered long-range diffusion in the gel-like membrane, an inherent consequence of the experimental condition, but such a phenomenon has repeatedly been reported previously (Teramura et al., 2006; Szabó et al., 2008; Liu et al., 2012; Vámosi et al., 2019). Coupling of a liganded ECD dimer to both active and inactive KD dimers, a key feature in the proposed model, has been experimentally observed in electron microscopy (Mi et al., 2011). Substantial controversy exists in the literature regarding constitutive, ligand-independent EGFR dimers. While several pieces of evidence point at their existence (Clayton et al., 2007; Szabó et al., 2008; Zanetti-Domingues et al., 2018), their transient nature and dependence on receptor expression levels has also been emphasized (Nagy et al., 2010; Low-Nam et al., 2011). Our model calculations show that such constitutive dimers harbor receptors with symmetric, inactive kinase dimers. This conclusion is in agreement with a recent study showing that mutations introduced into the active, asymmetric kinase dimer interface do not significantly affect the stability of ligand-independent, preformed dimers (Byrne et al., 2020). Due to the very low affinity of these dimeric species for binding of the first ligand, they hardly bind EGF at low ligand concentrations, i.e., the fraction of these preformed dimers is constant in this concentration range of EGF. When they do bind EGF beginning from the 1–10 nM range, they do so with positive cooperativity, a prediction, which is in accordance with previous single-molecule experiments (Teramura et al., 2006). There is a perplexing contradiction regarding the cooperativity of ligand binding in the EGFR system. While negative cooperativity has become widely accepted (Macdonald and Pike, 2008; Alvarado et al., 2010; Martin-Fernandez, 2012), positive cooperativity has also been repeatedly observed (Sherrill and Kyte, 1996; Lemmon et al., 1997; Teramura et al., 2006; Chung et al., 2010; Macdonald-Obermann and Pike, 2018). Our model predicts that the type of apparent cooperativity of EGF binding depends on receptor expression levels, and it is attributable to the different ligand binding properties of receptor dimers with the two different kinase dimers. Our observation and prediction that positive cooperativity increases as a function of receptor expression levels have already been reported (Lemmon et al., 1997). The fact that cooperativity of EGF binding depends on the relative abundance of receptors with active and inactive KDs and on receptor expression levels may account for the inconsistency in the literature in this regard.

Among dimers those harboring an inactive, symmetric kinase dimer are the dominant species in the absence or at low concentrations of EGF, while dimers with active, asymmetric kinase dimers are preferred at high ligand concentrations (**Supplementary Figure 8**). This tendency seems to prevent unintended kinase activation in the absence of stimulation, and to favor initiation of signaling at sufficiently high EGF concentrations. Although the dimerization tendency of unliganded monomers with an inactive KD is weaker than that of unliganded monomers with an active KD, dimers with an inactive KD in the absence or at low concentrations of EGF are favored for the following reasons: (i) the equilibrium between the inactive

and active KDs is shifted toward the inactive conformation (K_1 in **Table 2**); (ii) the binding affinity of dimers with inactive, symmetric kinase dimers for the first ligand is very weak. In contrast, dimers with active, asymmetric KD dimers are favored at high ligand concentrations, which is brought about by the positive linkage between ligand binding and dimer assembly if the KD is in the active conformation and by the inherently stronger dimerization tendency of monomers harboring an active KD.

We identified two conditions, depolymerization of actin filaments and inhibition of glycosylation, which reduced receptor affinity and abolished positive apparent cooperativity of EGF binding. Since the quality of these data did not allow for model fitting, only speculations can be put forward regarding the explanation. Both treatments may inhibit positive apparent cooperativity by reducing the local receptor concentration. Actin depolymerization may achieve this effect by abolishing confinement (Low-Nam et al., 2011), while deglycosylation may reduce the affinity of EGFR to putative raft-like domains or glycolipids (Furukawa et al., 2012). Since deglycosylation has been shown to alter the conformation of EGFR ECD and its orientation relative to the membrane, its affinity for dimerization and ligand binding is expected to be altered (Kaszuba et al., 2015). Since tunicamycin is a general inhibitor of N-glycosylation, it is also possible that the effect of this treatment is attributable to effects on the glycosylation of other proteins.

While the conformations of the extra- and intracellular domains are unlikely to be coupled in monomeric receptors, they can be indirectly linked to each other in dimers or higher order clusters. A possible explanation for the assignment of different EGF affinities to dimers with symmetric and asymmetric KD dimers invoking higher order clusters is provided below. Preformed, unliganded EGFR dimers harbor inactive, symmetric kinase dimers as revealed by the fitting and also supported by literature data (Byrne et al., 2020). Such preformed dimers have been found to form chains or polymers of dimers (Zanetti-Domingues et al., 2018). It is reasonable to assume, as suggested previously, that access of EGF to the ligand binding site of such receptors is blocked explaining their very low affinity for binding the first ligand. Ligand binding must remove these preformed dimers from these receptor polymers since their orientation would not allow cross-phosphorylation to happen. Once they are removed from the receptor polymers to form dimers (not forming larger clusters) (Needham et al., 2016), binding of the second ligand takes place much more easily leading to positive cooperativity. Dimers harboring active kinase domains (asymmetric KD dimers) are not incorporated to dimer chains, therefore the inherent negative cooperativity of the ECD is manifested in their case. Successful fitting of the experimental data using these assumptions implies that the influence of higher-order clusters on the affinity of EGF binding to receptors should not be overlooked.

The proposed model has important implications for interpreting the action of tyrosine kinase inhibitors. These inhibitors not only block the enzymatic activity of the KD, but they also alter the abundance of different molecular species. In particular, EGFR with an active kinase domain has a stronger dimerization tendency than receptors with

inactive kinase domains (Table 2). In addition, they also differ in terms of their propensity to form receptor oligomers as explained in the previous paragraph. Therefore, the effect of kinase inhibitors on EGF binding is determined by how they shift the concentration of different receptor states. Inhibitors stabilizing the active conformation of the kinase (e.g., erlotinib) enhance dimerization, a proposition supported by our homo-FRET experiments and previous data (Lichtner et al., 2001; Anido et al., 2003; Coban et al., 2015). In contrast, lapatinib, stabilizing the inactive conformation of the kinase, does not bring about such an increase in receptor dimerization in agreement with previous data (Bublil et al., 2010). Since the kinase in the majority of receptors is already in the inactive conformation in the absence of inhibitors (Table 2), the effect of lapatinib, stabilizing the inactive conformation of the KD, on the monomer/dimer equilibrium is much less pronounced than that of erlotinib. In light of the effect of kinase inhibitors on the monomer/dimer equilibrium, inhibitors stabilizing the inactive conformation of the kinase seem to be more potent and safer from a theoretical point of view.

In conclusion, the model developed in the current manuscript provides a comprehensive view on the molecular transitions taking place upon EGF binding to its receptor. Although different experimental approaches can capture distinct steps of the ligand-induced alterations in the conformation and assembly of receptor dimers, practically none of them can decipher all of them in a quantitative manner. Global analysis of EGF binding equilibria allowed us to generate a model providing insight into most steps of the activation pathway at a pseudo-molecular level.

DATA AVAILABILITY STATEMENT

All datasets presented in this study are included in the article/Supplementary Material.

REFERENCES

- Alvarado, D., Klein, D. E., and Lemmon, M. A. (2010). Structural basis for negative cooperativity in growth factor binding to an EGF receptor. *Cell* 142, 568–579. doi: 10.1016/j.cell.2010.07.015
- Anido, J., Matar, P., Albanell, J., Guzman, M., Rojo, F., Arribas, J., et al. (2003). ZD1839, a specific epidermal growth factor receptor (EGFR) tyrosine kinase inhibitor, induces the formation of inactive EGFR/HER2 and EGFR/HER3 heterodimers and prevents heregulin signaling in HER2-overexpressing breast cancer cells. *Clin. Cancer Res.* 9, 1274–1283.
- Bellot, F., Moolenaar, W., Kris, R., Mirakhur, B., Verlaan, I., Ullrich, A., et al. (1990). High-affinity epidermal growth factor binding is specifically reduced by a monoclonal antibody, and appears necessary for early responses. *J. Cell. Biol.* 110, 491–502. doi: 10.1083/jcb.110.2.491
- Bessman, N. J., Bagchi, A., Ferguson, K. M., and Lemmon, M. A. (2014). Complex relationship between ligand binding and dimerization in the epidermal growth factor receptor. *Cell Rep.* 9, 1306–1317. doi: 10.1016/j.celrep.2014.10.010
- Brock, R., Hamelers, I. H., and Jovin, T. M. (1999). Comparison of fixation protocols for adherent cultured cells applied to a GFP fusion protein of the epidermal growth factor receptor. *Cytometry* 35, 353–362. doi: 10.1002/(sici)1097-0320(19990401)35:4<353::aid-cyto8>3.0.co;2-m
- Bublil, E. M., Pines, G., Patel, G., Fruhwirth, G., Ng, T., and Yarden, Y. (2010). Kinase-mediated quasi-dimers of EGFR. *FASEB J.* 24, 4744–4755. doi: 10.1096/fj.10-166199

AUTHOR CONTRIBUTIONS

TH carried out and analyzed most of the experiments and wrote the initial version of the manuscript. TV and IR contributed to the flow cytometric and confocal microscopic experiments, respectively. TK performed part of the experiments with compounds modifying actin polymerization and protein glycosylation. JS advised about the flow cytometric experiments and revised the manuscript. PN conceived, supervised and funded the project, developed the mathematical model and revised the manuscript. All authors contributed to the article and approved the submitted version.

FUNDING

The work was supported by research grants from the National Research, Development and Innovation Office, Hungary (K120302, GINOP-2.3.2-15-2016-00020, GINOP-2.3.2-15-2016-00044, EFOP-3.6.3-VEKOP-16-2017-00009).

ACKNOWLEDGMENTS

We would like to express our gratitude to Thomas M. Jovin (Max Planck Institute for Biophysical Chemistry, Göttingen) for his mentorship and scientific advice during the initial stages of this project.

SUPPLEMENTARY MATERIAL

The Supplementary Material for this article can be found online at: <https://www.frontiersin.org/articles/10.3389/fcell.2020.00776/full#supplementary-material>

- Byrne, P. O., Hristova, K., and Leahy, D. J. (2020). Ligand-independent EGFR oligomers do not rely on the active state asymmetric kinase dimer. *bioRxiv*. [Preprint]. 2020.04.24.056077.
- Campos-Gonzalez, R., and Glenney, J. R. Jr. (1991). Temperature-dependent tyrosine phosphorylation of microtubule-associated protein kinase in epidermal growth factor-stimulated human fibroblasts. *Cell Regul.* 2, 663–673. doi: 10.1091/mbc.2.8.663
- Chung, I., Akita, R., Vandlen, R., Toomre, D., Schlessinger, J., and Mellman, I. (2010). Spatial control of EGF receptor activation by reversible dimerization on living cells. *Nature* 464, 783–787. doi: 10.1038/nature08827
- Clayton, A. H., Tavarnesi, M. L., and Johns, T. G. (2007). Unligated epidermal growth factor receptor forms higher order oligomers within microclusters on A431 cells that are sensitive to tyrosine kinase inhibitor binding. *Biochemistry* 46, 4589–4597. doi: 10.1021/bi700002b
- Coban, O., Zanetti-Dominguez, L. C., Matthews, D. R., Rolfe, D. J., Weitsman, G., Barber, P. R., et al. (2015). Effect of phosphorylation on EGFR dimer stability probed by single-molecule dynamics and FRET/FLIM. *Biophys. J.* 108, 1013–1026. doi: 10.1016/j.bpj.2015.01.005
- Defize, L. H., Arndt-Jovin, D. J., Jovin, T. M., Boonstra, J., Meisenhelder, J., Hunter, T., et al. (1988). A431 cell variants lacking the blood group A antigen display increased high affinity epidermal growth factor-receptor number, protein-tyrosine kinase activity, and receptor turnover. *J. Cell. Biol.* 107, 939–949. doi: 10.1083/jcb.107.3.939

- Diwanji, D., Thaker, T., and Jura, N. (2019). More than the sum of the parts: toward full-length receptor tyrosine kinase structures. *IUBMB Life* 71, 706–720. doi: 10.1002/iub.2060
- Fleishman, S. J., Schlessinger, J., and Ben-Tal, N. A. (2002). putative molecular-activation switch in the transmembrane domain of erbB2. *Proc. Natl. Acad. Sci. U.S.A.* 99, 15937–15940. doi: 10.1073/pnas.252640799
- Freed, D. M., Bessman, N. J., Kiyatkin, A., Salazar-Cavazos, E., Byrne, P. O., Moore, J. O., et al. (2017). EGFR ligands differentially stabilize receptor dimers to specify signaling kinetics. *Cell* 171, 683–695.e18. doi: 10.1016/j.cell.2017.09.017
- Furukawa, K., Ohkawa, Y., Yamauchi, Y., Hamamura, K., Ohmi, Y., and Furukawa, K. (2012). Fine tuning of cell signals by glycosylation. *J. Biochem.* 151, 573–578. doi: 10.1093/jb/mvs043
- Gadella, T. W. Jr., and Jovin, T. M. (1995). Oligomerization of epidermal growth factor receptors on A431 cells studied by time-resolved fluorescence imaging microscopy. A stereochemical model for tyrosine kinase receptor activation. *J. Cell. Biol.* 129, 1543–1558. doi: 10.1083/jcb.129.6.1543
- Garrett, T. P., McKern, N. M., Lou, M., Elleman, T. C., Adams, T. E., Lovrecz, G. O., et al. (2002). Crystal structure of a truncated epidermal growth factor receptor extracellular domain bound to transforming growth factor alpha. *Cell* 110, 763–773. doi: 10.1016/s0092-8674(02)00940-6
- Hofman, E. G., Bader, A. N., Voortman, J., van den Heuvel, D. J., Sigismund, S., Verkleij, A. J., et al. (2010). Ligand-induced EGF receptor oligomerization is kinase-dependent and enhances internalization. *J. Biol. Chem.* 285, 39481–39489. doi: 10.1074/jbc.m110.164731
- Jovin, T. M. (1979). “Fluorescence polarization and energy transfer: theory and application,” in *Flow Cytometry and Sorting*, eds M. Melamed, P. Mullaney, and M. Mendelsohn, (New York, NY: John Wiley & Sons), 137–165.
- Jovin, T. M. (2014). Pinning down the EGF receptor. *Biophys. J.* 107, 2486–2488. doi: 10.1016/j.bpj.2014.10.037
- Jura, N., Endres, N. F., Engel, K., Deindl, S., Das, R., Lamers, M. H., et al. (2009). Mechanism for activation of the EGF receptor catalytic domain by the juxtamembrane segment. *Cell* 137, 1293–1307. doi: 10.1016/j.cell.2009.04.025
- Kaplan, M., Narasimhan, S., de Heus, C., Mance, D., van Doorn, S., Houben, K., et al. (2016). EGFR dynamics change during activation in native membranes as revealed by NMR. *Cell* 167, 1241–1251.e11. doi: 10.1016/j.cell.2016.10.038
- Kaszuba, K., Grzybek, M., Orlowski, A., Danne, R., Rog, T., Simons, K., et al. (2015). N-glycosylation as determinant of epidermal growth factor receptor conformation in membranes. *Proc. Natl. Acad. Sci. U.S.A.* 112, 4334–4339. doi: 10.1073/pnas.1503262112
- Klein, P., Mattoon, D., Lemmon, M. A., and Schlessinger, J. A. (2004). structure-based model for ligand binding and dimerization of EGF receptors. *Proc. Natl. Acad. Sci. U.S.A.* 101, 929–934. doi: 10.1073/pnas.0307285101
- Kovacs, E., Zorn, J. A., Huang, Y., Barros, T., and Kuriyan, J. A. (2015). structural perspective on the regulation of the epidermal growth factor receptor. *Annu. Rev. Biochem.* 84, 739–764. doi: 10.1146/annurev-biochem-060614-034402
- Kovács, T., Batta, G., Hajdu, T., Szabó, A., Váradi, T., Zákány, F., et al. (2016). The dipole potential modifies the clustering and ligand binding affinity of ErbB proteins and their signaling efficiency. *Sci. Rep.* 6:35850.
- Kremers, G. J., and Goedhart, J. (2009). “Visible fluorescent proteins for FRET,” in *Laboratory Techniques in Biochemistry and Molecular Biology*, ed. T. W. J. Gadella, Vol. 33 (Amsterdam: Elsevier), 171–223. doi: 10.1016/s0075-7535(08)00005-3
- Landau, M., Fleishman, S. J., and Ben-Tal, N. A. (2004). putative mechanism for downregulation of the catalytic activity of the EGF receptor via direct contact between its kinase and C-terminal domains. *Structure* 12, 2265–2275. doi: 10.1016/j.str.2004.10.006
- Lemmon, M. A. (2009). Ligand-induced ErbB receptor dimerization. *Exp. Cell Res.* 315, 638–648. doi: 10.1016/j.yexcr.2008.10.024
- Lemmon, M. A., Bu, Z., Ladbury, J. E., Zhou, M., Pinchasi, D., Lax, I., et al. (1997). Two EGF molecules contribute additively to stabilization of the EGFR dimer. *EMBO J.* 16, 281–294. doi: 10.1093/emboj/16.2.281
- Lichter, R. B., Menrad, A., Sommer, A., Klar, U., and Schneider, M. R. (2001). Signaling-inactive epidermal growth factor receptor/ligand complexes in intact carcinoma cells by quinazoline tyrosine kinase inhibitors. *Cancer Res.* 61, 5790–5795.
- Lidke, D. S., Lidke, K. A., Rieger, B., Jovin, T. M., and Arndt-Jovin, D. J. (2005). Reaching out for signals: filopodia sense EGF and respond by directed retrograde transport of activated receptors. *J. Cell. Biol.* 170, 619–626.
- Lidke, D. S., Nagy, P., Barisas, B. G., Heintzmann, R., Post, J. N., Lidke, K. A., et al. (2003). Imaging molecular interactions in cells by dynamic and static fluorescence anisotropy (rFLIM and emFRET). *Biochem. Soc. Trans.* 31(Pt 5), 1020–1027. doi: 10.1042/bst0311020
- Liu, P., Cleveland, T. E. IV, Bouyain, S., Byrne, P. O., Longo, P. A., and Leahy, D. J. (2012). A single ligand is sufficient to activate EGFR dimers. *Proc. Natl. Acad. Sci. U.S.A.* 109, 10861–10866. doi: 10.1073/pnas.1201114109
- Low-Nam, S. T., Lidke, K. A., Cutler, P. J., Roovers, R. C., van Bergen En Henegouwen, P. M., Wilson, B. S., et al. (2011). ErbB1 dimerization is promoted by domain co-confinement and stabilized by ligand binding. *Nat. Struct. Mol. Biol.* 18, 1244–1249. doi: 10.1038/nsmb.2135
- Macdonald, J. L., and Pike, L. J. (2008). Heterogeneity in EGF-binding affinities arises from negative cooperativity in an aggregating system. *Proc. Natl. Acad. Sci. U.S.A.* 105, 112–117. doi: 10.1073/pnas.0707080105
- Macdonald-Obermann, J. L., and Pike, L. J. (2018). Allosteric regulation of epidermal growth factor (EGF) receptor ligand binding by tyrosine kinase inhibitors. *J. Biol. Chem.* 293, 13401–13414. doi: 10.1074/jbc.ra118.004139
- Martin-Fernandez, M. L. (2012). Human epidermal growth factor receptor (HER1) aligned on the plasma membrane adopts key features of *Drosophila* EGFR asymmetry. *Biochem. Soc. Trans.* 40, 184–188. doi: 10.1042/bst20110692
- Mi, L. Z., Lu, C., Li, Z., Nishida, N., Walz, T., and Springer, T. A. (2011). Simultaneous visualization of the extracellular and cytoplasmic domains of the epidermal growth factor receptor. *Nat. Struct. Mol. Biol.* 18, 984–989.
- Moehren, G., Markevich, N., Demin, O., Kiyatkin, A., Goryanin, I., Hoek, J. B., et al. (2002). Temperature dependence of the epidermal growth factor receptor signaling network can be accounted for by a kinetic model. *Biochemistry* 41, 306–320. doi: 10.1021/bi011506c
- Moriki, T., Maruyama, H., and Maruyama, I. N. (2001). Activation of preformed EGFR receptor dimers by ligand-induced rotation of the transmembrane domain. *J. Mol. Biol.* 311, 1011–1026. doi: 10.1006/jmbi.2001.4923
- Nagy, P., Claus, J., Jovin, T. M., and Arndt-Jovin, D. J. (2010). Distribution of resting and ligand-bound ErbB1 and ErbB2 receptor tyrosine kinases in living cells using number and brightness analysis. *Proc. Natl. Acad. Sci. U.S.A.* 107, 16524–16529. doi: 10.1073/pnas.1002642107
- Needham, S. R., Roberts, S. K., Arkhipov, A., Mysore, V. P., Tynan, C. J., Zanetti-Domingues, L. C., et al. (2016). EGFR oligomerization organizes kinase-active dimers into competent signalling platforms. *Nat. Commun.* 7:13307.
- Ogiso, H., Ishitani, R., Nureki, O., Fukai, S., Yamanaka, M., Kim, J. H., et al. (2002). Crystal structure of the complex of human epidermal growth factor and receptor extracellular domains. *Cell* 110, 775–787.
- Özcan, F., Klein, P., Lemmon, M. A., Lax, I., and Schlessinger, J. (2006). On the nature of low- and high-affinity EGF receptors on living cells. *Proc. Natl. Acad. Sci. U.S.A.* 103, 5735–5740. doi: 10.1073/pnas.0601469103
- Pike, L. J. (2012). Negative co-operativity in the EGF receptor. *Biochem. Soc. Trans.* 40, 15–19. doi: 10.1042/bst20110610
- Runnels, L. W., and Scarlata, S. F. (1995). Theory and application of fluorescence homotransfer to melittin oligomerization. *Biophys. J.* 69, 1569–1583. doi: 10.1016/s0006-3495(95)80030-5
- Shan, Y., Eastwood, M. P., Zhang, X., Kim, E. T., Arkhipov, A., Dror, R. O., et al. (2012). Oncogenic mutations counteract intrinsic disorder in the EGFR kinase and promote receptor dimerization. *Cell* 149, 860–870. doi: 10.1016/j.cell.2012.02.063
- Sherrill, J. M., and Kyte, J. (1996). Activation of epidermal growth factor receptor by epidermal growth factor. *Biochemistry* 35, 5705–5718. doi: 10.1021/bi9602268
- Stamos, J., Sliwkowski, M. X., and Eigenbrot, C. (2002). Structure of the epidermal growth factor receptor kinase domain alone and in complex with a 4-anilinoquinazoline inhibitor. *J. Biol. Chem.* 277, 46265–46272. doi: 10.1074/jbc.m207135200
- Szabó, A., Horváth, G., Szöllösi, J., and Nagy, P. (2008). Quantitative characterization of the large-scale association of ErbB1 and ErbB2 by flow cytometric homo-FRET measurements. *Biophys. J.* 95, 2086–2096. doi: 10.1529/biophysj.108.133371
- Teramura, Y., Ichinose, J., Takagi, H., Nishida, K., Yanagida, T., and Sako, Y. (2006). Single-molecule analysis of epidermal growth factor binding on the surface of living cells. *EMBO J.* 25, 4215–4222. doi: 10.1038/sj.emboj.7601308
- Valley, C. C., Arndt-Jovin, D. J., Karedla, N., Steinkamp, M. P., Chizhik, A. I., Hlavacek, W. S., et al. (2015). Enhanced dimerization drives ligand-independent

- activity of mutant epidermal growth factor receptor in lung cancer. *Mol. Biol. Cell.* 26, 4087–4099. doi: 10.1091/mbc.e15-05-0269
- Vámosi, G., Friedlander-Brock, E., Ibrahim, S. M., Brock, R., Szöllösi, J., and Vereb, G. (2019). EGF receptor stalls upon activation as evidenced by complementary fluorescence correlation spectroscopy and fluorescence recovery after photobleaching measurements. *Int. J. Mol. Sci.* 20:3370. doi: 10.3390/ijms20133370
- Volkmer, A., Subramaniam, V., Birch, D. J., and Jovin, T. M. (2000). One- and two-photon excited fluorescence lifetimes and anisotropy decays of green fluorescent proteins. *Biophys. J.* 78, 1589–1598. doi: 10.1016/s0006-3495(00)76711-7
- Wagner, M. J., Stacey, M. M., Liu, B. A., and Pawson, T. (2013). Molecular mechanisms of SH2- and PTB-domain-containing proteins in receptor tyrosine kinase signaling. *Cold Spring Harb. Perspect. Biol.* 5:a008987. doi: 10.1101/cshperspect.a008987
- Wiegant, F. A., Blok, F. J., Defize, L. H., Linnemans, W. A., Verkley, A. J., and Boonstra, J. (1986). Epidermal growth factor receptors associated to cytoskeletal elements of epidermoid carcinoma (A431) cells. *J. Cell. Biol.* 103, 87–94. doi: 10.1083/jcb.103.1.87
- Wood, E. R., Truesdale, A. T., McDonald, O. B., Yuan, D., Hassell, A., Dickerson, S. H., et al. (2004). A unique structure for epidermal growth factor receptor bound to GW572016 (Lapatinib): relationships among protein conformation, inhibitor off-rate, and receptor activity in tumor cells. *Cancer Res.* 64, 6652–6659. doi: 10.1158/0008-5472.can-04-1168
- Wyman, J., and Gill, S. J. (1990). *Binding and Linkage. Functional Chemistry of Biological Macromolecules*. Mill Valley, CA: University Science Books.
- Yang, F., Moss, L. G., and Phillips, G. N. Jr. (1996). The molecular structure of green fluorescent protein. *Nat. Biotechnol.* 14, 1246–1251.
- Yarden, Y., and Sliwkowski, M. X. (2001). Untangling the ErbB signalling network. *Nat. Rev. Mol. Cell. Biol.* 2, 127–137. doi: 10.1038/35052073
- Yates, A., Chan, C. C., Callard, R. E., George, A. J., and Stark, J. (2001). An approach to modelling in immunology. *Brief Bioinform.* 2, 245–257. doi: 10.1093/bib/2.3.245
- Yeow, E. K., and Clayton, A. H. (2007). Enumeration of oligomerization states of membrane proteins in living cells by homo-FRET spectroscopy and microscopy: theory and application. *Biophys. J.* 92, 3098–3104. doi: 10.1529/biophysj.106.099424
- Zákány, F., Kovács, T., Panyi, G., and Varga, Z. (2020). Direct and indirect cholesterol effects on membrane proteins with special focus on potassium channels. *Biochim. Biophys. Acta Mol. Cell. Biol. Lipids* 1865:158706. doi: 10.1016/j.bbalip.2020.158706
- Zanetti-Domingues, L. C., Korovesis, D., Needham, S. R., Tynan, C. J., Sagawa, S., Roberts, S. K., et al. (2018). The architecture of EGFR's basal complexes reveals autoinhibition mechanisms in dimers and oligomers. *Nat. Commun.* 9:4325.
- Zhang, J., Yang, P. L., and Gray, N. S. (2009). Targeting cancer with small molecule kinase inhibitors. *Nat. Rev. Cancer* 9, 28–39. doi: 10.1038/nrc2559
- Zhang, X., Gureasko, J., Shen, K., Cole, P. A., and Kuriyan, J. (2006). An allosteric mechanism for activation of the kinase domain of epidermal growth factor receptor. *Cell* 125, 1137–1149. doi: 10.1016/j.cell.2006.05.013
- Ziomkiewicz, I., Loman, A., Klement, R., Fritsch, C., Klymchenko, A. S., Bunt, G., et al. (2013). Dynamic conformational transitions of the EGF receptor in living mammalian cells determined by FRET and fluorescence lifetime imaging microscopy. *Cytom. A* 83, 794–805. doi: 10.1002/cyto.a.22311

Conflict of Interest: The authors declare that the research was conducted in the absence of any commercial or financial relationships that could be construed as a potential conflict of interest.

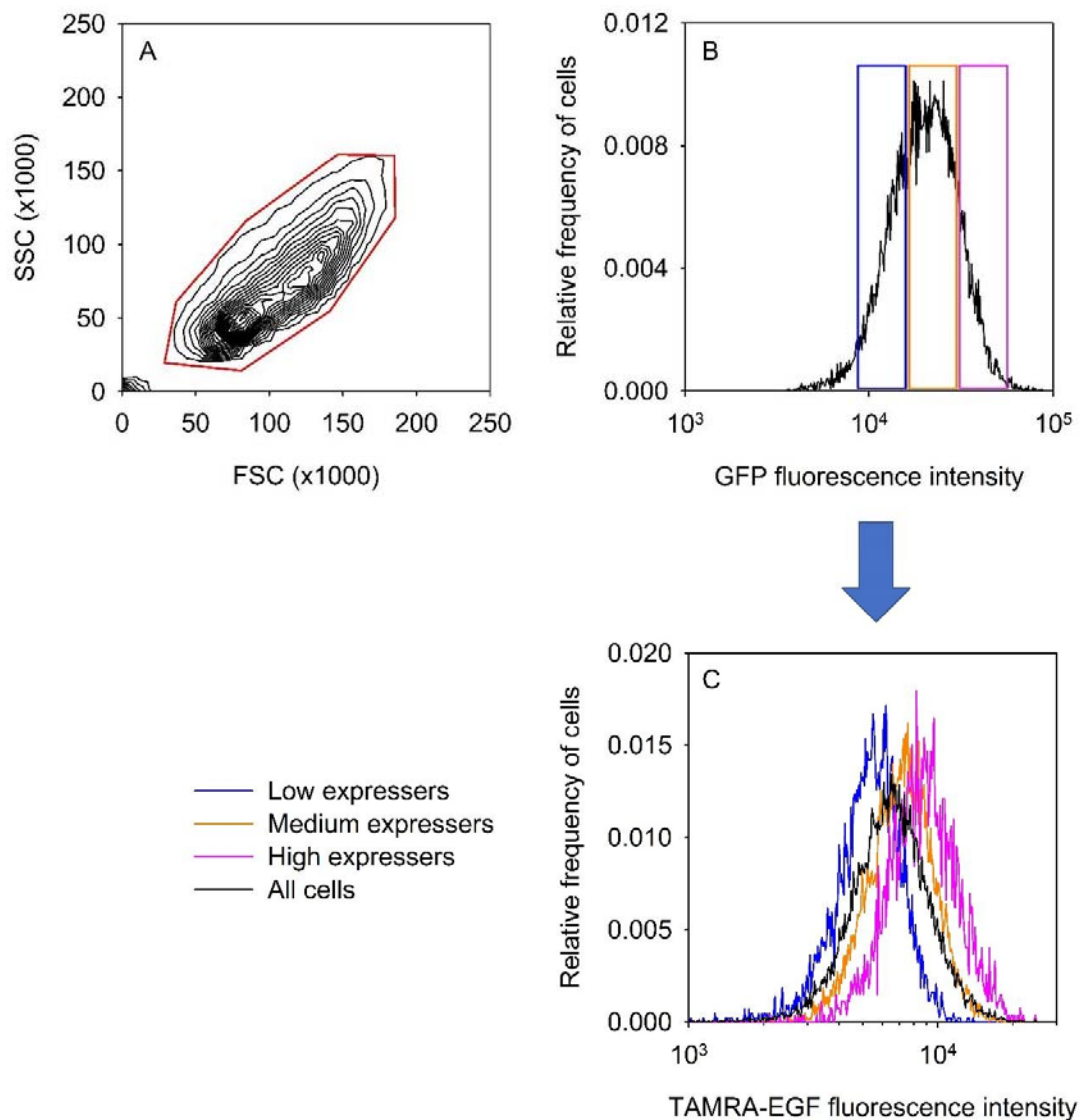
Copyright © 2020 Hajdu, Váradi, Rebenku, Kovács, Szöllösi and Nagy. This is an open-access article distributed under the terms of the Creative Commons Attribution License (CC BY). The use, distribution or reproduction in other forums is permitted, provided the original author(s) and the copyright owner(s) are credited and that the original publication in this journal is cited, in accordance with accepted academic practice. No use, distribution or reproduction is permitted which does not comply with these terms.

Supplementary Material

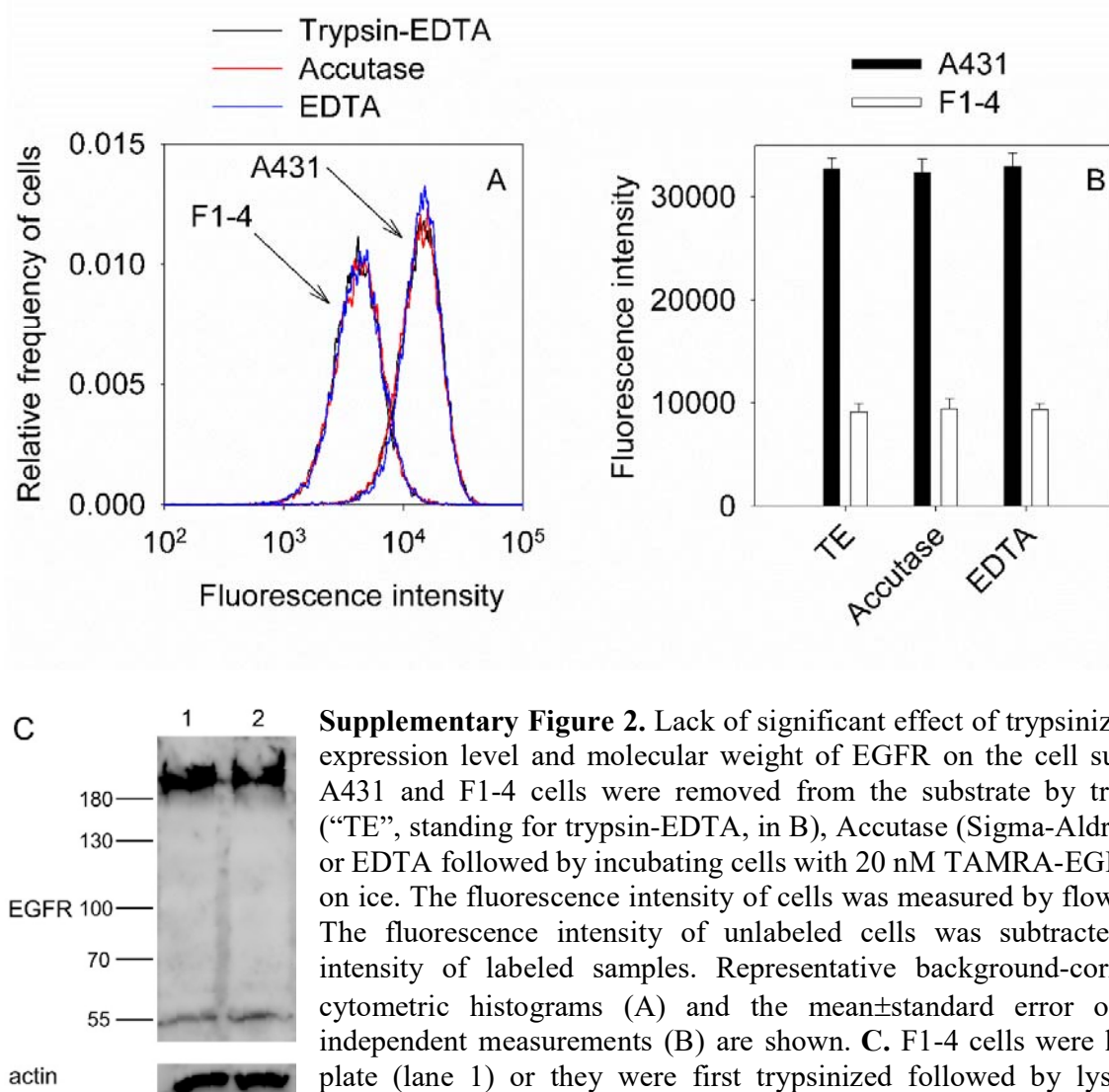
Comprehensive model for epidermal growth factor receptor ligand binding involving conformational states of the extracellular and the kinase domains

**Tímea Hajdu, Tímea Váradi, István Rebenku, Tamás Kovács, János Szöllősi,
Peter Nagy**

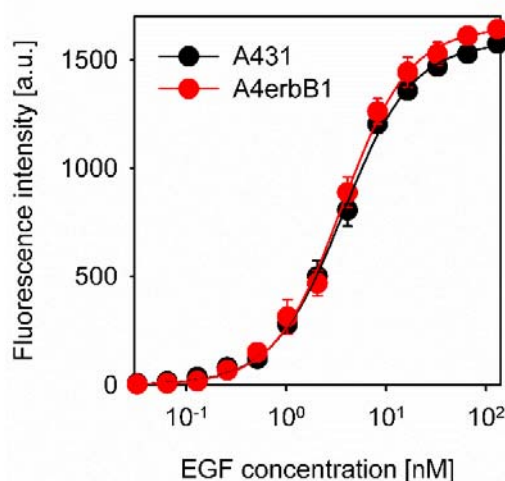
1 Supplementary figures



Supplementary Figure 1. Principle of selecting cell subpopulations with different levels of EGFR expression. Intact cells were selected by gating on the forward scatter (FSC) vs. side-scatter (SSC) contour plot. The selected cells are within the red polygon gate (A). The GFP fluorescence intensity histogram of these cells was further gated dividing the cells into high, medium and low expressers of EGFR-GFP (purple, orange and blue markers, respectively, panel B). The fluorescence intensity of TAMRA-EGF, representing cell-bound EGF, was separately plotted for the four cell populations followed by determining the mean of each histogram (C). The mean TAMRA-EGF fluorescence intensities were converted to the number of cell-bound EGF molecules by equating the maximum TAMRA-EGF fluorescence intensity (taken from fitting the Hill equation to the EGF concentration dependence of TAMRA-EGF fluorescence) with the number of EGFR/cell determined by flow cytometric calibration with Qifikit.

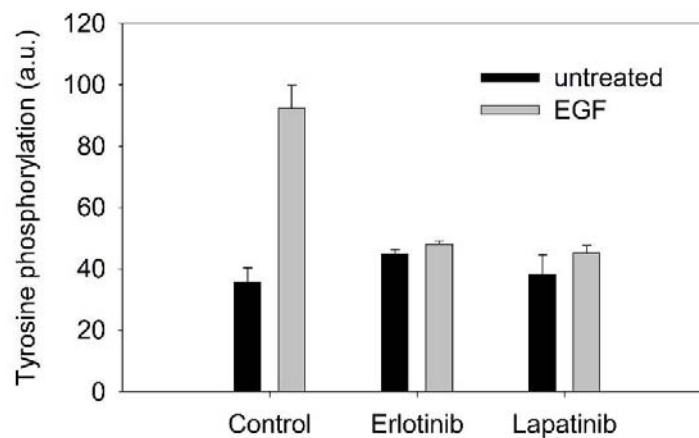
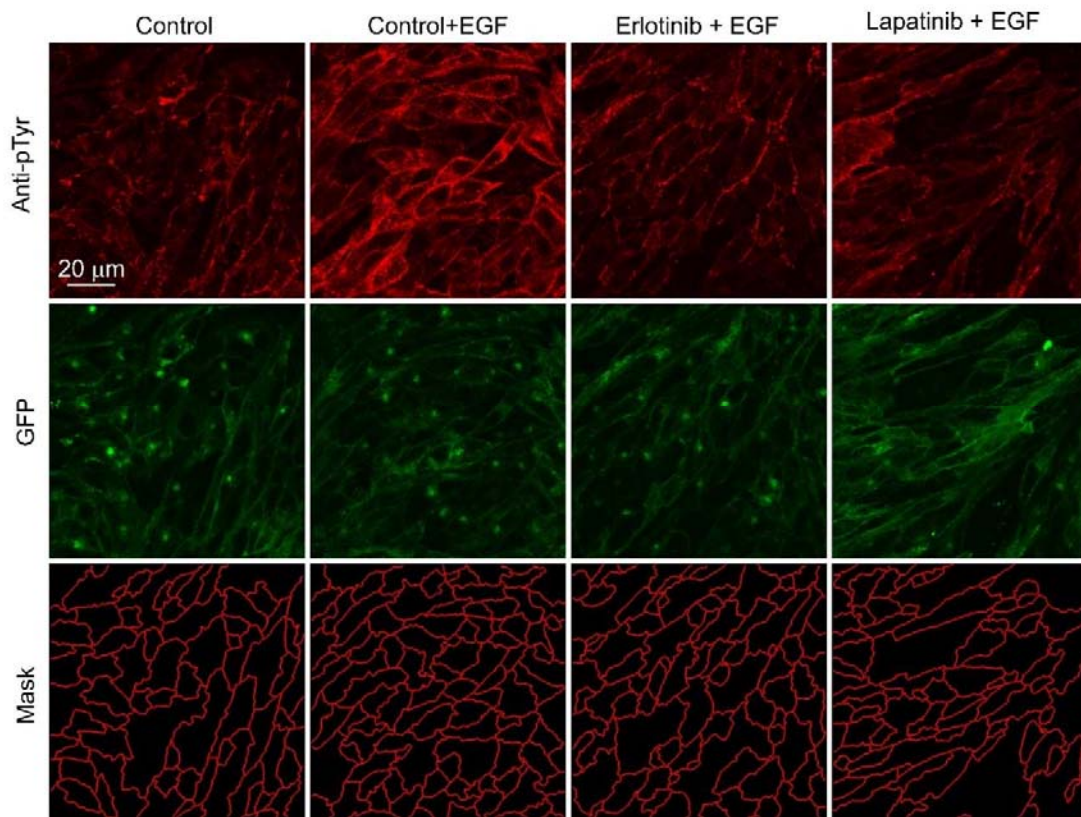


Supplementary Figure 2. Lack of significant effect of trypsinization on the expression level and molecular weight of EGFR on the cell surface. **A-B.** A431 and F1-4 cells were removed from the substrate by trypsinization (“TE”, standing for trypsin-EDTA, in B), Accutase (Sigma-Aldrich, A6964) or EDTA followed by incubating cells with 20 nM TAMRA-EGF for 60 min on ice. The fluorescence intensity of cells was measured by flow cytometry. The fluorescence intensity of unlabeled cells was subtracted from the intensity of labeled samples. Representative background-corrected flow cytometric histograms (A) and the mean \pm standard error of the three independent measurements (B) are shown. **C.** F1-4 cells were lysed on the plate (lane 1) or they were first trypsinized followed by lysis (lane 2). Proteins were separated based on molecular weight on a 7% polyacrylamide gel followed by Western blotting. The membranes were labeled with an anti-EGFR antibody (clone F4, Sigma-Aldrich; top image) or with an anti-actin antibody (clone AC40, Sigma-Aldrich; bottom image) followed by enhanced chemiluminescence to visualize the bands. The numbers beside the blots display the molecular weight in kDa.

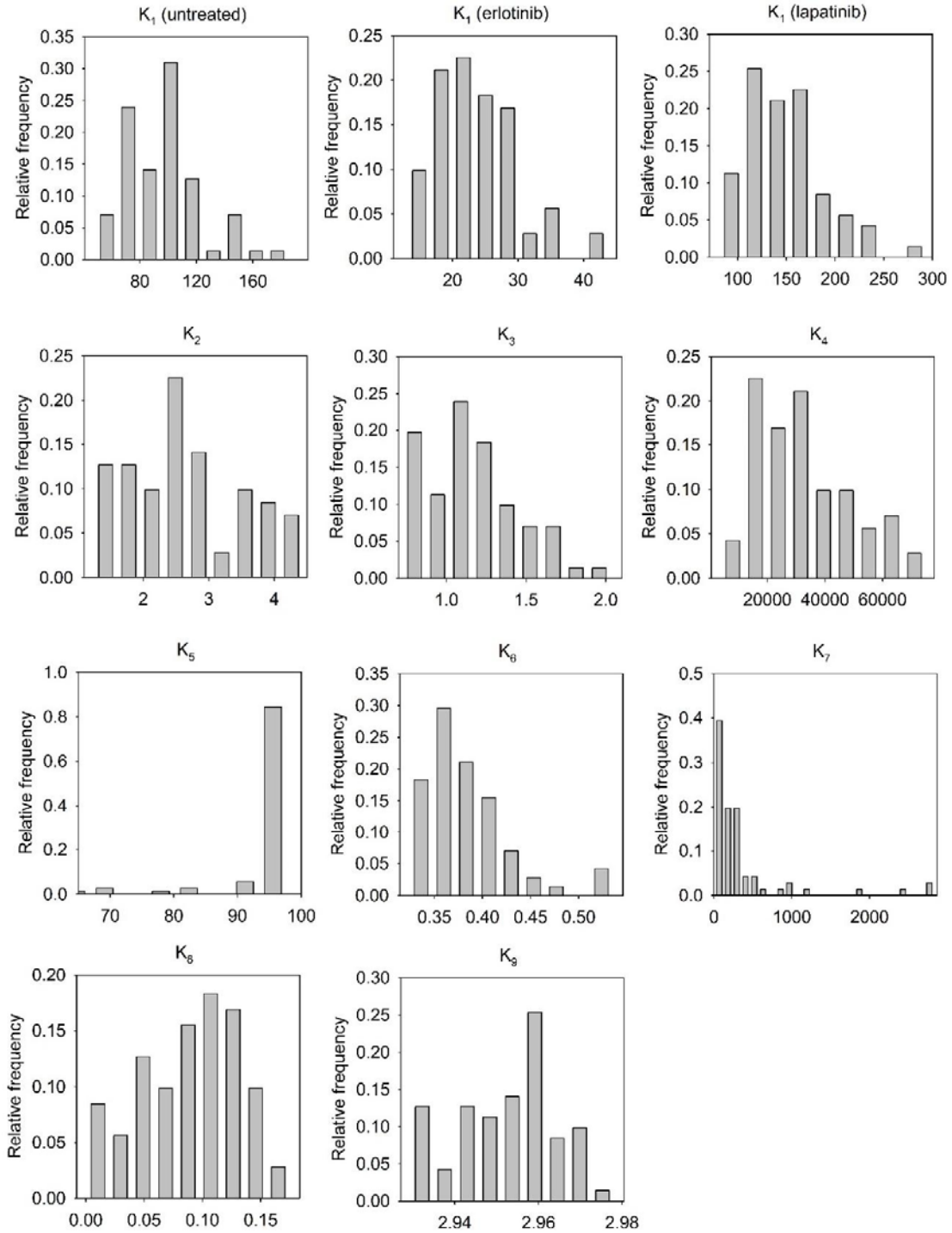


	A431	A4erbB1
K_d	3.8 ± 0.02 nM	3.7 ± 0.02 nM
n	1.28 ± 0.02	1.32 ± 0.02

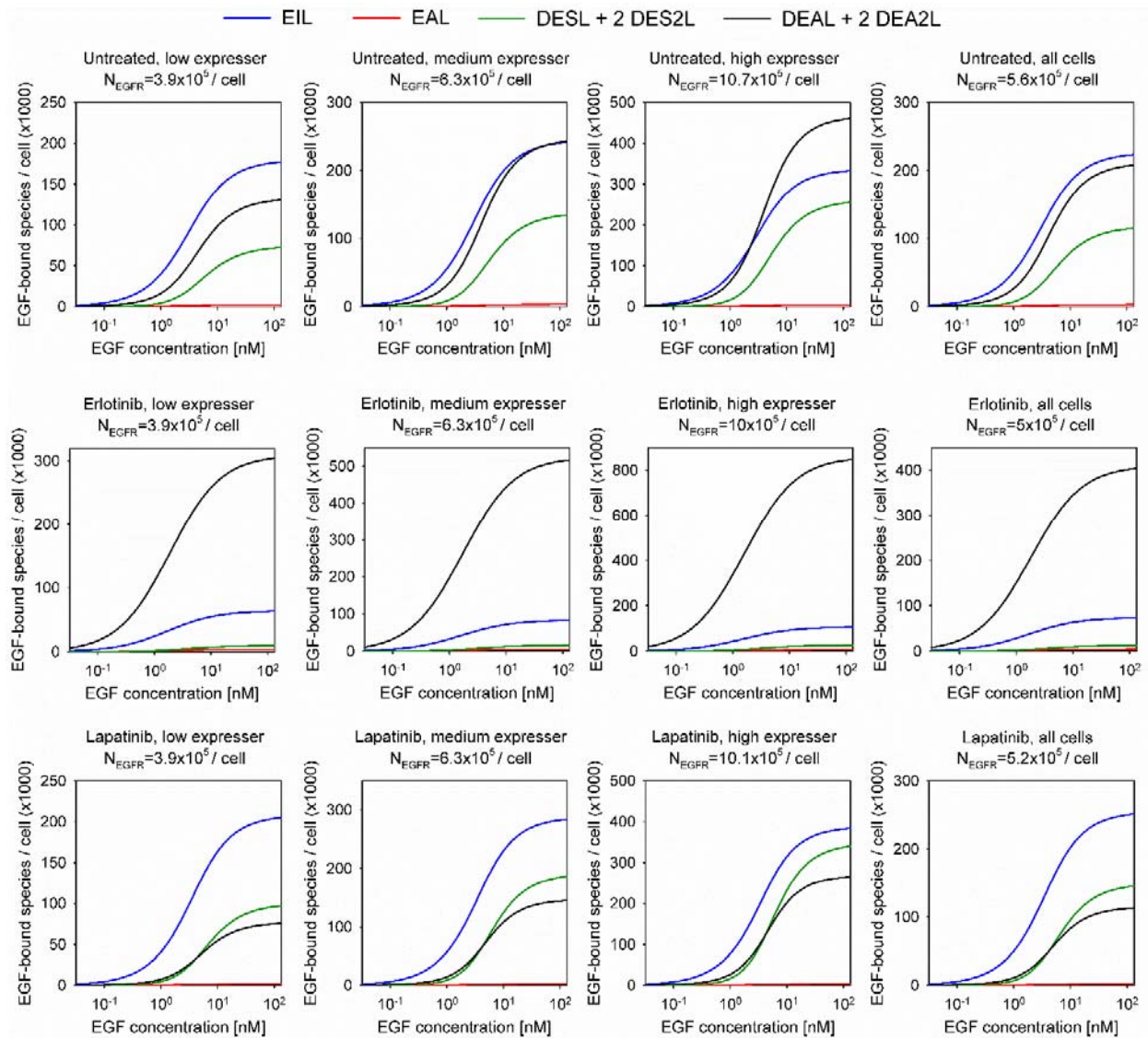
Supplementary Figure 3. The apparent cooperativity and affinity of EGF binding to EGFR is not altered by GFP. A431 cells (ATCC catalog number: CRL-1555) were stably transfected with the same EGFR-GFP plasmid used throughout the experiments reported in the current manuscript. This subline of A431, named A4erbB1, was kindly provided by Donna Arndt-Jovin (Max Planck Institute for Biophysical Chemistry, Göttingen, Germany). The EGFR expression level of both cell lines was determined by flow cytometric calibration using Qifikit (Agilent Technologies, Santa Clara, CA). Although A4erbB1 expresses ~2.9 million EGFRs/cell as opposed to ~2 million EGFRs/cell on A431, gating on GFP fluorescence intensity in A4erbB1 cells, as described in Suppl. Fig. 1, was used for selecting a subpopulation whose total EGFR expression was ~2 million/cell. The ratio of endogenous, dark EGFR to EGFR-GFP in A4erbB1 cells is approximately 2:1. Both cell types were incubated with a concentration series of TAMRA-EGF for 60 min on ice followed by flow cytometry. The mean of three independent measurements (\pm SEM) is shown by the symbols. The Hill equation was fitted to the data (shown by the continuous lines) revealing apparent dissociations constants and cooperativities identical within experimental error for the two cell lines. If the dimerization propensity of EGFR-GFP, its ligand binding affinity or its interaction with wild-type EGFR were any different from those of native EGFR, the apparent K_d or Hill coefficient characterizing A4erbB1 cells would be different from those of A431 cells. Since the curves characterizing the two cell lines perfectly overlap each other, we conclude that the GFP tag does not significantly modify the ligand binding and dimerization properties of EGFR.



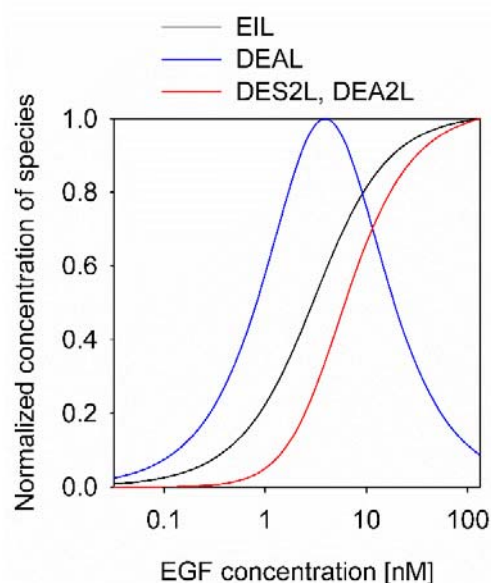
Supplementary Figure 4. Effect of kinase inhibitors on EGF-induced tyrosine phosphorylation. F1-4 cells were serum-starved overnight followed by treatment with 5 μM erlotinib or lapatinib at 37°C for 60 min. Cells were stimulated with 130 nM EGF at 37°C for 15 min followed by fixation, permeabilization and secondary staining with an anti-pTyr antibody (PY99, Santa Cruz Biotechnology) and AlexaFluor647-goat anti-mouse IgG. The GFP fluorescence corresponds to EGFR-GFP expression in the F1-4 cells. The membrane was identified with manually-seeded watershed segmentation and the intensities were analyzed only in the membrane masks. Representative images are shown in the top panel, while the evaluation of three independent measurements is displayed in the bar chart at the bottom. The error bars represent the standard error of the mean.



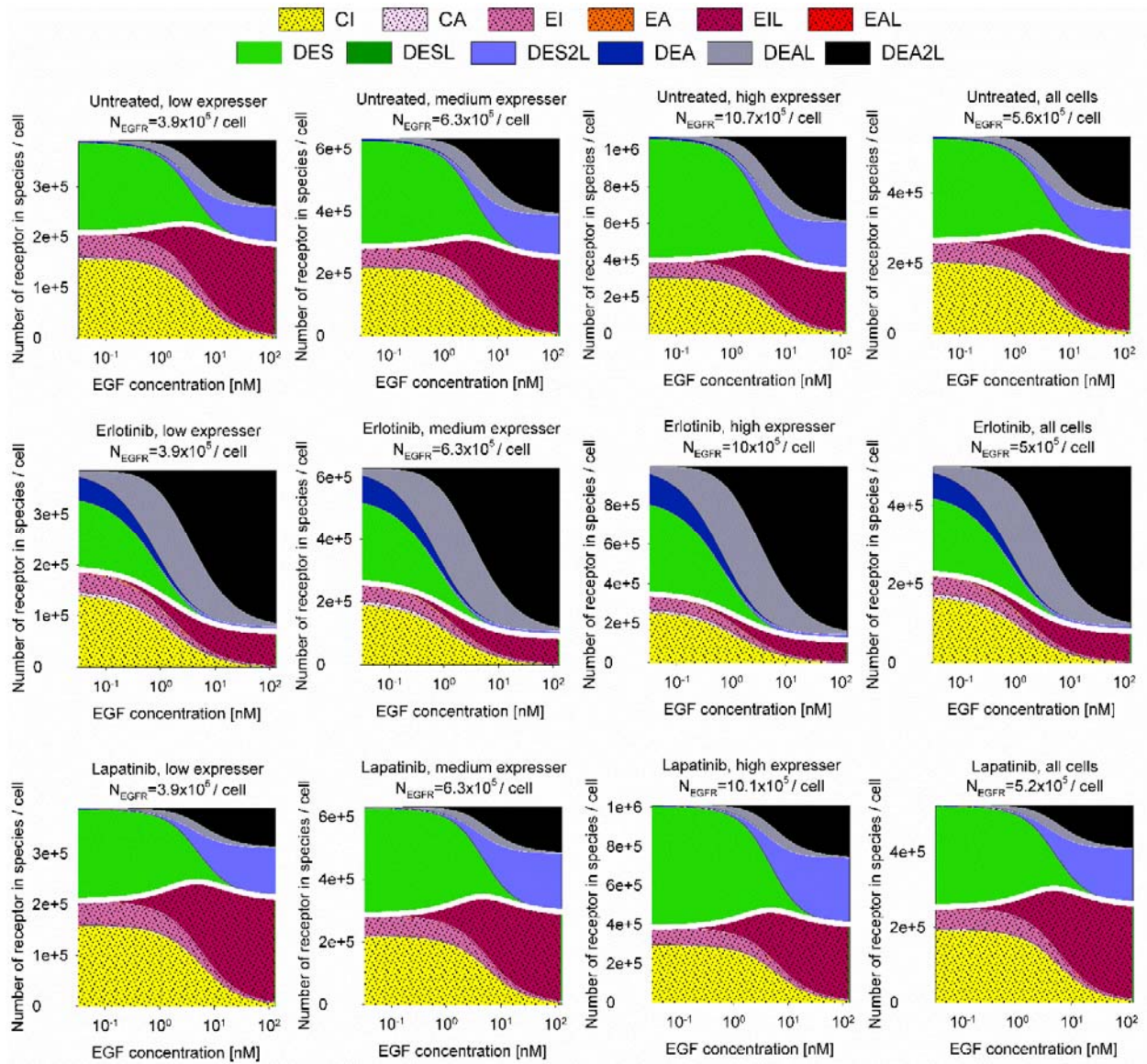
Supplementary Figure 5. Distribution of model parameters obtained from multiple fitting of the experimental results. The experimental data shown in Figure 3 of the manuscript was fitted 100-times, and the distributions of the 11 model parameters are shown by the histograms. The confidence intervals of the parameters, shown in Table 2 of the main text, were estimated from these data.



Supplementary Figure 6. Binding of EGF to different monomeric and dimeric receptor species. Equilibrium binding of EGF was calculated according to the parameters presented in Table 2 of the main text. Calculations were separately performed for control cells and cells treated with kinase inhibitors exhibiting different EGFR expressions. The number of EGF molecules bound to monomeric receptors with inactive (EIL) and active (EAL) kinase domains as well as to dimeric receptors with symmetric (DESL + 2 DES2L) and asymmetric (DEAL + 2 DEA2L) kinase domain dimers are shown in the figure. The amount of dimeric receptor species binding two EGF molecules (DES2L, DEA2L) is multiplied by two so that the displayed curves represent the amount of bound growth factor.

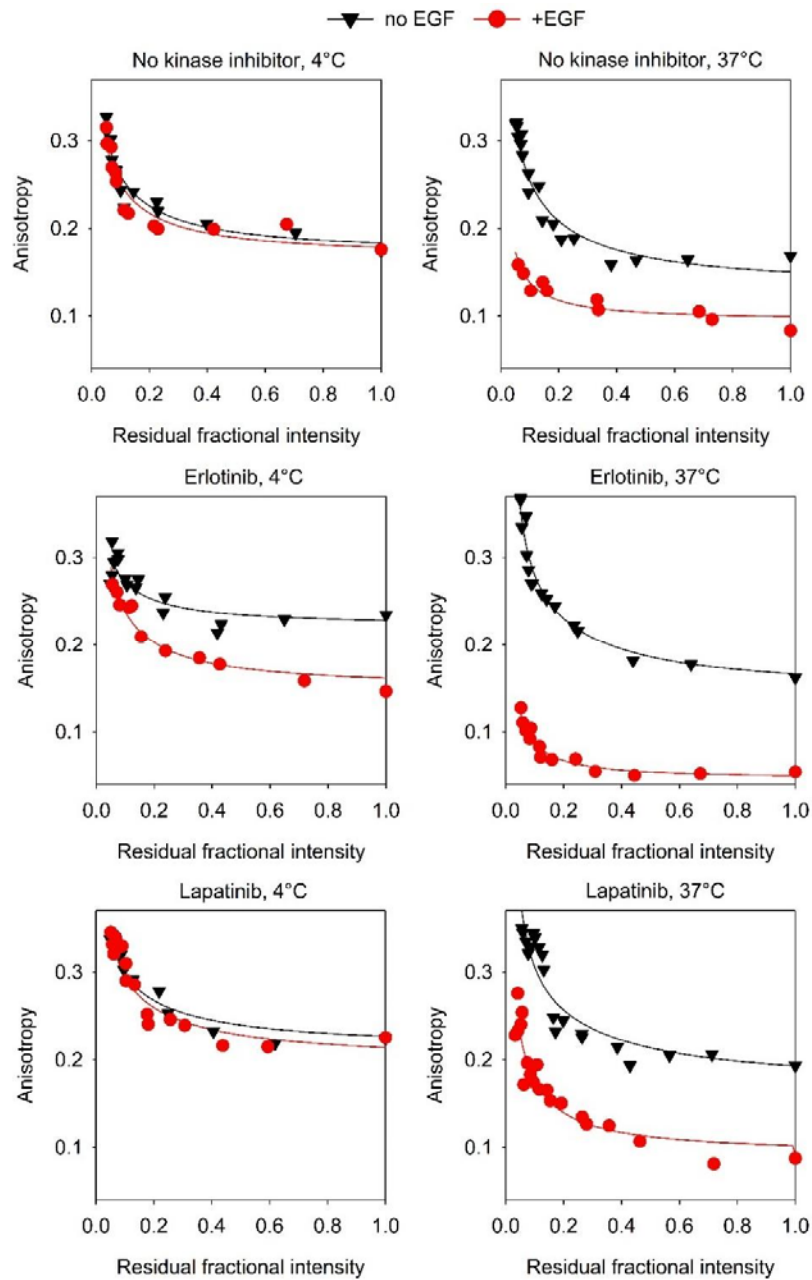


Supplementary Figure 7. Binding of EGF to different receptor species. The concentration of EGF-bound molecular species, normalized to their maximal values, were calculated according to parameters presented in Table 2 and displayed for the four species significantly binding the ligand under any of the experimental conditions (EIL –ligand-bound receptor with inactive KD; DEAL – singly liganded dimer with asymmetric KD dimer; DES2L, DEA2L – doubly-liganded dimers with symmetric and asymmetric KD dimers, respectively; the curves of these two latter species overlap). Since these normalized values do not change as a function of receptor expression or the presence or absence of an inhibitor, only the results for the low expresser subpopulation of the control sample are shown.

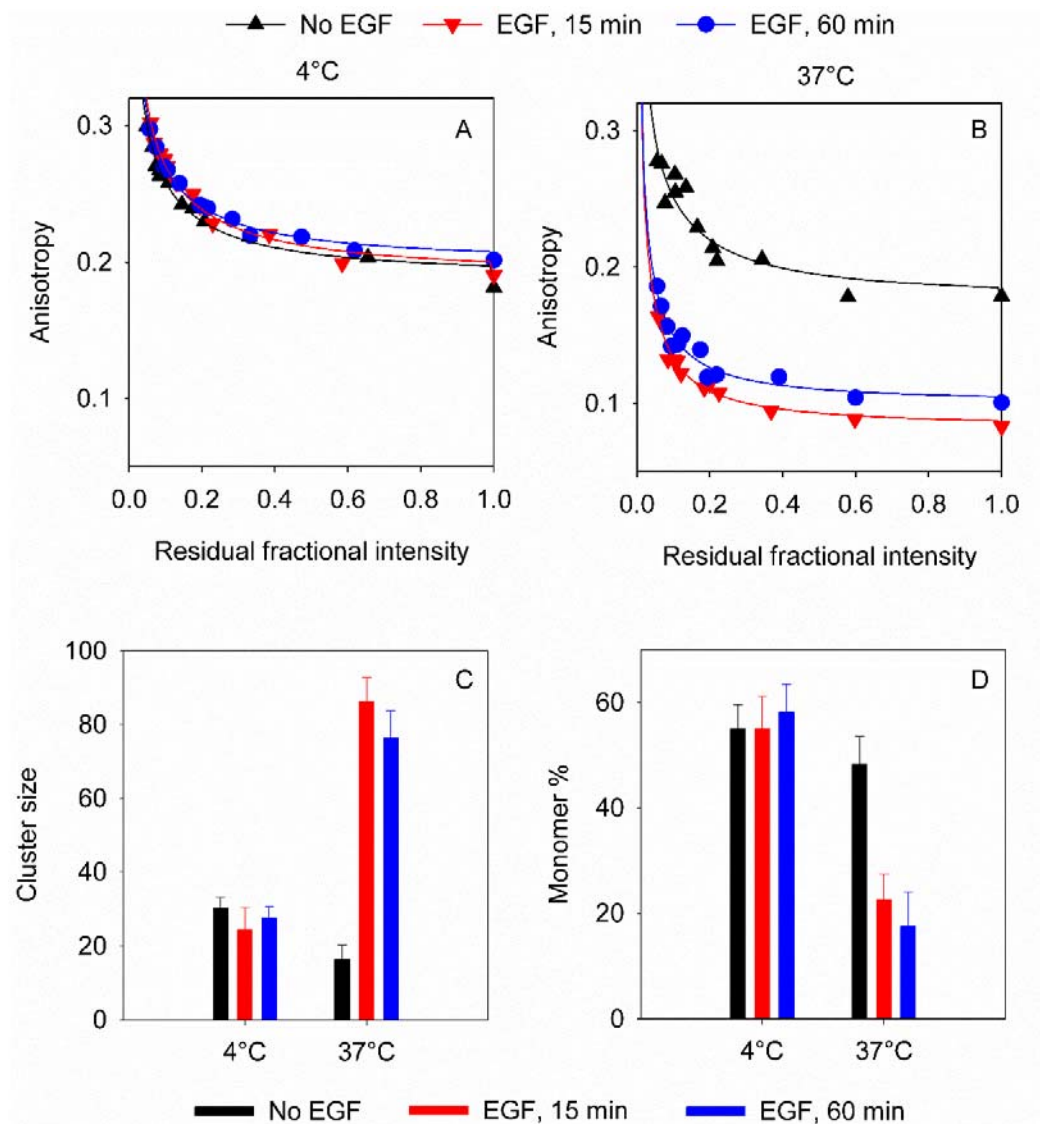


Supplementary Figure 8. EGF concentration dependent changes of monomeric and dimeric EGFR species. The amount of each receptor species is displayed in area plots as a function of EGF concentration for control and kinase inhibitor-treated cells exhibiting different receptor expression levels. The graph shows the number of receptors present in certain species, i.e. the concentration of dimeric species is multiplied by two. The thick white line separates the upper and bottom part of the plots corresponding to dimeric and monomeric receptor species, respectively. The calculation was performed according to the best fit parameters shown in Table 2 of the main text. Monomeric species whose concentrations are sufficient so that they are observable in the graphs: CI – closed ECD, inactive KD; EI – extended ECD, inactive KD; EIL – extended ECD with bound EGF, inactive KD. Monomeric species whose concentrations are too low to appear in the graphs: CA – closed ECD, active KD; EA – extended ECD, active KD; EAL – extended ECD with bound EGF, active KD. Dimeric species whose concentrations are sufficient so that they are observable in the graphs: DES – extended ECD, symmetric KD dimer; DES2L – extended ECD with two bound EGFRs, symmetric KD dimer; DEA – extended ECD, asymmetric KD; DEAL – extended ECD with one bound EGF, asymmetric KD; DEA2L –

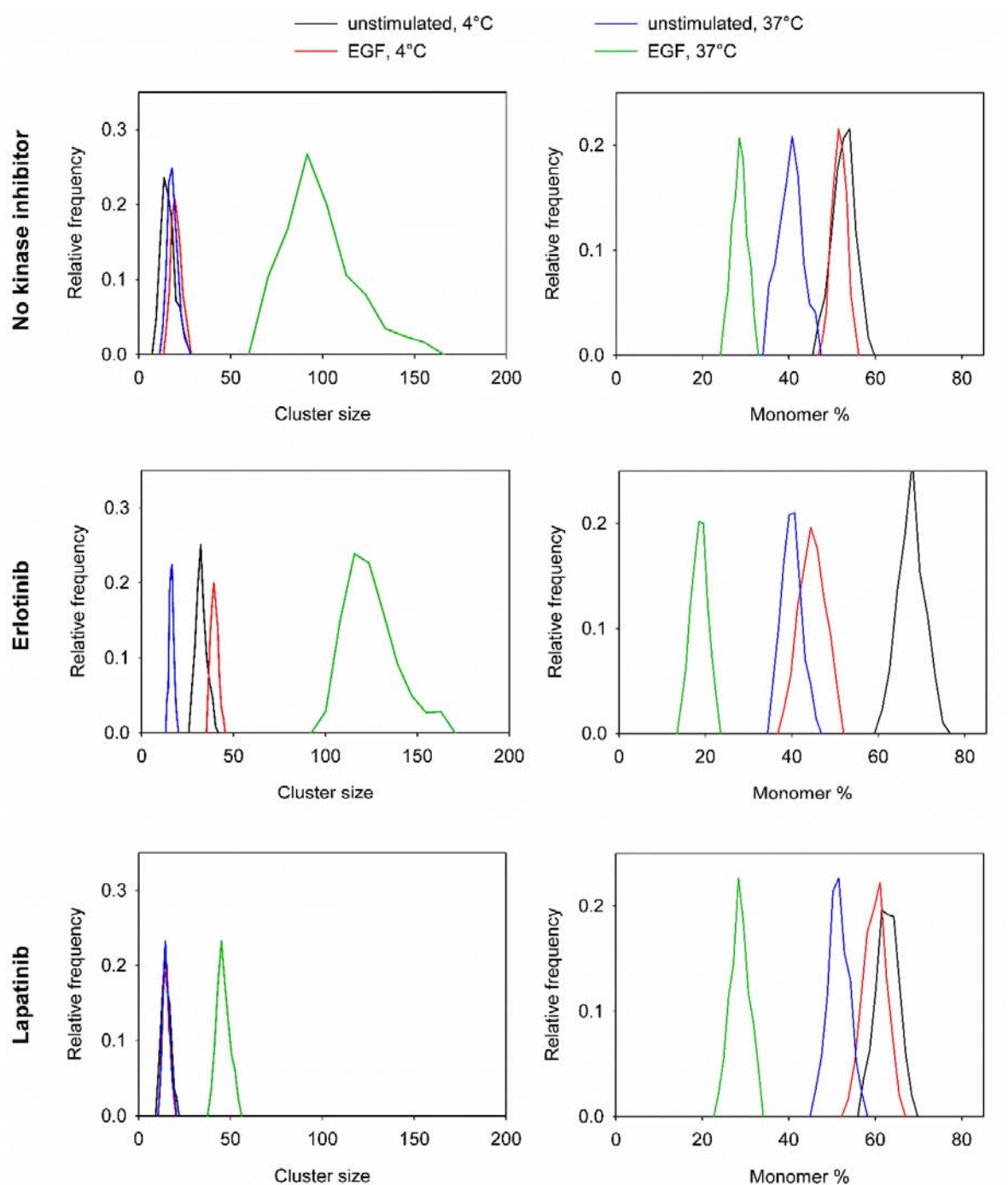
extended ECD with two bound EGFs, asymmetric KD. Dimeric species whose concentration is too low to appear in the graphs: DESL – extended ECD with one bound EGF, symmetric KD dimer.



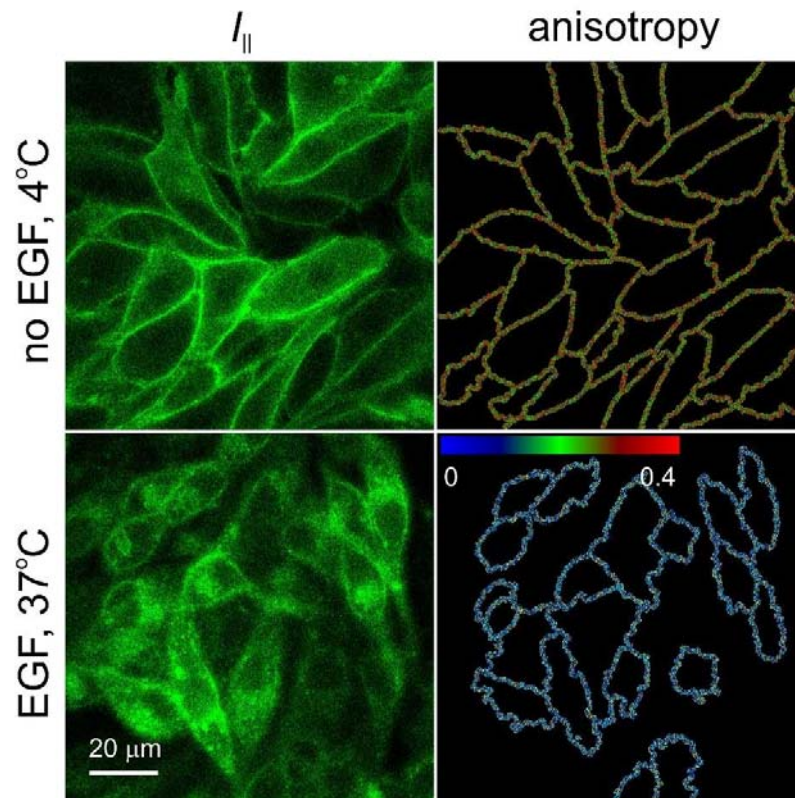
Supplementary Figure 9. Representative homo-FRET experiments of EGFR homoclustering in quiescent and growth factor-stimulated cells. F1-4 cells, stably transfected with EGFR-GFP, were serum-starved overnight. If indicated, cells were pretreated with kinase inhibitors (5 μ M, 1h, 37°C) followed by stimulation with 130 nM EGF for 15 minutes at 4°C or 37°C. Anisotropy was measured by polarized detection of GFP fluorescence in unbleached cells and in cells in which GFP fluorescence was photobleached by illumination at 405 nm. The symbols represent the anisotropy values determined from confocal microscopic images plotted as a function of residual fractional GFP intensity. The lines correspond to fitting of a model describing the anisotropy of a mixture of monomeric and clustered receptors to the measured data (1).



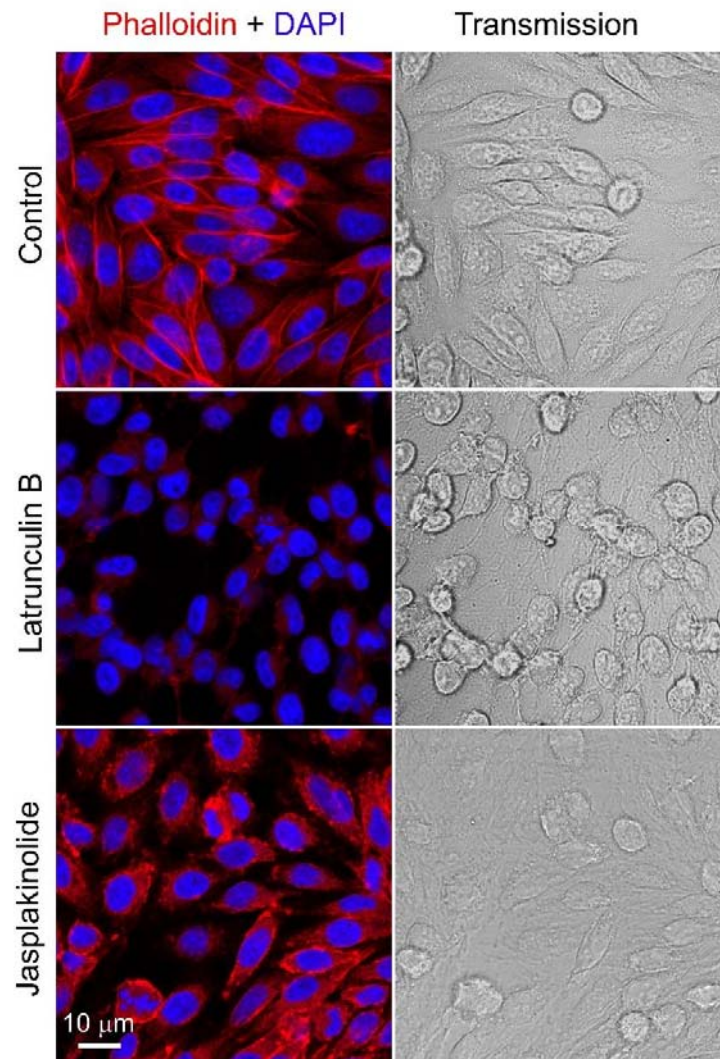
Supplementary Figure 10. Time-dependence of EGF-induced homoclustering of EGFR at 4°C and 37°C. The anisotropy of control and EGF-stimulated cells was measured by microscopy. The anisotropy was measured at different residual fractional intensities generated by bleaching of GFP. Representative data and their fits from experiments carried out at 4°C and 37°C are shown in A and B, respectively. Fitting revealed the cluster size and the monomer fraction (C, D). The error bars represent the standard error of the mean.



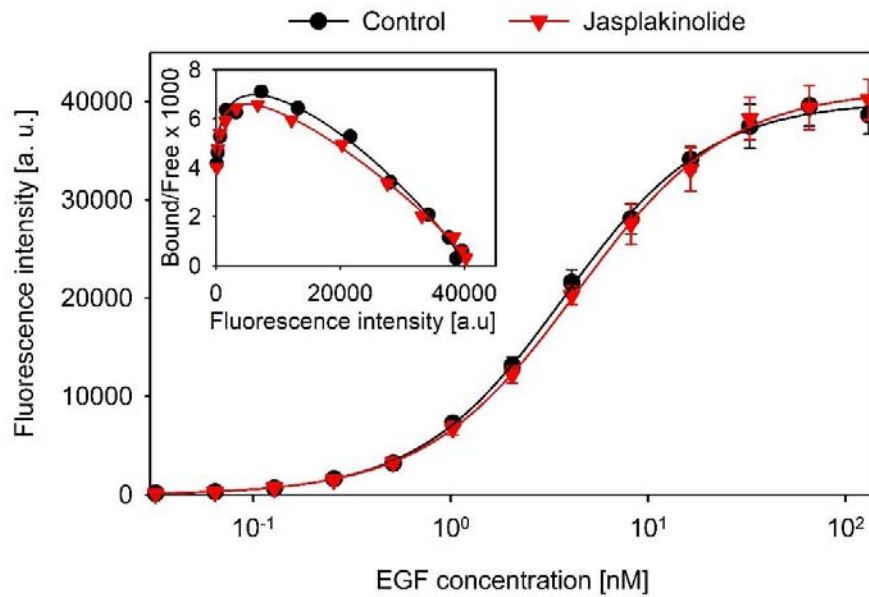
Supplementary Figure 11. Confidence intervals of cluster size and monomer percentage estimated from homo-FRET measurements. The measured anisotropy curves, shown in Suppl. Fig. 9, and the measurement errors were used for generating 500 simulated curves that were fitted resulting in 500 cluster sizes and monomer percentages. The distribution of these values, showing the reliability of the estimation, are displayed in the graphs. The number of histogram bins was determined according to Sturges' rule.



Supplementary Figure 12. Representative anisotropy images of control and EGF-stimulated cells. Control, unstimulated F1-4 cells and those incubated with 130 nM EGF at 4°C for 15 min were imaged using polarized detection of fluorescence. Since GFP was not photobleached, these images correspond to the initial condition (residual fractional intensity=1) in Suppl. Fig. 9 and 10. Fluorescence images recorded with polarizers parallel to the polarization of excitation are shown on the left. The cell membrane was identified using manually-seeded watershed segmentation followed by calculating the anisotropy in the membrane mask, which is shown in color-coded images on the right.

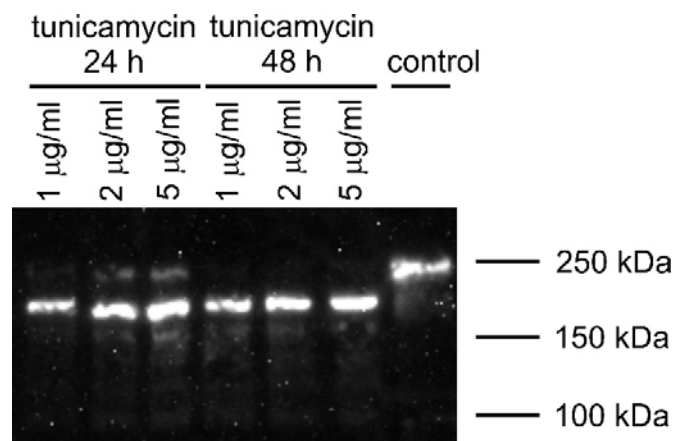


Supplementary Figure 13. Effect of latrunculin B and jasplakinolide treatment on the organization of actin filaments. Cells were treated with 2 μ M latrunculin B for 10 minutes or by 1 μ M jasplakinolide for 30 minutes followed by permeabilization in acetone and staining with 4 μ g/ml tetramethylrhodamine-labeled phalloidin and 10 μ g/ml DAPI to visualize actin filaments and the nucleus, respectively. The overlay of confocal microscopic fluorescence images and the transmission images are shown in the figure. The scale bar applies to all three conditions.

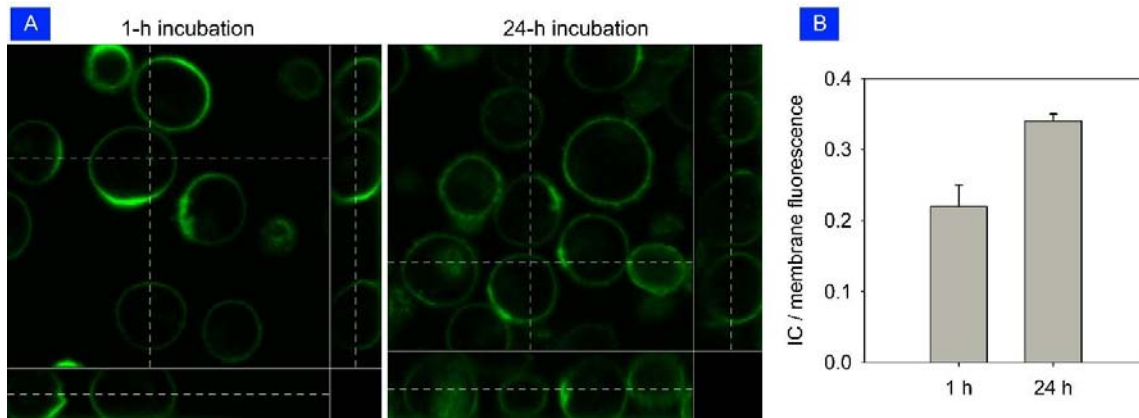


	Untreated	Jasplakinolide
K_d [nM]	3.7 ± 0.3	4.3 ± 0.3
n	1.18 ± 0.03	1.13 ± 0.05

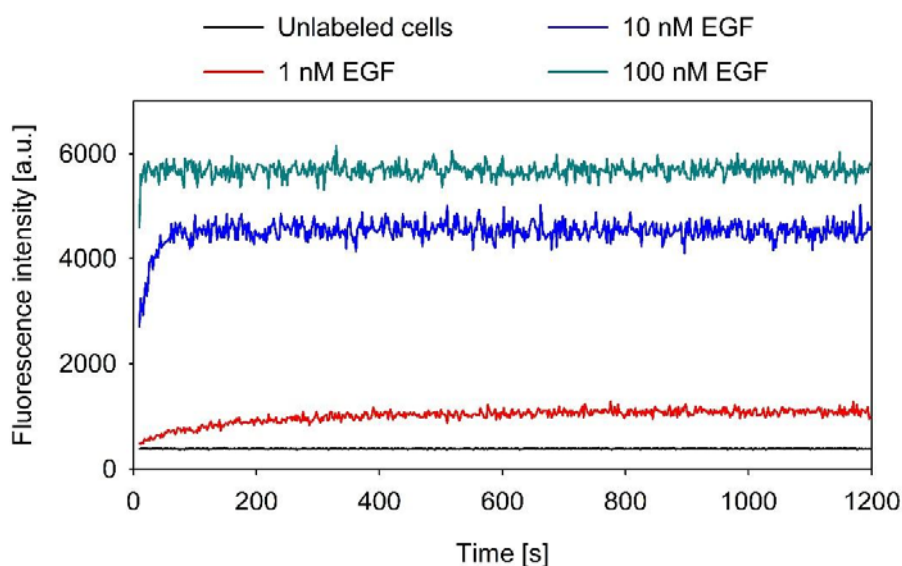
Supplementary Figure 14. The effect of jasplakinolide on EGF binding. F1-4 cells were incubated in the presence of 1 μ M jasplakinolide for 30 min at 37°C or left untreated. Cells were incubated with a concentration series of TAMRA-EGF and equilibrium binding was measured as described in Materials and Methods. The symbols display the measured data points (\pm SD), and the lines are fits of the Hill equation, the result of which is displayed in the table below the graph.



Supplementary Figure 15. Tunicamycin-induced inhibition of glycosylation shifts the molecular weight of EGFR. F1-4 cells were treated with the indicated concentrations of tunicamycin for 24 or 48 h. Proteins were separated by polyacrylamide gel electrophoresis. The EGFR on the membranes was labeled with anti-EGFR antibody (clone F4, Sigma Aldrich), and the lanes were visualized by enhanced chemiluminescence.



Supplementary Figure 16. Impact of 24-h incubation with fluorescent EGF on the distribution of EGF within cells. Cells were incubated with fluorescent EGF for 1 h or 24 h, and images of both samples were recorded with confocal microscopy. Orthogonal views of representative images are shown in A. Pictures were segmented with manually-seeded watershed segmentation to identify the plasma membrane. Pixels inside the membrane mask constituted the intracellular mask. The fluorescence intensity in the plasma membrane and in the intracellular space was calculated, and their ratio is plotted in part B. The difference between the ratios corresponding to the 1-h and 24-h incubations was significant (Student's t-test, $p < 0.01$).



Supplementary Figure 17. Kinetics of EGF binding to cells measured by flow cytometry. Control cells or cells incubated with three different concentrations of TAMRA-EGF (1 nM, 10 nM, 100 nM) were analyzed. The sample holder of the instrument was adjusted to 4°C to mimic the conditions applied during the binding studies. Data acquisition was started immediately after adding EGF to the samples. Since the acquisition time was also saved in the list-mode files, a time-correlated analysis of cell-bound EGF could be performed. Fluorescence intensities were averaged for a sliding window width of 5 s. The experiments revealed that equilibrium is reached before 1 h, the duration of the incubation time in the equilibrium binding experiments, independent of the concentration of EGF used.

2 Supplementary theory

2.1 Estimation of ligand depletion

The total molar quantity (m_{total}) of EGF added to the incubation volume (V), in which the concentration of the growth factor was c_{EGF} , was calculated according to the following equation:

$$m_{\text{total}} = c_{\text{EGF}} V \quad (\text{S1})$$

In order to estimate the molar quantity of bound EGF the mean intensity of each sample (I) normalized to the saturation intensity, obtained from the Hill fits (I_{max}), was assumed to represent the fractional saturation (f) of EGFRs with EGF:

$$f = \frac{I}{I_{\text{max}}} \quad (\text{S2})$$

The molar quantity of bound EGF was calculated by multiplying the product of this fractional saturation with the number of EGFRs/cell, determined by flow cytometric calibration (N_{receptor}), and with the number of cells in the incubation volume (N_{cell}), followed by dividing with Avogadro's number (N_A):

$$m_{\text{bound}} = \frac{f N_{\text{receptor}} N_{\text{cell}}}{N_A} \quad (\text{S3})$$

The percent of cell-bound growth factor, $m_{\text{bound}} / m_{\text{total}}$, was under 10% for all experimental conditions.

2.2 Evaluation of the negative cooperativity model about its predictions for EGFR species

The model proposed by Macdonald and Pike involves the dimerization of EGFR monomers disregarding the extended-closed structural transition of the ECD and the conformation of the KD (2). The model is described by the following equations:

$$[M][M] = L_{20} [D] \quad (\text{S4})$$

$$[M][EGF] = K_{11} [MEGF] \quad (\text{S5})$$

$$[D][EGF] = K_{21} [DEGF] \quad (\text{S6})$$

$$[DEGF][EGF] = K_{22} [D2EGF] \quad (\text{S7})$$

$$\text{signal} = [MEGF] + [DEGF] + 2[D2EGF] \quad (\text{S8})$$

$$[R_{\text{tot}}] = [M] + [MEGF] + 2([D] + [DEGF] + [D2EGF]) \quad (\text{S9})$$

where M and D are the monomeric and dimeric receptor, respectively, without bound ligand, $MEGF$ is the liganded monomer, $DEGF$ and $D2EGF$ are the singly and doubly liganded receptor dimer,

respectively. L_{20} is the dissociation constant for the receptor dimer, K_{11} is the dissociation constant of the receptor monomer for EGF, and K_{21} and K_{22} are the dissociation constants for binding of the first and second ligand to the dimer, respectively. Equation (S8) describes the cell-bound signal, while equation (S9) expresses the conservation of the receptor. The Matlab function containing the solutions for all species is provided below. The function selects that root series as the meaningful solution in which all concentrations are positive.

```
function
[boundSignal,allSpecies,whichRoot]=boundEGFpike(l20,k11,k21,k22,rtot,egf)
% 1 m - monomer unliganded receptor
% 2 megf - monomer ligand-bound receptor
% 3 d - unliganded dimer
% 4 degf - dimer with one EGF
% 5 d2egf - dimer with two EGFs

signal1=(1/8).*egf.*k11.^(-2).*egf.^2+(egf+k21).*k22.^(-2).*((-2).*(egf+ ...
k11).*k21.^2.*k22.^2.*l20+4.*egf.*k11.^2.*(egf+k22).*(2.*egf+k22) ...
.*rtot+k21.*k22.*((egf+k11).*(2.*egf.*k11+(-1).*egf.*k22+k11.*k22) ...
.*l20+4.*k11.^2.*(2.*egf+k22).*rtot)+2.*egf.*k11.*((egf.*k21.* ...
k22.*l20+k11.*k21.*k22.*l20).^2+8.*k11.^2.*k21.*k22.*(egf.^2+(egf+ ...
k21).*k22).*l20.*rtot).^((1/2)+(-1).*egf.*k22.*((egf.*k21.*k22.* ...
l20+k11.*k21.*k22.*l20).^2+8.*k11.^2.*k21.*k22.*(egf.^2+(egf+k21) ...
.*k22).*l20.*rtot).^((1/2)+k11.*k22.*((egf.*k21.*k22.*l20+k11.* ...
k21.*k22.*l20).^2+8.*k11.^2.*k21.*k22.*(egf.^2+(egf+k21).*k22).* ...
l20.*rtot).^((1/2)+(-2).*k21.*k22.*((egf.*k21.*k22.*l20+k11.*k21.* ...
k22.*l20).^2+8.*k11.^2.*k21.*k22.*(egf.^2+(egf+k21).*k22).*l20.* ...
rtot).^((1/2)));
m1=(-1/4).*k11.^(-1).*(egf.^2+(egf+k21).*k22).^(-1).*((egf+k11).* ...
k21.*k22.*l20+(k21.*k22.*l20.*((egf+k11).^2.*k21.*k22.*l20+8.* ...
k11.^2.*(egf.^2+(egf+k21).*k22).*rtot)).^(1/2));
megf1=(-1/4).*egf.*k11.^(-2).*(egf.^2+(egf+k21).*k22).^(-1).*((egf+k11) ...
.*k21.*k22.*l20+(k21.*k22.*l20.*((egf+k11).^2.*k21.*k22.*l20+8.* ...
k11.^2.*(egf.^2+(egf+k21).*k22).*rtot)).^(1/2));
d1=(1/8).*k11.^(-2).*k21.*k22.*(egf.^2+(egf+k21).*k22).^(-2).*(4.* ...
egf.*k11.^2.*(egf+k22).*rtot+k21.*k22.*((egf+k11).^2.*l20+4.* ...
k11.^2.*rtot)+egf.*((egf.*k21.*k22.*l20+k11.*k21.*k22.*l20).^2+8.* ...
k11.^2.*k21.*k22.*(egf.^2+(egf+k21).*k22).*l20.*rtot).^((1/2)+k11.* ...
((egf.*k21.*k22.*l20+k11.*k21.*k22.*l20).^2+8.*k11.^2.*k21.*k22.* ...
egf.^2+(egf+k21).*k22).*l20.*rtot).^((1/2)));
degf1=(1/8).*egf.*k11.^(-2).*k22.*(egf.^2+(egf+k21).*k22).^(-2).*(4.* ...
egf.*k11.^2.*(egf+k22).*rtot+k21.*k22.*((egf+k11).^2.*l20+4.* ...
k11.^2.*rtot)+egf.*((egf.*k21.*k22.*l20+k11.*k21.*k22.*l20).^2+8.* ...
k11.^2.*k21.*k22.*(egf.^2+(egf+k21).*k22).*l20.*rtot).^((1/2)+k11.* ...
((egf.*k21.*k22.*l20+k11.*k21.*k22.*l20).^2+8.*k11.^2.*k21.*k22.* ...
egf.^2+(egf+k21).*k22).*l20.*rtot).^((1/2)));
d2egf1=(1/8).*egf.^2.*k11.^(-2).*(egf.^2+(egf+k21).*k22).^(-2).*(4.*egf.* ...
k11.^2.*(egf+k22).*rtot+k21.*k22.*((egf+k11).^2.*l20+4.*k11.^2.* ...
rtot)+egf.*((egf.*k21.*k22.*l20+k11.*k21.*k22.*l20).^2+8.*k11.^2.* ...
k21.*k22.*(egf.^2+(egf+k21).*k22).*l20.*rtot).^((1/2)+k11.*((egf.* ...
k21.*k22.*l20+k11.*k21.*k22.*l20).^2+8.*k11.^2.*k21.*k22.*(egf.^2+ ...
(egf+k21).*k22).*l20.*rtot).^((1/2)));
signal2=(1/8).*egf.*k11.^(-2).*(egf.^2+(egf+k21).*k22).^(-2).*((-2).*(egf+ ...
k11).*k21.^2.*k22.^2.*l20+4.*egf.*k11.^2.*(egf+k22).*(2.*egf+k22) ...
.*rtot+k21.*k22.*((egf+k11).*(2.*egf.*k11+(-1).*egf.*k22+k11.*k22) ...
.*l20+4.*k11.^2.*(2.*egf+k22).*rtot)+(-2).*egf.*k11.*((egf.*k21.* ...
```

```

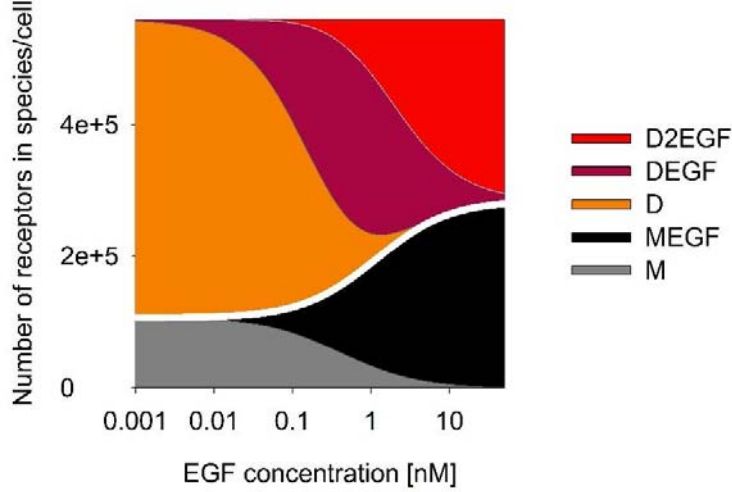
k22.*l20+k11.*k21.*k22.*l20).^2+8.*k11.^2.*k21.*k22.*(egf.^2+(egf+ ...
k21).*k22).*l20.*rtot).^(1/2)+egf.*k22.*((egf.*k21.*k22.*l20+k11.* ...
k21.*k22.*l20).^2+8.*k11.^2.*k21.*k22.*(egf.^2+(egf+k21).*k22).* ...
l20.*rtot).^(1/2)+(-1).*k11.*k22.*((egf.*k21.*k22.*l20+k11.*k21.* ...
k22.*l20).^2+8.*k11.^2.*k21.*k22.*(egf.^2+(egf+k21).*k22).*l20.* ...
rtot).^(1/2)+2.*k21.*k22.*((egf.*k21.*k22.*l20+k11.*k21.*k22.*l20) ...
.^2+8.*k11.^2.*k21.*k22.*(egf.^2+(egf+k21).*k22).*l20.*rtot).^( ...
1/2));
m2=(1/4).*k11.^(-1).*(egf.^2+(egf+k21).*k22).^(-1).*((( -1).*egf+(-1) ...
.*k11).*k21.*k22.*l20+(k21.*k22.*l20.*((egf+k11).^2.*k21.*k22.* ...
l20+8.*k11.^2.*(egf.^2+(egf+k21).*k22).*rtot)).^(1/2));
megf2=(1/4).*egf.*k11.^(-2).*(egf.^2+(egf+k21).*k22).^(-1).*((( -1).*egf+ ...
(-1).*k11).*k21.*k22.*l20+(k21.*k22.*l20.*((egf+k11).^2.*k21.* ...
k22.*l20+8.*k11.^2.*(egf.^2+(egf+k21).*k22).*rtot)).^(1/2));
d2=(1/8).*k11.^(-2).*k21.*k22.*(egf.^2+(egf+k21).*k22).^(-2).*(4.* ...
egf.*k11.^2.*(egf+k22).*rtot+k21.*k22.*((egf+k11).^2.*l20+4.* ...
k11.^2.*rtot)+(-1).*egf.*((egf.*k21.*k22.*l20+k11.*k21.*k22.*l20) ...
.^2+8.*k11.^2.*k21.*k22.*(egf.^2+(egf+k21).*k22).*l20.*rtot).^( ...
1/2)+(-1).*k11.*((egf.*k21.*k22.*l20+k11.*k21.*k22.*l20).^2+8.* ...
k11.^2.*k21.*k22.*(egf.^2+(egf+k21).*k22).*l20.*rtot).^(1/2));
degf2=(1/8).*egf.*k11.^(-2).*k22.*(egf.^2+(egf+k21).*k22).^(-2).*(4.* ...
egf.*k11.^2.*(egf+k22).*rtot+k21.*k22.*((egf+k11).^2.*l20+4.* ...
k11.^2.*rtot)+(-1).*egf.*((egf.*k21.*k22.*l20+k11.*k21.*k22.*l20) ...
.^2+8.*k11.^2.*k21.*k22.*(egf.^2+(egf+k21).*k22).*l20.*rtot).^( ...
1/2)+(-1).*k11.*((egf.*k21.*k22.*l20+k11.*k21.*k22.*l20).^2+8.* ...
k11.^2.*k21.*k22.*(egf.^2+(egf+k21).*k22).*l20.*rtot).^(1/2));
d2egf2=(1/8).*egf.^2.*k11.^(-2).*(egf.^2+(egf+k21).*k22).^(-2).*(4.*egf.* ...
k11.^2.*(egf+k22).*rtot+k21.*k22.*((egf+k11).^2.*l20+4.*k11.^2.* ...
rtot)+(-1).*egf.*((egf.*k21.*k22.*l20+k11.*k21.*k22.*l20).^2+8.* ...
k11.^2.*k21.*k22.*(egf.^2+(egf+k21).*k22).*l20.*rtot).^(1/2)+(-1) ...
.*k11.*((egf.*k21.*k22.*l20+k11.*k21.*k22.*l20).^2+8.*k11.^2.* ...
k21.*k22.*(egf.^2+(egf+k21).*k22).*l20.*rtot).^(1/2));

numOfElements=numel([signal1,m1,megf1,d1,degf1,d2egf1]);
if sum(sum([signal1,m1,megf1,d1,degf1,d2egf1]>=0))==numOfElements
    boundSignal=signal1;
    allSpecies=[m1,megf1,d1,degf1,d2egf1];
    whichRoot=1;
elseif sum(sum([signal2,m2,megf2,d2,degf2,d2egf2]>=0))==numOfElements
    boundSignal=signal2;
    allSpecies=[m2,megf2,d2,degf2,d2egf2];
    whichRoot=2;
else
    boundSignal=nan;
    allSpecies=nan;
    whichRoot=0;
end

```

While association constants were used in the original paper, dissociation constants are used in the above derivation in order to maintain compatibility with our model described in the main text. Taking this fact into consideration the model parameters are the following: $K_{11}=0.2174$ nM, $K_{21}=0.1887$ nM, $K_{22}=2.94$ nM, $L_{20}=5 \cdot 10^4$ receptors/cell. Using these constants and an expression level of $R_{\text{tot}}=5.6 \cdot 10^5$

receptors/cell, corresponding to the F1-4 cells used in the current manuscript, predictions for the different molecular species are shown in the figure below:



The thick white line separates monomeric and dimeric receptor species from each other. According to the model the overwhelming majority of receptors are present in preformed, constitutive dimers at an expression level of $5 \cdot 10^5$ /cell. The graph also predicts that EGF induces a decline in the number of receptors in dimers. This unexpected conclusion, which is the consequence of the significantly lower homodimerization tendency of liganded monomers as compared to unliganded ones, follows from the parameters of the model, and it has been pointed out by the authors as well.

2.3 Analysis of the kinetics of reaching the equilibrium by a receptor dimer

We aimed at characterizing what kind of effect the lack of reaching an equilibrium exerts on the apparent cooperativity of EGF binding. First, we set up a system of differential equations describing the binding kinetics of the ligand:

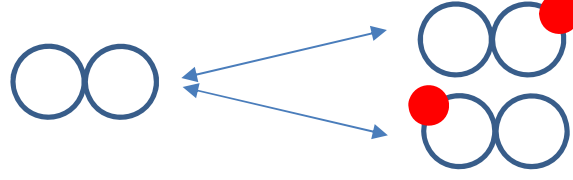
$$\frac{dR0(t)}{dt} = -2k_{1,ON} R0(t) c_{EGF} + k_{1,OFF} R1(t) \quad (S10)$$

$$\frac{dR1(t)}{dt} = 2k_{1,ON} R0(t) c_{EGF} - k_{1,OFF} R1(t) - k_{2,ON} R1(t) c_{EGF} + 2k_{2,OFF} R2(t) \quad (S11)$$

$$\frac{dR2(t)}{dt} = k_{2,ON} R1(t) c_{EGF} - 2k_{2,OFF} R2(t) \quad (S12)$$

where $R0$, $R1$ and $R2$ are concentrations of the unoccupied, singly and doubly liganded dimers, respectively, c_{EGF} is the concentration of EGF in the solution. $k_{1,ON}$ and $k_{1,OFF}$ are the association and dissociation rate constants of EGF for the first binding site, and $k_{2,ON}$ and $k_{2,OFF}$ are the same parameters for the second binding site. Multiplication with two of certain terms on the right-hand side of the equations takes the fact into account that certain transitions can take place via two, kinetically different

ways, e.g. the $RO \rightarrow RI$ step can be accomplished by the ligand associating with either one of the receptor monomers:



The above differential equation system can be rewritten as a matrix differential equation as follows:

$$\begin{pmatrix} RO'(t) \\ R1'(t) \\ R2'(t) \end{pmatrix} = \mathbf{A} \begin{pmatrix} RO(t) \\ R1(t) \\ R2(t) \end{pmatrix} \quad (\text{S13})$$

$$\mathbf{A} = \begin{pmatrix} -2k_{1,\text{ON}}c_{\text{EGF}} & k_{1,\text{OFF}} & 0 \\ 2k_{1,\text{ON}}c_{\text{EGF}} & -k_{1,\text{OFF}} - k_{2,\text{ON}}c_{\text{EGF}} & 2k_{2,\text{OFF}} \\ 0 & k_{2,\text{ON}}c_{\text{EGF}} & -2k_{2,\text{OFF}} \end{pmatrix}$$

The general solution of the equation above is given below:

$$\begin{pmatrix} RO(t) \\ R1(t) \\ R2(t) \end{pmatrix} = C_1 e^{-\lambda_1 t} \mathbf{v}_1 + C_2 e^{-\lambda_2 t} \mathbf{v}_2 + C_3 e^{-\lambda_3 t} \mathbf{v}_3 \quad (\text{S14})$$

where C_1 , C_2 and C_3 are the eigenvalues of matrix \mathbf{A} , and \mathbf{v}_1 , \mathbf{v}_2 and \mathbf{v}_3 are the eigenvectors of matrix \mathbf{A} . The eigenvalues and eigenvectors were found using Mathematica. The specific solution corresponding to the current problem was found by setting the initial concentrations as follows:

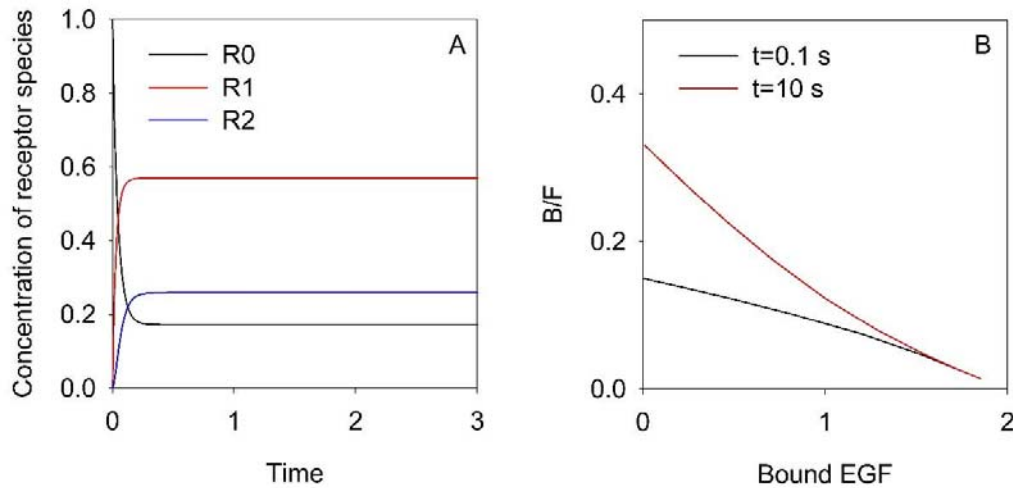
$$RO(t) = R_{\text{tot}}, \quad R1(t) = R2(t) = 0 \quad (\text{S15})$$

For reasons described above the dissociation constants of EGF for the 1st and 2nd binding sites are given by the following equations:

$$K_{d,1} = \frac{k_{1,\text{OFF}}}{2k_{1,\text{ON}}}, \quad K_{d,2} = \frac{2k_{2,\text{OFF}}}{k_{2,\text{ON}}} \quad (\text{S16})$$

In order to reveal the effect of the lack of reaching equilibrium binding conditions, the following, arbitrary dissociation constants generating negative cooperativity were used: $K_{d1}=3$ nM, $K_{d2}=12$ nM. Assuming $k_{1,\text{ON}}=k_{2,\text{ON}}=1$, the dissociation rate constants were calculated and substituted into the solution of the differential equation system. The kinetics of ligand binding were calculated at an EGF concentration of 10 nM (panel A). Next, we analyzed the dependence of cell-bound EGF at two time points corresponding to before ($t=0.1$ s) and after ($t=10$ s) reaching the equilibrium. The Scatchard plots in panel B demonstrate that the concave-up plot corresponding to $t=10$ s, indicative of negative

cooperativity, is converted to a concave-down curve at $t=0.1$ s implying positive cooperativity. Fitting of the binding curves with the Hill equation confirmed the conclusions reached based on the Scatchard plots ($K_d=8.2$ nM, $n=0.88$ at $t=10$ s; $K_d=11$ nM, $n=1.1$ at $t=0.1$ s).



3 References

1. Szabó A, Horváth G, Szöllősi J, Nagy P. Quantitative characterization of the large-scale association of ErbB1 and ErbB2 by flow cytometric homo-FRET measurements. *Biophys J.* 2008;95(4):2086-96.
2. Macdonald JL, Pike LJ. Heterogeneity in EGF-binding affinities arises from negative cooperativity in an aggregating system. *Proc Natl Acad Sci U S A.* 2008;105(1):112-7.

```

function [boundSignal,allSpecies,whichRoot]=boundEGF(varargin)
% input arguments:
% 3 inputs: ks, rtot, egfcc
% 12 inputs: k1, k2, ..., k10, rtot, egfcc
% k1 - equilibrium between inactive and active kinase
% k2 - equilibrium between closed and extended ECD
% k3 - ligand binding by an extended monomer
% k4 - dimerization of EI
% k5 - first ligand binding of DES
% k6 - second ligand binding of DES
% k7 - dimerization of EA
% k8 - first ligand binding of DEA
% k9 - second ligand binding of DEA
%
% output arguments: boundSignal, allSpecies (ci, ca, ei, ea, eil, eal, des,
desl, des2l, dea, deal, dea2l}, whichRoot
%
% 1 ci - closed ECD, inhibited KD
% 2 ca - closed, active KD
% 3 ei - extended, inhibited KD
% 4 ea - extended, active KD
% 5 eil - extended, inhibited KD + EGF
% 6 eal - extended, active KD + EGF
% 7 des - dimer of extended, inhibited (symmetric) KD
% 8 desl - dimer of extended, inhibited (symmetric) KD + EGF
% 9 des2l - dimer of extended, inhibited (symmetric) KD + 2 EGF
% 10 dea - dimer of extended, active (asymmetric) KD
% 11 deal - dimer of extended, active (asymmetric) KD + EGF
% 12 dea2l - dimer of extended, active (asymmetric) KD + 2 EGF
if nargin==11
    k1=varargin{1};
    k2=varargin{2};
    k3=varargin{3};
    k4=varargin{4};
    k5=varargin{5};
    k6=varargin{6};
    k7=varargin{7};
    k8=varargin{8};
    k9=varargin{9};
    rtot=varargin{10};
    egf=varargin{11};
elseif nargin==3
    k1=varargin{1}(1);
    k2=varargin{1}(2);
    k3=varargin{1}(3);
    k4=varargin{1}(4);
    k5=varargin{1}(5);
    k6=varargin{1}(6);
    k7=varargin{1}(7);
    k8=varargin{1}(8);
    k9=varargin{1}(9);
    rtot=varargin{2};
    egf=varargin{3};
else
    error('Number of arguments must be 3 or 11.');
```

end

```

% first series of roots
```

```

egfbound1=(1/8).*egf.*k1.^(-1).*(egf.^2.*k3.*k4.*k5.*k6+k3.*(egf.*k4.*k5.*
...
k6+k4.*k5.*k6.*k8+k1.^2.*(egf.^2+(egf+k5).*k6).*k7.*k8).*k9).^(-2) ...
.*(8.*egf.^3.*k1.*k3.^2.*(k4.*k5.*k6+k1.^2.*k7.*k8.*k9).^2.*rtot+ ...
egf.^2.*k1.*k6.*k9.*((-1).*(1+k1).^2.*k4.*k5.*k6.*k7.*k8.*(k4.*k5+ ...
k1.^2.*k7.*k8).*k9+2.*(1+k1).^2.*(1+k2).*k3.*k4.*k5.*k7.*k8.*(k4.* ...
k5.*k6+k1.^2.*k7.*k8.*k9)+12.*k3.^2.*(k4.*k5+k1.^2.*k7.*k8).*(k4.* ...
k5.*k6+k1.^2.*k7.*k8.*k9).*rtot)+k6.*k9.*(2.*k1.^4.*(1+k2).*k3.* ...
k4.*(k3+k2.*k3+(-2).*k5).*k5.*k6.*k7.^2.*k8.^2.*k9+k1.^5.*k3.*k5.* ...
k6.*k7.^2.*k8.^2.*k9.*((1+k2).*k4.*(k3+k2.*k3+(-2).*k5)+4.*k3.* ...
rtot)+k4.*k5.*(k3+k2.*k3+(-2).*k8).*(k1.^2.*k4.*k5.*k6.*k7.*k8.* ...
k9.*((1+k1).^2.*(egf+k3+k2.*k3).^2.*k4.*k5.*k6.*k7.*k8.*k9+8.* ...
k3.^2.*(egf.^2.*k4.*k5.*k6+(egf.*k4.*k5.*k6+k4.*k5.*k6.*k8+k1.^2.* ...
(egf.^2+(egf+k5).*k6).*k7.*k8).*k9).*rtot)).^(1/2)+k1.^2.*k7.*k8.* ...
(2.*(1+k2).^2.*k3.^2.*k4.^2.*k5.^2.*k6.*k9+(-2).*k5.*(k1.^2.*k4.* ...
k5.*k6.*k7.*k8.*k9.*((1+k1).^2.*(egf+k3+k2.*k3).^2.*k4.*k5.*k6.* ...
k7.*k8.*k9+8.*k3.^2.*(egf.^2.*k4.*k5.*k6+(egf.*k4.*k5.*k6+k4.*k5.* ...
k6.*k8+k1.^2.*k7.*k8).*k9).*rtot)).^(1/2)+k1.^2.*k4.*k5.*k6.* ...
k7.*k8.*k9.*((1+k1).^2.*(egf+k3+k2.*k3).^2.*k4.*k5.*k6.*k7.*k8.* ...
k9+8.*k3.^2.*(egf.^2.*k4.*k5.*k6+(egf.*k4.*k5.*k6+k4.*k5.*k6.*k8+ ...
k1.^2.*(egf.^2+(egf+k5).*k6).*k7.*k8).*k9).*rtot)).^(1/2)))+ ...
k1.^3.*k7.*k8.*(k3.^2.*k4.*k5.*k6.*k9.*((1+k2).^2.*(k4.*k5+k7.*k8) ...
+4.*(k5+k8).*rtot)+(-2).*k5.*(k1.^2.*k4.*k5.*k6.*k7.*k8.*k9.*((1+ ...
k1).^2.*(egf+k3+k2.*k3).^2.*k4.*k5.*k6.*k7.*k8.*k9+8.*k3.^2.*( ...
egf.^2.*k4.*k5.*k6+(egf.*k4.*k5.*k6+k4.*k5.*k6.*k8+k1.^2.*(egf.^2+ ...
(egf+k5).*k6).*k7.*k8).*k9).*rtot)).^(1/2)+(1+k2).*k3.*((-2).*k4.* ...
k5.^2.*k6.*(k4+k7).*k8.*k9+(k1.^2.*k4.*k5.*k6.*k7.*k8.*k9.*((1+k1) ...
.^2.*(egf+k3+k2.*k3).^2.*k4.*k5.*k6.*k7.*k8.*k9+8.*k3.^2.*( ...
egf.^2.*k4.*k5.*k6+(egf.*k4.*k5.*k6+k4.*k5.*k6.*k8+k1.^2.*(egf.^2+ ...
(egf+k5).*k6).*k7.*k8).*k9).*rtot)).^(1/2))+k1.*k4.*k5.*(k3.^2.* ...
k4.*k5.*k6.*k8.*k9.*((1+k2).^2.*k7+4.*rtot))+(-2).*k8.*(k1.^2.*k4.* ...
k5.*k6.*k7.*k8.*k9.*((1+k1).^2.*(egf+k3+k2.*k3).^2.*k4.*k5.*k6.* ...
k7.*k8.*k9+8.*k3.^2.*(egf.^2.*k4.*k5.*k6+(egf.*k4.*k5.*k6+k4.*k5.* ...
k6.*k8+k1.^2.*(egf.^2+(egf+k5).*k6).*k7.*k8).*k9).*rtot)).^(1/2)+ ...
(1+k2).*k3.*((-2).*k4.*k5.*k6.*k7.*k8.^2.*k9+(k1.^2.*k4.*k5.*k6.* ...
k7.*k8.*k9.*((1+k1).^2.*(egf+k3+k2.*k3).^2.*k4.*k5.*k6.*k7.*k8.* ...
k9+8.*k3.^2.*(egf.^2.*k4.*k5.*k6+(egf.*k4.*k5.*k6+k4.*k5.*k6.*k8+ ...
k1.^2.*(egf.^2+(egf+k5).*k6).*k7.*k8).*k9).*rtot)).^(1/2)))+egf.* ...
(4.*k1.^4.*k4.*k5.*k6.*((1+k2).^2.*k3.^2+(-1).*k5.*k6).*k7.^2.* ...
k8.^2.*k9.^2+k4.*k5.*k6.*(2.*(1+k2).*k3+(-1).*k9).*(k1.^2.*k4.* ...
k5.*k6.*k7.*k8.*k9.*((1+k1).^2.*(egf+k3+k2.*k3).^2.*k4.*k5.*k6.* ...
k7.*k8.*k9+8.*k3.^2.*(egf.^2.*k4.*k5.*k6+(egf.*k4.*k5.*k6+k4.*k5.* ...
k6.*k8+k1.^2.*(egf.^2+(egf+k5).*k6).*k7.*k8).*k9).*rtot)).^(1/2)+ ...
2.*k1.^5.*k6.*k7.^2.*k8.^2.*k9.^2.*((-1).*k4.*k5.^2.*k6+k3.^2.*(( ...
1+k2).^2.*k4.*k5+2.*(2.*k5+k6).*rtot))+k1.^3.*k7.*k8.*k9.*(2.* ...
k3.^2.*k4.*k5.*k6.*((1+k2).^2.*(k4.*k5.*k6+k7.*k8.*k9)+4.*(k5.*k6+ ...
(k6+k8).*k9).*rtot)+2.*(1+k2).*k3.*(k1.^2.*k4.*k5.*k6.*k7.*k8.* ...
k9.*((1+k1).^2.*(egf+k3+k2.*k3).^2.*k4.*k5.*k6.*k7.*k8.*k9+8.* ...
k3.^2.*(egf.^2.*k4.*k5.*k6+(egf.*k4.*k5.*k6+k4.*k5.*k6.*k8+k1.^2.* ...
(egf.^2+(egf+k5).*k6).*k7.*k8).*k9).*rtot)).^(1/2)+k6.*((-2).*k4.* ...
k5.^2.*k6.*(k4+k7).*k8.*k9+(-1).*(k1.^2.*k4.*k5.*k6.*k7.*k8.*k9.* ...
(1+k1).^2.*(egf+k3+k2.*k3).^2.*k4.*k5.*k6.*k7.*k8.*k9+8.*k3.^2.*( ...
egf.^2.*k4.*k5.*k6+(egf.*k4.*k5.*k6+k4.*k5.*k6.*k8+k1.^2.*(egf.^2+ ...
(egf+k5).*k6).*k7.*k8).*k9).*rtot)).^(1/2))+k1.^2.*k7.*k8.*k9.* ...
4.*(1+k2).^2.*k3.^2.*k4.^2.*k5.^2.*k6.^2+2.*(1+k2).*k3.*(k1.^2.* ...
k4.*k5.*k6.*k7.*k8.*k9.*((1+k1).^2.*(egf+k3+k2.*k3).^2.*k4.*k5.*

```

$$\begin{aligned}
& k6.*k7.*k8.*k9+8.*k3.^2.*(egf.^2.*k4.*k5.*k6+(egf.*k4.*k5.*k6+k4.* \\
& k5.*k6.*k8+k1.^2.*(egf.^2+(egf+k5).*k6).*k7.*k8).*k9).^2.*(1/2)+(-1).*k6.*(4.*k4.^2.*k5.^2.*k6.*k8.*k9+(k1.^2.*k4.*k5.*k6.* \\
& k7.*k8.*k9.*((1+k1).^2.*(egf+k3+k2.*k3).^2.*k4.*k5.*k6.*k7.*k8.* \\
& k9+8.*k3.^2.*(egf.^2.*k4.*k5.*k6+(egf.*k4.*k5.*k6+k4.*k5.*k6.*k8+ \\
& k1.^2.*(egf.^2+(egf+k5).*k6).*k7.*k8).*k9).^2.*(1/2)))+k1.* \\
& k4.*k5.*k6.*(2.*k3.^2.*k4.*k5.*k6.*k9.*((1+k2).^2.*k7.*k8+2.*(2.* \\
& k8+k9).*rtot)+2.*(1+k2).*k3.*(k1.^2.*k4.*k5.*k6.*k7.*k8.*k9.*((1+ \\
& k1).^2.*(egf+k3+k2.*k3).^2.*k4.*k5.*k6.*k7.*k8.*k9+8.*k3.^2.*(\\
& egf.^2.*k4.*k5.*k6+(egf.*k4.*k5.*k6+k4.*k5.*k6.*k8+k1.^2.*(egf.^2+ \\
& (egf+k5).*k6).*k7.*k8).*k9).^2.*(1/2)+(-1).*k9.*(2.*k4.*k5.* \\
& k6.*k7.*k8.^2.*k9+(k1.^2.*k4.*k5.*k6.*k7.*k8.*k9.*((1+k1).^2.*(\\
& egf+k3+k2.*k3).^2.*k4.*k5.*k6.*k7.*k8.*k9+8.*k3.^2.*(egf.^2.*k4.* \\
& k5.*k6+(egf.*k4.*k5.*k6+k4.*k5.*k6.*k8+k1.^2.*(egf.^2+(egf+k5).* \\
& k6).*k7.*k8).*k9).^2.*(1/2)))));
\end{aligned}$$

$$\begin{aligned}
cil &= (1/4).*k2.*k3.^{(-1)}.*(egf.^2.*k4.*k5.*k6+(egf.*k4.*k5.*k6+k4.*k5.* \\
& k6.*k8+k1.^2.*(egf.^2+(egf+k5).*k6).*k7.*k8).*k9)^{(-1)}.*((-1).* \\
& k1.*(1+k1).*(egf+k3+k2.*k3).*k4.*k5.*k6.*k7.*k8.*k9+(-1).*(k1.^2.* \\
& k4.*k5.*k6.*k7.*k8.*k9.*((1+k1).^2.*(egf+k3+k2.*k3).^2.*k4.*k5.* \\
& k6.*k7.*k8.*k9+8.*k3.^2.*(egf.^2.*k4.*k5.*k6+(egf.*k4.*k5.*k6+k4.* \\
& k5.*k6.*k8+k1.^2.*(egf.^2+(egf+k5).*k6).*k7.*k8).*k9).^2.*(1/2)));
\end{aligned}$$

$$\begin{aligned}
cal &= (1/4).*k1.^{(-1)}.*k2.*k3.^{(-1)}.*(egf.^2.*k4.*k5.*k6+(egf.*k4.*k5.* \\
& k6+k4.*k5.*k6.*k8+k1.^2.*(egf.^2+(egf+k5).*k6).*k7.*k8).*k9)^{(-1)}.* \\
& *((-1).*k1.*(1+k1).*(egf+k3+k2.*k3).*k4.*k5.*k6.*k7.*k8.*k9+(-1).* \\
& *(k1.^2.*k4.*k5.*k6.*k7.*k8.*k9.*((1+k1).^2.*(egf+k3+k2.*k3).^2.* \\
& k4.*k5.*k6.*k7.*k8.*k9+8.*k3.^2.*(egf.^2.*k4.*k5.*k6+(egf.*k4.* \\
& k5.*k6+k4.*k5.*k6.*k8+k1.^2.*(egf.^2+(egf+k5).*k6).*k7.*k8).*k9).* \\
& rtot)).^2.*(1/2));
\end{aligned}$$

$$\begin{aligned}
eil &= (-1/4).*k3.^{(-1)}.*(egf.^2.*k4.*k5.*k6+(egf.*k4.*k5.*k6+k4.*k5.* \\
& k6.*k8+k1.^2.*(egf.^2+(egf+k5).*k6).*k7.*k8).*k9)^{(-1)}.*(k1.*(1+ \\
& k1).*(egf+k3+k2.*k3).*k4.*k5.*k6.*k7.*k8.*k9+(k1.^2.*k4.*k5.*k6.* \\
& k7.*k8.*k9.*((1+k1).^2.*(egf+k3+k2.*k3).^2.*k4.*k5.*k6.*k7.*k8.* \\
& k9+8.*k3.^2.*(egf.^2.*k4.*k5.*k6+(egf.*k4.*k5.*k6+k4.*k5.*k6.*k8+ \\
& k1.^2.*(egf.^2+(egf+k5).*k6).*k7.*k8).*k9).^2.*(1/2)));
\end{aligned}$$

$$\begin{aligned}
eal &= (-1/4).*k1.^{(-1)}.*k3.^{(-1)}.*(egf.^2.*k4.*k5.*k6+(egf.*k4.*k5.*k6+ \\
& k4.*k5.*k6.*k8+k1.^2.*(egf.^2+(egf+k5).*k6).*k7.*k8).*k9)^{(-1)}.*(\\
& k1.*(1+k1).*(egf+k3+k2.*k3).*k4.*k5.*k6.*k7.*k8.*k9+(k1.^2.*k4.* \\
& k5.*k6.*k7.*k8.*k9.*((1+k1).^2.*(egf+k3+k2.*k3).^2.*k4.*k5.*k6.* \\
& k7.*k8.*k9+8.*k3.^2.*(egf.^2.*k4.*k5.*k6+(egf.*k4.*k5.*k6+k4.*k5.* \\
& k6.*k8+k1.^2.*(egf.^2+(egf+k5).*k6).*k7.*k8).*k9).^2.*(1/2)));
\end{aligned}$$

$$\begin{aligned}
eill &= (1/4).*egf.*k3.^{(-2)}.*(egf.^2.*k4.*k5.*k6+(egf.*k4.*k5.*k6+k4.* \\
& k5.*k6.*k8+k1.^2.*(egf.^2+(egf+k5).*k6).*k7.*k8).*k9)^{(-1)}.*((-1).* \\
& *k1.*(1+k1).*(egf+k3+k2.*k3).*k4.*k5.*k6.*k7.*k8.*k9+(-1).*(
\end{aligned}$$


```

k1.^2.*k4.*k5.*k6.*k7.*k8.*k9.*( (1+k1).^2.*(egf+k3+k2.*k3).^2.* ...
k4.*k5.*k6.*k7.*k8.*k9+8.*k3.^2.*(egf.^2.*k4.*k5.*k6+(egf.*k4.* ...
k5.*k6+k4.*k5.*k6.*k8+k1.^2.*(egf.^2+(egf+k5).*k6).*k7.*k8).*k9).* ...
rtot)).^(1/2));

```

```

eall=(1/4).*egf.*k1.^(-1).*k3.^(-2).* (egf.^2.*k4.*k5.*k6+(egf.*k4.*k5.* ...
k6+k4.*k5.*k6.*k8+k1.^2.*(egf.^2+(egf+k5).*k6).*k7.*k8).*k9).^(-1) ...
.*((-1).*k1.*(1+k1)).*(egf+k3+k2.*k3).*k4.*k5.*k6.*k7.*k8.*k9+(-1) ...
.*(k1.^2.*k4.*k5.*k6.*k7.*k8.*k9.*( (1+k1).^2.*(egf+k3+k2.*k3).^2.* ...
k4.*k5.*k6.*k7.*k8.*k9+8.*k3.^2.*(egf.^2.*k4.*k5.*k6+(egf.*k4.* ...
k5.*k6+k4.*k5.*k6.*k8+k1.^2.*(egf.^2+(egf+k5).*k6).*k7.*k8).*k9).* ...
rtot)).^(1/2));

```

```

des1=(1/8).*k1.*k5.*k6.*k7.*k8.*k9.*(egf.^2.*k3.*k4.*k5.*k6+k3.*(egf.* ...
k4.*k5.*k6+k4.*k5.*k6.*k8+k1.^2.*(egf.^2+(egf+k5).*k6).*k7.*k8).* ...
k9).^(-2).* (egf.^2.*k1.*( (1+k1).^2.*k4.*k5.*k6.*k7.*k8.*k9+4.* ...
k3.^2.*(k4.*k5.*k6+k1.^2.*k7.*k8.*k9).*rtot)+k3.*(2.*k1.^2.*(1+k2) ...
.^2.*k3.*k4.*k5.*k6.*k7.*k8.*k9+k1.^3.*k3.*k5.*k6.*k7.*k8.*k9.*( ...
1+k2).^2.*k4+4.*rtot)+k1.*k3.*k4.*k5.*k6.*k8.*k9.*( (1+k2).^2.*k7+ ...
4.*rtot)+(1+k2)).*(k1.^2.*k4.*k5.*k6.*k7.*k8.*k9.*( (1+k1).^2.*(egf+ ...
k3+k2.*k3).^2.*k4.*k5.*k6.*k7.*k8.*k9+8.*k3.^2.*(egf.^2.*k4.*k5.* ...
k6+(egf.*k4.*k5.*k6+k4.*k5.*k6.*k8+k1.^2.*(egf.^2+(egf+k5).*k6).* ...
k7.*k8).*k9).*rtot)).^(1/2)+k1.*(1+k2)).*(k1.^2.*k4.*k5.*k6.*k7.* ...
k8.*k9.*( (1+k1).^2.*(egf+k3+k2.*k3).^2.*k4.*k5.*k6.*k7.*k8.*k9+8.* ...
k3.^2.*(egf.^2.*k4.*k5.*k6+(egf.*k4.*k5.*k6+k4.*k5.*k6.*k8+k1.^2.* ...
(egf.^2+(egf+k5).*k6).*k7.*k8).*k9).*rtot)).^(1/2))+egf.*( (k1.^2.* ...
k4.*k5.*k6.*k7.*k8.*k9.*( (1+k1).^2.*(egf+k3+k2.*k3).^2.*k4.*k5.* ...
k6.*k7.*k8.*k9+8.*k3.^2.*(egf.^2.*k4.*k5.*k6+(egf.*k4.*k5.*k6+k4.* ...
k5.*k6.*k8+k1.^2.*(egf.^2+(egf+k5).*k6).*k7.*k8).*k9).*rtot)).^( ...
1/2)+k1.*(2.*k3.*k6.*k9.*( (1+k1).^2.*(1+k2)).*k4.*k5.*k7.*k8+2.* ...
k3.*(k4.*k5+k1.^2.*k7.*k8).*rtot)+(k1.^2.*k4.*k5.*k6.*k7.*k8.*k9.* ...
((1+k1).^2.*(egf+k3+k2.*k3).^2.*k4.*k5.*k6.*k7.*k8.*k9+8.*k3.^2.*( ...
egf.^2.*k4.*k5.*k6+(egf.*k4.*k5.*k6+k4.*k5.*k6.*k8+k1.^2.*(egf.^2+ ...
(egf+k5).*k6).*k7.*k8).*k9).*rtot)).^(1/2)))));

```

```

deall=(1/8).*k1.^(-1).*k4.*k5.*k6.*k8.*k9.*(egf.^2.*k3.*k4.*k5.*k6+k3.*( ...
egf.*k4.*k5.*k6+k4.*k5.*k6.*k8+k1.^2.*(egf.^2+(egf+k5).*k6).*k7.* ...
k8).*k9).^(-2).* (egf.^2.*k1.*( (1+k1).^2.*k4.*k5.*k6.*k7.*k8.*k9+ ...
4.*k3.^2.*(k4.*k5.*k6+k1.^2.*k7.*k8.*k9).*rtot)+k3.*(2.*k1.^2.*(1+ ...
k2).^2.*k3.*k4.*k5.*k6.*k7.*k8.*k9+k1.^3.*k3.*k5.*k6.*k7.*k8.*k9.* ...
((1+k2).^2.*k4+4.*rtot)+k1.*k3.*k4.*k5.*k6.*k8.*k9.*( (1+k2).^2.* ...
k7+4.*rtot)+(1+k2)).*(k1.^2.*k4.*k5.*k6.*k7.*k8.*k9.*( (1+k1).^2.*( ...
egf+k3+k2.*k3).^2.*k4.*k5.*k6.*k7.*k8.*k9+8.*k3.^2.*(egf.^2.*k4.* ...
k5.*k6+(egf.*k4.*k5.*k6+k4.*k5.*k6.*k8+k1.^2.*(egf.^2+(egf+k5).* ...
k6).*k7.*k8).*k9).*rtot)).^(1/2)+k1.*(1+k2)).*(k1.^2.*k4.*k5.*k6.* ...
k7.*k8.*k9.*( (1+k1).^2.*(egf+k3+k2.*k3).^2.*k4.*k5.*k6.*k7.*k8.* ...
k9+8.*k3.^2.*(egf.^2.*k4.*k5.*k6+(egf.*k4.*k5.*k6+k4.*k5.*k6.*k8+ ...
k1.^2.*(egf.^2+(egf+k5).*k6).*k7.*k8).*k9).*rtot)).^(1/2))+egf.*( ...
k1.^2.*k4.*k5.*k6.*k7.*k8.*k9.*( (1+k1).^2.*(egf+k3+k2.*k3).^2.* ...
k4.*k5.*k6.*k7.*k8.*k9+8.*k3.^2.*(egf.^2.*k4.*k5.*k6+(egf.*k4.* ...
k5.*k6+k4.*k5.*k6.*k8+k1.^2.*(egf.^2+(egf+k5).*k6).*k7.*k8).*k9).* ...
rtot)).^(1/2)+k1.*(2.*k3.*k6.*k9.*( (1+k1).^2.*(1+k2)).*k4.*k5.*k7.* ...
k8+2.*k3.*(k4.*k5+k1.^2.*k7.*k8).*rtot)+(k1.^2.*k4.*k5.*k6.*k7.* ...

```

```

k8.*k9.*((1+k1).^2.*(egf+k3+k2.*k3).^2.*k4.*k5.*k6.*k7.*k8.*k9+8.* ...
k3.^2.*(egf.^2.*k4.*k5.*k6+(egf.*k4.*k5.*k6+k4.*k5.*k6.*k8+k1.^2.* ...
(egf.^2+(egf+k5).*k6).*k7.*k8).*k9).*rtot)).^(1/2)))));

```

```

des11=(1/8).*egf.*k1.*k6.*k7.*k8.*k9.*(egf.^2.*k3.*k4.*k5.*k6+k3.*(egf.* ...
k4.*k5.*k6+k4.*k5.*k6.*k8+k1.^2.*(egf.^2+(egf+k5).*k6).*k7.*k8).* ...
k9).^(-2).*(egf.^2.*k1.*((1+k1).^2.*k4.*k5.*k6.*k7.*k8.*k9+4.* ...
k3.^2.*(k4.*k5.*k6+k1.^2.*k7.*k8.*k9).*rtot)+k3.*(2.*k1.^2.*(1+k2) ...
.^2.*k3.*k4.*k5.*k6.*k7.*k8.*k9+k1.^3.*k3.*k5.*k6.*k7.*k8.*k9.*(( ...
1+k2).^2.*k4+4.*rtot)+k1.*k3.*k4.*k5.*k6.*k8.*k9.*((1+k2).^2.*k7+ ...
4.*rtot)+(1+k2).*(k1.^2.*k4.*k5.*k6.*k7.*k8.*k9.*((1+k1).^2.*(egf+ ...
k3+k2.*k3).^2.*k4.*k5.*k6.*k7.*k8.*k9+8.*k3.^2.*(egf.^2.*k4.*k5.* ...
k6+(egf.*k4.*k5.*k6+k4.*k5.*k6.*k8+k1.^2.*(egf.^2+(egf+k5).*k6).* ...
k7.*k8).*k9).*rtot)).^(1/2)+k1.*(1+k2).*(k1.^2.*k4.*k5.*k6.*k7.* ...
k8.*k9.*((1+k1).^2.*(egf+k3+k2.*k3).^2.*k4.*k5.*k6.*k7.*k8.*k9+8.* ...
k3.^2.*(egf.^2.*k4.*k5.*k6+(egf.*k4.*k5.*k6+k4.*k5.*k6.*k8+k1.^2.* ...
(egf.^2+(egf+k5).*k6).*k7.*k8).*k9).*rtot)).^(1/2))+egf.*((k1.^2.* ...
k4.*k5.*k6.*k7.*k8.*k9.*((1+k1).^2.*(egf+k3+k2.*k3).^2.*k4.*k5.* ...
k6.*k7.*k8.*k9+8.*k3.^2.*(egf.^2.*k4.*k5.*k6+(egf.*k4.*k5.*k6+k4.* ...
k5.*k6.*k8+k1.^2.*(egf.^2+(egf+k5).*k6).*k7.*k8).*k9).*rtot)).^( ...
1/2)+k1.*(2.*k3.*k6.*k9.*((1+k1).^2.*(1+k2).*k4.*k5.*k7.*k8+2.* ...
k3.*(k4.*k5+k1.^2.*k7.*k8).*rtot)+(k1.^2.*k4.*k5.*k6.*k7.*k8.*k9.* ...
((1+k1).^2.*(egf+k3+k2.*k3).^2.*k4.*k5.*k6.*k7.*k8.*k9+8.*k3.^2.*( ...
egf.^2.*k4.*k5.*k6+(egf.*k4.*k5.*k6+k4.*k5.*k6.*k8+k1.^2.*(egf.^2+ ...
(egf+k5).*k6).*k7.*k8).*k9).*rtot)).^(1/2)))));

```

```

des211=(1/8).*egf.^2.*k1.*k7.*k8.*k9.*(egf.^2.*k3.*k4.*k5.*k6+k3.*(egf.* ...
k4.*k5.*k6+k4.*k5.*k6.*k8+k1.^2.*(egf.^2+(egf+k5).*k6).*k7.*k8).* ...
k9).^(-2).*(egf.^2.*k1.*((1+k1).^2.*k4.*k5.*k6.*k7.*k8.*k9+4.* ...
k3.^2.*(k4.*k5.*k6+k1.^2.*k7.*k8.*k9).*rtot)+k3.*(2.*k1.^2.*(1+k2) ...
.^2.*k3.*k4.*k5.*k6.*k7.*k8.*k9+k1.^3.*k3.*k5.*k6.*k7.*k8.*k9.*(( ...
1+k2).^2.*k4+4.*rtot)+k1.*k3.*k4.*k5.*k6.*k8.*k9.*((1+k2).^2.*k7+ ...
4.*rtot)+(1+k2).*(k1.^2.*k4.*k5.*k6.*k7.*k8.*k9.*((1+k1).^2.*(egf+ ...
k3+k2.*k3).^2.*k4.*k5.*k6.*k7.*k8.*k9+8.*k3.^2.*(egf.^2.*k4.*k5.* ...
k6+(egf.*k4.*k5.*k6+k4.*k5.*k6.*k8+k1.^2.*(egf.^2+(egf+k5).*k6).* ...
k7.*k8).*k9).*rtot)).^(1/2)+k1.*(1+k2).*(k1.^2.*k4.*k5.*k6.*k7.* ...
k8.*k9.*((1+k1).^2.*(egf+k3+k2.*k3).^2.*k4.*k5.*k6.*k7.*k8.*k9+8.* ...
k3.^2.*(egf.^2.*k4.*k5.*k6+(egf.*k4.*k5.*k6+k4.*k5.*k6.*k8+k1.^2.* ...
(egf.^2+(egf+k5).*k6).*k7.*k8).*k9).*rtot)).^(1/2))+egf.*((k1.^2.* ...
k4.*k5.*k6.*k7.*k8.*k9.*((1+k1).^2.*(egf+k3+k2.*k3).^2.*k4.*k5.* ...
k6.*k7.*k8.*k9+8.*k3.^2.*(egf.^2.*k4.*k5.*k6+(egf.*k4.*k5.*k6+k4.* ...
k5.*k6.*k8+k1.^2.*(egf.^2+(egf+k5).*k6).*k7.*k8).*k9).*rtot)).^( ...
1/2)+k1.*(2.*k3.*k6.*k9.*((1+k1).^2.*(1+k2).*k4.*k5.*k7.*k8+2.* ...
k3.*(k4.*k5+k1.^2.*k7.*k8).*rtot)+(k1.^2.*k4.*k5.*k6.*k7.*k8.*k9.* ...
((1+k1).^2.*(egf+k3+k2.*k3).^2.*k4.*k5.*k6.*k7.*k8.*k9+8.*k3.^2.*( ...
egf.^2.*k4.*k5.*k6+(egf.*k4.*k5.*k6+k4.*k5.*k6.*k8+k1.^2.*(egf.^2+ ...
(egf+k5).*k6).*k7.*k8).*k9).*rtot)).^(1/2)))));

```

```

deall1=(1/8).*egf.*k1.^(-1).*k4.*k5.*k6.*k9.*(egf.^2.*k3.*k4.*k5.*k6+k3.* ...
(egf.*k4.*k5.*k6+k4.*k5.*k6.*k8+k1.^2.*(egf.^2+(egf+k5).*k6).*k7.* ...
k8).*k9).^(-2).*(egf.^2.*k1.*((1+k1).^2.*k4.*k5.*k6.*k7.*k8.*k9+ ...
4.*k3.^2.*(k4.*k5.*k6+k1.^2.*k7.*k8.*k9).*rtot)+k3.*(2.*k1.^2.*(1+ ...
k2).^2.*k3.*k4.*k5.*k6.*k7.*k8.*k9+k1.^3.*k3.*k5.*k6.*k7.*k8.*k9.* ...

```

```

((1+k2).^2.*k4+4.*rtot)+k1.*k3.*k4.*k5.*k6.*k8.*k9.*((1+k2).^2.* ...
k7+4.*rtot)+(1+k2).*(k1.^2.*k4.*k5.*k6.*k7.*k8.*k9.*((1+k1).^2.*( ...
egf+k3+k2.*k3).^2.*k4.*k5.*k6.*k7.*k8.*k9+8.*k3.^2.*(egf.^2.*k4.* ...
k5.*k6+(egf.*k4.*k5.*k6+k4.*k5.*k6.*k8+k1.^2.*(egf.^2+(egf+k5).* ...
k6).*k7.*k8).*k9).*rtot)).^(1/2)+k1.*(1+k2).*(k1.^2.*k4.*k5.*k6.* ...
k7.*k8.*k9.*((1+k1).^2.*(egf+k3+k2.*k3).^2.*k4.*k5.*k6.*k7.*k8.* ...
k9+8.*k3.^2.*(egf.^2.*k4.*k5.*k6+(egf.*k4.*k5.*k6+k4.*k5.*k6.*k8+ ...
k1.^2.*(egf.^2+(egf+k5).*k6).*k7.*k8).*k9).*rtot)).^(1/2))+egf.*(( ...
k1.^2.*k4.*k5.*k6.*k7.*k8.*k9.*((1+k1).^2.*(egf+k3+k2.*k3).^2.* ...
k4.*k5.*k6.*k7.*k8.*k9+8.*k3.^2.*(egf.^2.*k4.*k5.*k6+(egf.*k4.* ...
k5.*k6+k4.*k5.*k6.*k8+k1.^2.*(egf.^2+(egf+k5).*k6).*k7.*k8).*k9).* ...
rtot)).^(1/2)+k1.*(2.*k3.*k6.*k9.*((1+k1).^2.*(1+k2).*k4.*k5.*k7.* ...
k8+2.*k3.*(k4.*k5+k1.^2.*k7.*k8).*rtot)+(k1.^2.*k4.*k5.*k6.*k7.* ...
k8.*k9.*((1+k1).^2.*(egf+k3+k2.*k3).^2.*k4.*k5.*k6.*k7.*k8.*k9+8.* ...
k3.^2.*(egf.^2.*k4.*k5.*k6+(egf.*k4.*k5.*k6+k4.*k5.*k6.*k8+k1.^2.* ...
(egf.^2+(egf+k5).*k6).*k7.*k8).*k9).*rtot)).^(1/2)))));

dea2l1=(1/8).*egf.^2.*k1.^(-1).*k4.*k5.*k6.*(egf.^2.*k3.*k4.*k5.*k6+k3.*( ...
egf.*k4.*k5.*k6+k4.*k5.*k6.*k8+k1.^2.*(egf.^2+(egf+k5).*k6).*k7.* ...
k8).*k9).^(-2).*(egf.^2.*k1.*((1+k1).^2.*k4.*k5.*k6.*k7.*k8.*k9+ ...
4.*k3.^2.*(k4.*k5.*k6+k1.^2.*k7.*k8.*k9).*rtot)+k3.*(2.*k1.^2.*(1+ ...
k2).^2.*k3.*k4.*k5.*k6.*k7.*k8.*k9+k1.^3.*k3.*k5.*k6.*k7.*k8.*k9.* ...
((1+k2).^2.*k4+4.*rtot)+k1.*k3.*k4.*k5.*k6.*k8.*k9.*((1+k2).^2.* ...
k7+4.*rtot)+(1+k2).*(k1.^2.*k4.*k5.*k6.*k7.*k8.*k9.*((1+k1).^2.*( ...
egf+k3+k2.*k3).^2.*k4.*k5.*k6.*k7.*k8.*k9+8.*k3.^2.*(egf.^2.*k4.* ...
k5.*k6+(egf.*k4.*k5.*k6+k4.*k5.*k6.*k8+k1.^2.*(egf.^2+(egf+k5).* ...
k6).*k7.*k8).*k9).*rtot)).^(1/2)+k1.*(1+k2).*(k1.^2.*k4.*k5.*k6.* ...
k7.*k8.*k9.*((1+k1).^2.*(egf+k3+k2.*k3).^2.*k4.*k5.*k6.*k7.*k8.* ...
k9+8.*k3.^2.*(egf.^2.*k4.*k5.*k6+(egf.*k4.*k5.*k6+k4.*k5.*k6.*k8+ ...
k1.^2.*(egf.^2+(egf+k5).*k6).*k7.*k8).*k9).*rtot)).^(1/2))+egf.*(( ...
k1.^2.*k4.*k5.*k6.*k7.*k8.*k9.*((1+k1).^2.*(egf+k3+k2.*k3).^2.* ...
k4.*k5.*k6.*k7.*k8.*k9+8.*k3.^2.*(egf.^2.*k4.*k5.*k6+(egf.*k4.* ...
k5.*k6+k4.*k5.*k6.*k8+k1.^2.*(egf.^2+(egf+k5).*k6).*k7.*k8).*k9).* ...
rtot)).^(1/2)+k1.*(2.*k3.*k6.*k9.*((1+k1).^2.*(1+k2).*k4.*k5.*k7.* ...
k8+2.*k3.*(k4.*k5+k1.^2.*k7.*k8).*rtot)+(k1.^2.*k4.*k5.*k6.*k7.* ...
k8.*k9.*((1+k1).^2.*(egf+k3+k2.*k3).^2.*k4.*k5.*k6.*k7.*k8.*k9+8.* ...
k3.^2.*(egf.^2.*k4.*k5.*k6+(egf.*k4.*k5.*k6+k4.*k5.*k6.*k8+k1.^2.* ...
(egf.^2+(egf+k5).*k6).*k7.*k8).*k9).*rtot)).^(1/2)))));

% second series of roots
egfbound2=(1/8).*egf.*k1.^(-1).*(egf.^2.*k3.*k4.*k5.*k6+k3.*(egf.*k4.*k5.*
...
k6+k4.*k5.*k6.*k8+k1.^2.*(egf.^2+(egf+k5).*k6).*k7.*k8).*k9).^(-2) ...
.*(8.*egf.^3.*k1.*k3.^2.*(k4.*k5.*k6+k1.^2.*k7.*k8.*k9).^2.*rtot+ ...
egf.^2.*k1.*k6.*k9.*((-1).*(1+k1).^2.*k4.*k5.*k6.*k7.*k8).*(k4.*k5+ ...
k1.^2.*k7.*k8).*k9+2.*(1+k1).^2.*(1+k2).*k3.*k4.*k5.*k7.*k8).*(k4.* ...
k5.*k6+k1.^2.*k7.*k8.*k9)+12.*k3.^2.*(k4.*k5+k1.^2.*k7.*k8).*(k4.* ...
k5.*k6+k1.^2.*k7.*k8.*k9).*rtot)+egf.*(4.*k1.^4.*k4.*k5.*k6.*((1+ ...
k2).^2.*k3.^2+(-1).*k5.*k6).*k7.^2.*k8.^2.*k9.^2+k4.*k5.*k6.*((-2) ...
.*(1+k2).*k3+k9).*(k1.^2.*k4.*k5.*k6.*k7.*k8.*k9.*((1+k1).^2.*( ...
egf+k3+k2.*k3).^2.*k4.*k5.*k6.*k7.*k8.*k9+8.*k3.^2.*(egf.^2.*k4.* ...
k5.*k6+(egf.*k4.*k5.*k6+k4.*k5.*k6.*k8+k1.^2.*(egf.^2+(egf+k5).* ...
k6).*k7.*k8).*k9).*rtot)).^(1/2)+2.*k1.^5.*k6.*k7.^2.*k8.^2.* ...
k9.^2.*((-1).*k4.*k5.^2.*k6+k3.^2.*(1+k2).^2.*k4.*k5+2.*(2.*k5+ ...
k6).*rtot))+k1.^2.*k7.*k8.*k9.*(4.*(1+k2).^2.*k3.^2.*k4.^2.* ...
k5.^2.*k6.^2+(-2).*(1+k2).*k3.*(k1.^2.*k4.*k5.*k6.*k7.*k8.*k9.*((

```

```

(1+k1).^2.*(egf+k3+k2.*k3).^2.*k4.*k5.*k6.*k7.*k8.*k9+8.*k3.^2.*(egf.^2.*k4.*k5.*k6+(egf.*k4.*k5.*k6+k4.*k5.*k6.*k8+k1.^2.*(egf.^2+(egf+k5).*k6).*k7.*k8).*k9).*rtot)).^(1/2)+k6.*((-4).*k4.^2.*k5.^2.*k6.*k8.*k9+(k1.^2.*k4.*k5.*k6.*k7.*k8.*k9.*((1+k1).^2.*(egf+k3+k2.*k3).^2.*k4.*k5.*k6.*k7.*k8.*k9+8.*k3.^2.*(egf.^2.*k4.*k5.*k6+(egf.*k4.*k5.*k6+k4.*k5.*k6.*k8+k1.^2.*(egf.^2+(egf+k5).*k6).*k7.*k8).*k9).*rtot)).^(1/2)))+k1.^3.*k7.*k8.*k9.*(2.*k3.^2.*k4.*k5.*k6.*((1+k2).^2.*(k4.*k5.*k6+k7.*k8.*k9)+4.*(k5.*k6+(k6+k8).*k9).*rtot))+(-2).*(1+k2).*k3.*(k1.^2.*k4.*k5.*k6.*k7.*k8.*k9.*((1+k1).^2.*(egf+k3+k2.*k3).^2.*k4.*k5.*k6.*k7.*k8.*k9+8.*k3.^2.*(egf.^2.*k4.*k5.*k6+(egf.*k4.*k5.*k6+k4.*k5.*k6.*k8+k1.^2.*(egf.^2+(egf+k5).*k6).*k7.*k8).*k9).*rtot)).^(1/2)+k6.*((-2).*k4.*k5.^2.*k6.*(k4+k7)).*k8.*k9+(k1.^2.*k4.*k5.*k6.*k7.*k8.*k9.*((1+k1).^2.*(egf+k3+k2.*k3).^2.*k4.*k5.*k6.*k7.*k8.*k9+8.*k3.^2.*(egf.^2.*k4.*k5.*k6+(egf.*k4.*k5.*k6+k4.*k5.*k6.*k8+k1.^2.*(egf.^2+(egf+k5).*k6).*k7.*k8).*k9).*rtot)).^(1/2)))+k1.*k4.*k5.*k6.*(2.*k3.^2.*k4.*k5.*k6.*k9.*((1+k2).^2.*k7.*k8+2.*(2.*k8+k9).*rtot))+(-2).*(1+k2).*k3.*(k1.^2.*k4.*k5.*k6.*k7.*k8.*k9.*((1+k1).^2.*(egf+k3+k2.*k3).^2.*k4.*k5.*k6.*k7.*k8.*k9+8.*k3.^2.*(egf.^2.*k4.*k5.*k6+(egf.*k4.*k5.*k6+k4.*k5.*k6.*k8+k1.^2.*(egf.^2+(egf+k5).*k6).*k7.*k8).*k9).*rtot)).^(1/2)+k9.*((-2).*k4.*k5.*k6.*k7.*k8.^2.*k9+(k1.^2.*k4.*k5.*k6.*k7.*k8.*k9.*((1+k1).^2.*(egf+k3+k2.*k3).^2.*k4.*k5.*k6+(egf.*k4.*k5.*k6+k4.*k5.*k6.*k8+k1.^2.*(egf.^2+(egf+k5).*k6).*k7.*k8).*k9).*rtot)).^(1/2)))+k1.^2.*k7.*k8.*(2.*(1+k2).^2.*k3.^2.*k4.^2.*k5.^2.*k6.*k9+2.*k5.*(k1.^2.*k4.*k5.*k6.*k7.*k8.*k9.*((1+k1).^2.*(egf+k3+k2.*k3).^2.*k4.*k5.*k6.*k7.*k8.*k9+8.*k3.^2.*(egf.^2.*k4.*k5.*k6+(egf.*k4.*k5.*k6+k4.*k5.*k6.*k8+k1.^2.*(egf.^2+(egf+k5).*k6).*k7.*k8).*k9).*rtot)).^(1/2))+(-1).*(1+k2).*k3.*(4.*k4.^2.*k5.^2.*k6.*k8.*k9+(k1.^2.*k4.*k5.*k6.*k7.*k8.*k9.*((1+k1).^2.*(egf+k3+k2.*k3).^2.*k4.*k5.*k6.*k7.*k8.*k9+8.*k3.^2.*(egf.^2.*k4.*k5.*k6+(egf.*k4.*k5.*k6+k4.*k5.*k6.*k8+k1.^2.*(egf.^2+(egf+k5).*k6).*k7.*k8).*k9).*rtot)).^(1/2))+(-1).*(1+k2).*k3.*(2.*k4.*k5.^2.*k6.*(k4+k7).*k8.*k9+(k1.^2.*k4.*k5.*k6.*k7.*k8.*k9.*((1+k1).^2.*(egf+k3+k2.*k3).^2.*k4.*k5.*k6.*k7.*k8.*k9+8.*k3.^2.*(egf.^2.*k4.*k5.*k6+(egf.*k4.*k5.*k6+k4.*k5.*k6.*k8+k1.^2.*(egf.^2+(egf+k5).*k6).*k7.*k8).*k9).*rtot)).^(1/2)))+k1.*k4.*k5.*(k3.^2.*k4.*k5.*k6.*k8.*k9.*((1+k2).^2.*k7+4.*rtot)+2.*k8.*(k1.^2.*k4.*k5.*k6.*k7.*k8.*k9.*((1+k1).^2.*(egf+k3+k2.*k3).^2.*k4.*k5.*k6.*k7.*k8.*k9+8.*k3.^2.*(egf.^2.*k4.*k5.*k6+(egf.*k4.*k5.*k6+k4.*k5.*k6.*k8+k1.^2.*(egf.^2+(egf+k5).*k6).*k7.*k8).*k9).*rtot)).^(1/2))+(-1).*(1+k2).*k3.*(2.*k4.*k5.*k6.*k7.*k8.^2.*k9+(k1.^2.*k4.*k5.*k6.*k7.*k8.*k9.*((1+k1).^2.*(egf+k3+k2.*k3).^2.*k4.*k5.*k6.*k7.*k8.*k9+8.*k3.^2.*(egf.^2.*k4.*k5.*k6+(egf.*k4.*k5.*k6+k4.*k5.*k6.*k8+k1.^2.*(egf.^2+(egf+k5).*k6).*k7.*k8).*k9).*rtot)).^(1/2)))));

```

```
ci2=(1/4).*k2.*k3.^(-1).*(egf.^2.*k4.*k5.*k6+(egf.*k4.*k5.*k6+k4.*k5.*
k6.*k8+k1.^2.*(egf.^2+(egf+k5).*k6).*k7.*k8).*k9).^(-1).*((-1).*
k1.*(1+k1).*(egf+k3+k2.*k3).*k4.*k5.*k6.*k7.*k8.*k9+(k1.^2.*k4.*
k5.*k6.*k7.*k8.*k9.*((1+k1).^2.*(egf+k3+k2.*k3).^2.*k4.*k5.*k6.*
k7.*k8.*k9+8.*k3.^2.*(egf.^2.*k4.*k5.*k6+(egf.*k4.*k5.*k6+k4.*k5.*
k6.*k8+k1.^2.*(egf.^2+(egf+k5).*k6).*k7.*k8).*k9).*rtot)).^(1/2));
```

```
ca2=(1/4).*k1.^(-1).*k2.*k3.^(-1).*(egf.^2.*k4.*k5.*k6+(egf.*k4.*k5.*
k6+k4.*k5.*k6.*k8+k1.^2.*(egf.^2+(egf+k5).*k6).*k7.*k8).*k9).^(-1)
.*((-1).*k1.*(1+k1).*(egf+k3+k2.*k3).*k4.*k5.*k6.*k7.*k8.*k9+(
k1.^2.*k4.*k5.*k6.*k7.*k8.*k9.*((1+k1).^2.*(egf+k3+k2.*k3).^2.*
k4.*k5.*k6.*k7.*k8.*k9+8.*k3.^2.*(egf.^2.*k4.*k5.*k6+(egf.*k4.*
k5.*k6+k4.*k5.*k6.*k8+k1.^2.*(egf.^2+(egf+k5).*k6).*k7.*k8).*k9).*
rtot)).^(1/2));
```

```
ei2=(1/4).*k3.^(-1).*(egf.^2.*k4.*k5.*k6+(egf.*k4.*k5.*k6+k4.*k5.*k6.*
k8+k1.^2.*(egf.^2+(egf+k5).*k6).*k7.*k8).*k9).^(-1).*((-1).*k1.*(
1+k1).*(egf+k3+k2.*k3).*k4.*k5.*k6.*k7.*k8.*k9+(k1.^2.*k4.*k5.*
k6.*k7.*k8.*k9.*((1+k1).^2.*(egf+k3+k2.*k3).^2.*k4.*k5.*k6.*k7.*
k8.*k9+8.*k3.^2.*(egf.^2.*k4.*k5.*k6+(egf.*k4.*k5.*k6+k4.*k5.*k6.*
k8+k1.^2.*(egf.^2+(egf+k5).*k6).*k7.*k8).*k9).*rtot)).^(1/2));
```

```
ea2=(1/4).*k1.^(-1).*k3.^(-1).*(egf.^2.*k4.*k5.*k6+(egf.*k4.*k5.*k6+
k4.*k5.*k6.*k8+k1.^2.*(egf.^2+(egf+k5).*k6).*k7.*k8).*k9).^(-1).*(
(-1).*k1.*(1+k1).*(egf+k3+k2.*k3).*k4.*k5.*k6.*k7.*k8.*k9+(k1.^2.*
k4.*k5.*k6.*k7.*k8.*k9.*((1+k1).^2.*(egf+k3+k2.*k3).^2.*k4.*k5.*
k6.*k7.*k8.*k9+8.*k3.^2.*(egf.^2.*k4.*k5.*k6+(egf.*k4.*k5.*k6+k4.*
k5.*k6.*k8+k1.^2.*(egf.^2+(egf+k5).*k6).*k7.*k8).*k9).*rtot)).^(
1/2));
```

```
eil2=(1/4).*egf.*k3.^(-2).*(egf.^2.*k4.*k5.*k6+(egf.*k4.*k5.*k6+k4.*
k5.*k6.*k8+k1.^2.*(egf.^2+(egf+k5).*k6).*k7.*k8).*k9).^(-1).*((-1)
.*k1.*(1+k1).*(egf+k3+k2.*k3).*k4.*k5.*k6.*k7.*k8.*k9+(k1.^2.*k4.*
k5.*k6.*k7.*k8.*k9.*((1+k1).^2.*(egf+k3+k2.*k3).^2.*k4.*k5.*k6.*
k7.*k8.*k9+8.*k3.^2.*(egf.^2.*k4.*k5.*k6+(egf.*k4.*k5.*k6+k4.*k5.*
k6.*k8+k1.^2.*(egf.^2+(egf+k5).*k6).*k7.*k8).*k9).*rtot)).^(1/2));
```

```
eal2=(1/4).*egf.*k1.^(-1).*k3.^(-2).*(egf.^2.*k4.*k5.*k6+(egf.*k4.*k5.*
k6+k4.*k5.*k6.*k8+k1.^2.*(egf.^2+(egf+k5).*k6).*k7.*k8).*k9).^(-1)
.*((-1).*k1.*(1+k1).*(egf+k3+k2.*k3).*k4.*k5.*k6.*k7.*k8.*k9+(
k1.^2.*k4.*k5.*k6.*k7.*k8.*k9.*((1+k1).^2.*(egf+k3+k2.*k3).^2.*
k4.*k5.*k6.*k7.*k8.*k9+8.*k3.^2.*(egf.^2.*k4.*k5.*k6+(egf.*k4.*
k5.*k6+k4.*k5.*k6.*k8+k1.^2.*(egf.^2+(egf+k5).*k6).*k7.*k8).*k9).*
rtot)).^(1/2));
```



```

des2=(1/8).*k1.*k5.*k6.*k7.*k8.*k9.*(egf.^2.*k3.*k4.*k5.*k6+k3.*(egf.* ...
k4.*k5.*k6+k4.*k5.*k6.*k8+k1.^2.*(egf.^2+(egf+k5).*k6).*k7.*k8).* ...
k9).^(-2).*(egf.^2.*k1.*((1+k1).^2.*k4.*k5.*k6.*k7.*k8.*k9+4.* ...
k3.^2.*(k4.*k5.*k6+k1.^2.*k7.*k8.*k9).*rtot)+egf.*(2.*k1.*k3.*k6.* ...
k9.*((1+k1).^2.*(1+k2).*k4.*k5.*k7.*k8+2.*k3.*(k4.*k5+k1.^2.*k7.* ...
k8).*rtot)+(-1).*(k1.^2.*k4.*k5.*k6.*k7.*k8.*k9.*((1+k1).^2.*(egf+ ...
k3+k2.*k3).^2.*k4.*k5.*k6.*k7.*k8.*k9+8.*k3.^2.*(egf.^2.*k4.*k5.* ...
k6+(egf.*k4.*k5.*k6+k4.*k5.*k6.*k8+k1.^2.*(egf.^2+(egf+k5).*k6).* ...
k7.*k8).*k9).*rtot)).^(1/2)+(-1).*k1.*(k1.^2.*k4.*k5.*k6.*k7.*k8.* ...
k9.*((1+k1).^2.*(egf+k3+k2.*k3).^2.*k4.*k5.*k6.*k7.*k8.*k9+8.* ...
k3.^2.*(egf.^2.*k4.*k5.*k6+(egf.*k4.*k5.*k6+k4.*k5.*k6.*k8+k1.^2.* ...
(egf.^2+(egf+k5).*k6).*k7.*k8).*k9).*rtot)).^(1/2))+k3.*(2.* ...
k1.^2.*(1+k2).^2.*k3.*k4.*k5.*k6.*k7.*k8.*k9+k1.^3.*k3.*k5.*k6.* ...
k7.*k8.*k9.*((1+k2).^2.*k4+4.*rtot)+k1.*k3.*k4.*k5.*k6.*k8.*k9.*(( ...
1+k2).^2.*k7+4.*rtot)+(-1).*(1+k2).*(k1.^2.*k4.*k5.*k6.*k7.*k8.* ...
k9.*((1+k1).^2.*(egf+k3+k2.*k3).^2.*k4.*k5.*k6.*k7.*k8.*k9+8.* ...
k3.^2.*(egf.^2.*k4.*k5.*k6+(egf.*k4.*k5.*k6+k4.*k5.*k6.*k8+k1.^2.* ...
(egf.^2+(egf+k5).*k6).*k7.*k8).*k9).*rtot)).^(1/2)+(-1).*k1.*(1+ ...
k2).*(k1.^2.*k4.*k5.*k6.*k7.*k8.*k9.*((1+k1).^2.*(egf+k3+k2.*k3) ...
.^2.*k4.*k5.*k6.*k7.*k8.*k9+8.*k3.^2.*(egf.^2.*k4.*k5.*k6+(egf.* ...
k4.*k5.*k6+k4.*k5.*k6.*k8+k1.^2.*(egf.^2+(egf+k5).*k6).*k7.*k8).* ...
k9).*rtot)).^(1/2));

```

```

dea2=(1/8).*k1.^(-1).*k4.*k5.*k6.*k8.*k9.*(egf.^2.*k3.*k4.*k5.*k6+k3.*( ...
egf.*k4.*k5.*k6+k4.*k5.*k6.*k8+k1.^2.*(egf.^2+(egf+k5).*k6).*k7.* ...
k8).*k9).^(-2).*(egf.^2.*k1.*((1+k1).^2.*k4.*k5.*k6.*k7.*k8.*k9+ ...
4.*k3.^2.*(k4.*k5.*k6+k1.^2.*k7.*k8.*k9).*rtot)+egf.*(2.*k1.*k3.* ...
k6.*k9.*((1+k1).^2.*(1+k2).*k4.*k5.*k7.*k8+2.*k3.*(k4.*k5+k1.^2.* ...
k7.*k8).*rtot)+(-1).*(k1.^2.*k4.*k5.*k6.*k7.*k8.*k9.*((1+k1).^2.*( ...
egf+k3+k2.*k3).^2.*k4.*k5.*k6.*k7.*k8.*k9+8.*k3.^2.*(egf.^2.*k4.* ...
k5.*k6+(egf.*k4.*k5.*k6+k4.*k5.*k6.*k8+k1.^2.*(egf.^2+(egf+k5).* ...
k6).*k7.*k8).*k9).*rtot)).^(1/2)+(-1).*k1.*(k1.^2.*k4.*k5.*k6.* ...
k7.*k8.*k9.*((1+k1).^2.*(egf+k3+k2.*k3).^2.*k4.*k5.*k6.*k7.*k8.* ...
k9+8.*k3.^2.*(egf.^2.*k4.*k5.*k6+(egf.*k4.*k5.*k6+k4.*k5.*k6.*k8+ ...
k1.^2.*(egf.^2+(egf+k5).*k6).*k7.*k8).*k9).*rtot)).^(1/2))+k3.*( ...
2.*k1.^2.*(1+k2).^2.*k3.*k4.*k5.*k6.*k7.*k8.*k9+k1.^3.*k3.*k5.* ...
k6.*k7.*k8.*k9.*((1+k2).^2.*k4+4.*rtot)+k1.*k3.*k4.*k5.*k6.*k8.* ...
k9.*((1+k2).^2.*k7+4.*rtot)+(-1).*(1+k2).*(k1.^2.*k4.*k5.*k6.*k7.* ...
k8.*k9.*((1+k1).^2.*(egf+k3+k2.*k3).^2.*k4.*k5.*k6.*k7.*k8.*k9+8.* ...
k3.^2.*(egf.^2.*k4.*k5.*k6+(egf.*k4.*k5.*k6+k4.*k5.*k6.*k8+k1.^2.* ...
(egf.^2+(egf+k5).*k6).*k7.*k8).*k9).*rtot)).^(1/2)+(-1).*k1.*(1+ ...
k2).*(k1.^2.*k4.*k5.*k6.*k7.*k8.*k9.*((1+k1).^2.*(egf+k3+k2.*k3) ...
.^2.*k4.*k5.*k6.*k7.*k8.*k9+8.*k3.^2.*(egf.^2.*k4.*k5.*k6+(egf.* ...
k4.*k5.*k6+k4.*k5.*k6.*k8+k1.^2.*(egf.^2+(egf+k5).*k6).*k7.*k8).* ...
k9).*rtot)).^(1/2));

```

```

des12=(1/8).*egf.*k1.*k6.*k7.*k8.*k9.*(egf.^2.*k3.*k4.*k5.*k6+k3.*(egf.* ...
k4.*k5.*k6+k4.*k5.*k6.*k8+k1.^2.*(egf.^2+(egf+k5).*k6).*k7.*k8).* ...
k9).^(-2).*(egf.^2.*k1.*((1+k1).^2.*k4.*k5.*k6.*k7.*k8.*k9+4.* ...
k3.^2.*(k4.*k5.*k6+k1.^2.*k7.*k8.*k9).*rtot)+egf.*(2.*k1.*k3.*k6.* ...
k9.*((1+k1).^2.*(1+k2).*k4.*k5.*k7.*k8+2.*k3.*(k4.*k5+k1.^2.*k7.* ...
k8).*rtot)+(-1).*(k1.^2.*k4.*k5.*k6.*k7.*k8.*k9.*((1+k1).^2.*(egf+ ...
k3+k2.*k3).^2.*k4.*k5.*k6.*k7.*k8.*k9+8.*k3.^2.*(egf.^2.*k4.*k5.* ...
k6+(egf.*k4.*k5.*k6+k4.*k5.*k6.*k8+k1.^2.*(egf.^2+(egf+k5).*k6).* ...

```

$$\begin{aligned}
& k7.*k8).*k9).*rtot)).^{(1/2)}+(-1).*k1.*(k1.^2.*k4.*k5.*k6.*k7.*k8.* \\
& k9.*((1+k1).^2.*(egf+k3+k2.*k3).^2.*k4.*k5.*k6.*k7.*k8.*k9+8.* \\
& k3.^2.*(egf.^2.*k4.*k5.*k6+(egf.*k4.*k5.*k6+k4.*k5.*k6.*k8+k1.^2.* \\
& (egf.^2+(egf+k5).*k6).*k7.*k8).*k9).*rtot)).^{(1/2)}+k3.*(2.* \\
& k1.^2.*(1+k2).^2.*k3.*k4.*k5.*k6.*k7.*k8.*k9+k1.^3.*k3.*k5.*k6.* \\
& k7.*k8.*k9.*((1+k2).^2.*k4+4.*rtot)+k1.*k3.*k4.*k5.*k6.*k8.*k9.*((\\
& 1+k2).^2.*k7+4.*rtot)+(-1).*(1+k2).*(k1.^2.*k4.*k5.*k6.*k7.*k8.* \\
& k9.*((1+k1).^2.*(egf+k3+k2.*k3).^2.*k4.*k5.*k6.*k7.*k8.*k9+8.* \\
& k3.^2.*(egf.^2.*k4.*k5.*k6+(egf.*k4.*k5.*k6+k4.*k5.*k6.*k8+k1.^2.* \\
& (egf.^2+(egf+k5).*k6).*k7.*k8).*k9).*rtot)).^{(1/2)}+(-1).*k1.*(1+ \\
& k2).*(k1.^2.*k4.*k5.*k6.*k7.*k8.*k9.*((1+k1).^2.*(egf+k3+k2.*k3) \\
& .^2.*k4.*k5.*k6.*k7.*k8.*k9+8.*k3.^2.*(egf.^2.*k4.*k5.*k6+(egf.* \\
& k4.*k5.*k6+k4.*k5.*k6.*k8+k1.^2.*(egf.^2+(egf+k5).*k6).*k7.*k8).* \\
& k9).*rtot)).^{(1/2)}));
\end{aligned}$$

$$\begin{aligned}
des2l2=& (1/8).*egf.^2.*k1.*k7.*k8.*k9.*(egf.^2.*k3.*k4.*k5.*k6+k3.*(egf.* \\
& k4.*k5.*k6+k4.*k5.*k6.*k8+k1.^2.*(egf.^2+(egf+k5).*k6).*k7.*k8).* \\
& k9).^(-2).*(egf.^2.*k1.*((1+k1).^2.*k4.*k5.*k6.*k7.*k8.*k9+4.* \\
& k3.^2.*(k4.*k5.*k6+k1.^2.*k7.*k8.*k9).*rtot)+egf.*(2.*k1.*k3.*k6.* \\
& k9.*((1+k1).^2.*(1+k2).*k4.*k5.*k7.*k8+2.*k3.*(k4.*k5+k1.^2.*k7.* \\
& k8).*rtot)+(-1).*(k1.^2.*k4.*k5.*k6.*k7.*k8.*k9.*((1+k1).^2.*(egf+ \\
& k3+k2.*k3).^2.*k4.*k5.*k6.*k7.*k8.*k9+8.*k3.^2.*(egf.^2.*k4.*k5.* \\
& k6+(egf.*k4.*k5.*k6+k4.*k5.*k6.*k8+k1.^2.*(egf.^2+(egf+k5).*k6).* \\
& k7.*k8).*k9).*rtot)).^{(1/2)}+(-1).*k1.*(k1.^2.*k4.*k5.*k6.*k7.*k8.* \\
& k9.*((1+k1).^2.*(egf+k3+k2.*k3).^2.*k4.*k5.*k6.*k7.*k8.*k9+8.* \\
& k3.^2.*(egf.^2.*k4.*k5.*k6+(egf.*k4.*k5.*k6+k4.*k5.*k6.*k8+k1.^2.* \\
& (egf.^2+(egf+k5).*k6).*k7.*k8).*k9).*rtot)).^{(1/2)}+(-1).*k1.*(1+ \\
& k2).*(k1.^2.*k4.*k5.*k6.*k7.*k8.*k9.*((1+k1).^2.*(egf+k3+k2.*k3) \\
& .^2.*k4.*k5.*k6.*k7.*k8.*k9+8.*k3.^2.*(egf.^2.*k4.*k5.*k6+(egf.* \\
& k4.*k5.*k6+k4.*k5.*k6.*k8+k1.^2.*(egf.^2+(egf+k5).*k6).*k7.*k8).* \\
& k9).*rtot)).^{(1/2)}));
\end{aligned}$$

$$\begin{aligned}
deal2=& (1/8).*egf.*k1.^{(-1)}.*k4.*k5.*k6.*k9.*(egf.^2.*k3.*k4.*k5.*k6+k3.* \\
& (egf.*k4.*k5.*k6+k4.*k5.*k6.*k8+k1.^2.*(egf.^2+(egf+k5).*k6).*k7.* \\
& k8).*k9).^(-2).*(egf.^2.*k1.*((1+k1).^2.*k4.*k5.*k6.*k7.*k8.*k9+ \\
& 4.*k3.^2.*(k4.*k5.*k6+k1.^2.*k7.*k8.*k9).*rtot)+egf.*(2.*k1.*k3.* \\
& k6.*k9.*((1+k1).^2.*(1+k2).*k4.*k5.*k7.*k8+2.*k3.*(k4.*k5+k1.^2.* \\
& k7.*k8).*rtot)+(-1).*(k1.^2.*k4.*k5.*k6.*k7.*k8.*k9.*((1+k1).^2.*(\\
& egf+k3+k2.*k3).^2.*k4.*k5.*k6.*k7.*k8.*k9+8.*k3.^2.*(egf.^2.*k4.* \\
& k5.*k6+(egf.*k4.*k5.*k6+k4.*k5.*k6.*k8+k1.^2.*(egf.^2+(egf+k5).* \\
& k6).*k7.*k8).*k9).*rtot)).^{(1/2)}+(-1).*k1.*(k1.^2.*k4.*k5.*k6.* \\
& k7.*k8.*k9.*((1+k1).^2.*(egf+k3+k2.*k3).^2.*k4.*k5.*k6.*k7.*k8.* \\
& k9+8.*k3.^2.*(egf.^2.*k4.*k5.*k6+(egf.*k4.*k5.*k6+k4.*k5.*k6.*k8+ \\
& k1.^2.*(egf.^2+(egf+k5).*k6).*k7.*k8).*k9).*rtot)).^{(1/2)}+k3.*(\\
& 2.*k1.^2.*(1+k2).^2.*k3.*k4.*k5.*k6.*k7.*k8.*k9+k1.^3.*k3.*k5.* \\
& k6.*k7.*k8.*k9.*((1+k2).^2.*k4+4.*rtot)+k1.*k3.*k4.*k5.*k6.*k8.* \\
& k9.*((1+k2).^2.*k7+4.*rtot)+(-1).*(1+k2).*(k1.^2.*k4.*k5.*k6.*k7.* \\
& k8.*k9.*((1+k1).^2.*(egf+k3+k2.*k3).^2.*k4.*k5.*k6.*k7.*k8.*k9+8.*
\end{aligned}$$

```

k3.^2.*(egf.^2.*k4.*k5.*k6+(egf.*k4.*k5.*k6+k4.*k5.*k6.*k8+k1.^2.* ...
(egf.^2+(egf+k5).*(k6).*(k7.*k8).*(k9)).*rtot)).^(1/2)+(-1).*(k1.*(1+ ...
k2).*(k1.^2.*k4.*k5.*k6.*k7.*k8.*k9.*((1+k1).^2.*(egf+k3+k2.*k3) ...
.^2.*k4.*k5.*k6.*k7.*k8.*k9+8.*k3.^2.*(egf.^2.*k4.*k5.*k6+(egf.* ...
k4.*k5.*k6+k4.*k5.*k6.*k8+k1.^2.*(egf.^2+(egf+k5).*(k6).*(k7.*k8).*( ...
k9).*(rtot)).^(1/2)));

```

```

dea212=(1/8).*(egf.^2.*k1.^(-1).*(k4.*k5.*k6.*(egf.^2.*k3.*k4.*k5.*k6+k3.* ...
egf.*k4.*k5.*k6+k4.*k5.*k6.*k8+k1.^2.*(egf.^2+(egf+k5).*(k6).*(k7.* ...
k8).*(k9)).^(-2).*(egf.^2.*k1.*((1+k1).^2.*k4.*k5.*k6.*k7.*k8.*k9+ ...
4.*k3.^2.*(k4.*k5.*k6+k1.^2.*k7.*k8.*k9)).*rtot)+egf.*(2.*k1.*k3.* ...
k6.*k9.*((1+k1).^2.*(1+k2).*(k4.*k5.*k7.*k8+2.*k3.*(k4.*k5+k1.^2.* ...
k7.*k8)).*rtot)+(-1).*(k1.^2.*k4.*k5.*k6.*k7.*k8.*k9.*((1+k1).^2.*( ...
egf+k3+k2.*k3).^2.*k4.*k5.*k6.*k7.*k8.*k9+8.*k3.^2.*(egf.^2.*k4.* ...
k5.*k6+(egf.*k4.*k5.*k6+k4.*k5.*k6.*k8+k1.^2.*(egf.^2+(egf+k5).*( ...
k6).*(k7.*k8).*(k9)).*rtot)).^(1/2)+(-1).*(k1.*(k1.^2.*k4.*k5.*k6.* ...
k7.*k8.*k9.*((1+k1).^2.*(egf+k3+k2.*k3).^2.*k4.*k5.*k6.*k7.*k8.* ...
k9+8.*k3.^2.*(egf.^2.*k4.*k5.*k6+(egf.*k4.*k5.*k6+k4.*k5.*k6.*k8+ ...
k1.^2.*(egf.^2+(egf+k5).*(k6).*(k7.*k8).*(k9)).*rtot)).^(1/2))+k3.*( ...
2.*k1.^2.*(1+k2).^2.*k3.*k4.*k5.*k6.*k7.*k8.*k9+k1.^3.*k3.*k5.* ...
k6.*k7.*k8.*k9.*((1+k2).^2.*k4+4.*rtot)+k1.*k3.*k4.*k5.*k6.*k8.* ...
k9.*((1+k2).^2.*k7+4.*rtot)+(-1).*(1+k2).*(k1.^2.*k4.*k5.*k6.*k7.* ...
k8.*k9.*((1+k1).^2.*(egf+k3+k2.*k3).^2.*k4.*k5.*k6.*k7.*k8.*k9+8.* ...
k3.^2.*(egf.^2.*k4.*k5.*k6+(egf.*k4.*k5.*k6+k4.*k5.*k6.*k8+k1.^2.* ...
(egf.^2+(egf+k5).*(k6).*(k7.*k8).*(k9)).*rtot)).^(1/2)+(-1).*(k1.*(1+ ...
k2).*(k1.^2.*k4.*k5.*k6.*k7.*k8.*k9.*((1+k1).^2.*(egf+k3+k2.*k3) ...
.^2.*k4.*k5.*k6.*k7.*k8.*k9+8.*k3.^2.*(egf.^2.*k4.*k5.*k6+(egf.* ...
k4.*k5.*k6+k4.*k5.*k6.*k8+k1.^2.*(egf.^2+(egf+k5).*(k6).*(k7.*k8).*( ...
k9).*(rtot)).^(1/2)));

```

```

numOfElements=numel([egfbound1, cil, cal, eil, eal, eil1, eal1, des1, des11,
des211, deal, deal1, dea211]);
if sum(sum([egfbound1, cil, cal, eil, eal, eil1, eal1, des1, des11, des211,
deal, deal1, dea211]>=0))==numOfElements
    boundSignal=egfbound1;
    allSpecies=[cil, cal, eil, eal, eil1, eal1, des1, des11, des211, deal,
deal1, dea211];
    whichRoot=1;
elseif sum(sum([egfbound2, ci2, ca2, ei2, ea2, eil2, eal2, des2, des12,
des212, dea2, deal2, dea212]>=0))==numOfElements
    boundSignal=egfbound2;
    allSpecies=[ci2, ca2, ei2, ea2, eil2, eal2, des2, des12, des212, dea2,
deal2, dea212];
    whichRoot=2;
else
    boundSignal=nan;
    allSpecies=nan;
    whichRoot=0;
end

```

